Volume 15
Number 10
October 2024
Pages 3275–3626

RSC Medicinal Chemistry

rsc.li/medchem

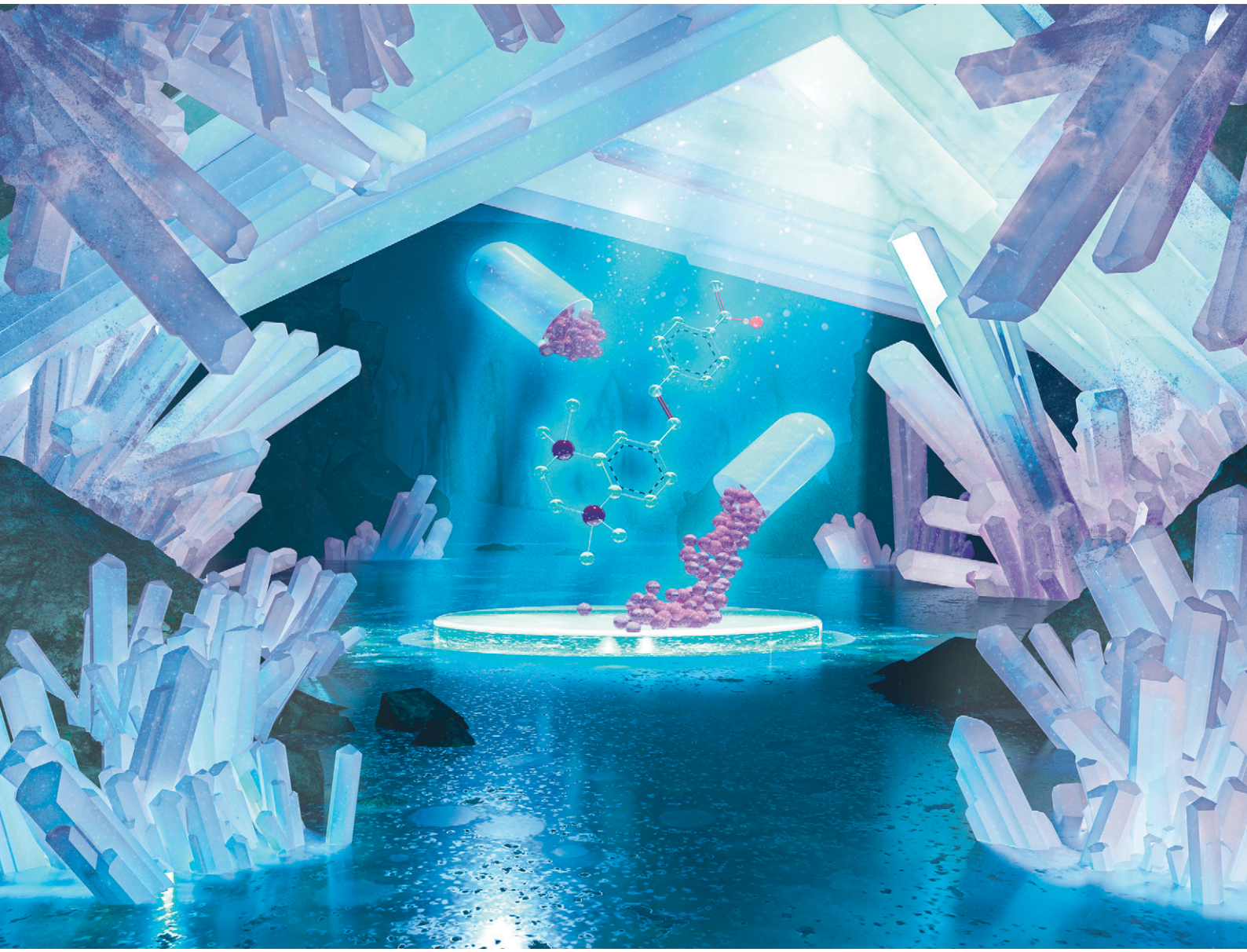

ISSN 2632-8682

ROYAL SOCIETY OF CHEMISTRY

REVIEW ARTICLE
Jenny-Lee Panayides, Darren Lyall Riley *et al.*
The role of silicon in drug discovery: a review

RSC Medicinal Chemistry

ROYAL SOCIETY OF CHEMISTRY

REVIEW

View Article Online
View Journal | View Issue

Cite this: *RSC Med. Chem.*, 2024, **15**, 3286

The role of silicon in drug discovery: a review

Jenny-Lee Panayides, *[a] Darren Lyall Riley, *[b] Felix Hasenmaile [c] and Willem A. L. van Otterlo [c]

Received 12th March 2024,
Accepted 7th June 2024

DOI: 10.1039/d4md00169a

rsc.li/medchem

This review aims to highlight the role of silicon in drug discovery. Silicon and carbon are often regarded as being similar with silicon located directly beneath carbon in the same group in the periodic table. That being noted, in many instances a clear dichotomy also exists between silicon and carbon, and these differences often lead to vastly different physiochemical and biological properties. As a result, the utility of silicon in drug discovery has attracted significant attention and has grown rapidly over the past decade. This review showcases some recent advances in synthetic organosilicon chemistry and examples of the ways in which silicon has been employed in the drug-discovery field.

Introduction

"*Silicon and carbon are alike in so many ways, and yet, they are so different. This dichotomy was behind a good portion of the interest in silicon chemistry in the 20th century... In recent decades, silicon has thoroughly penetrated areas as diverse as organic synthesis and microelectronics*" – Josef Michl, Editor, *Chemical Reviews*, 1995.[1]

Silicon, the 14th element in the periodic table, accounts for about a quarter of all the material in the Earth's crust.[2] It is however never found naturally in its elemental form, but

[a] *Pharmaceutical Technologies, Future Production: Chemicals, Council for Scientific and Industrial Research (CSIR), Meiring Naude Road, Brummeria, Pretoria, South Africa. E-mail: jpanayides@csir.co.za*
[b] *Department of Chemistry, Faculty of Natural and Agricultural Sciences, University of Pretoria, Lynnwood Road, Pretoria, South Africa. E-mail: darren.riley@up.ac.za*
[c] *Department of Chemistry and Polymer Science, Stellenbosch University, Matieland, Stellenbosch, 7600, South Africa*

Jenny-Lee Panayides

Dr Jenny-Lee Panayides is a Principal Researcher and Research Group Leader (Pharmaceutical Technologies) at the Council for Scientific and Industrial Research, South Africa. She holds a PhD in synthetic chemistry and microbiology (University of the Witwatersrand), and certification in advanced project management (University of Pretoria). Her early research supported malaria transmission-blocking drug discovery efforts through high-throughput screening cascades, while she has shifted her research focus in recent years to supporting the self-sufficiency of African pharmaceutical manufacturing. She now leads an applied research program focusing on the local production of active pharmaceutical ingredients, integrating continuous flow chemistry with intelligent process transformation, and provides thought leadership on various working groups in the pharmaceutical and 4IR technologies space.

Darren Lyall Riley

Prof. Riley obtained his doctorate in organic chemistry at the University of the Witwatersrand, Johannesburg, South Africa in 2007. This was followed by a post-doctoral fellowship at the same institution. In 2010 he was appointed as a principal scientist at iThemba Pharmaceuticals and thereafter returned to academia joining the University of Pretoria in 2013. His research interests include small molecule-based drug discovery and the application of flow chemistry for the development of more sustainable approaches for manufacturing pharmaceuticals.

always in combinations with other elements, especially oxygen. Despite its abundance, silicon plays only a minor role in living organisms. While inorganic forms, such as silica (SiO_2) or silicic acid ($Si(OH)_4$) are of importance in the biochemistry of algae and plants,[3] it has generally been accepted that there are no naturally occurring organosilicon compounds, *i.e.* compounds containing at least one silicon–carbon bond.[4]

Silicon in drug discovery

"*Some of the fundamental differences between carbon and silicon can lead to marked alterations in the physiochemical and biological properties of the silicon-containing analogues… and the resulting benefits can be exploited in the drug design process*" – Graham A. Showell, Amedis Pharmaceuticals Ltd.[5]

The design of new and improved drug-like compounds for the treatment of disease requires not only good activity and selectivity but also low toxicity and physiologically acceptable pharmacokinetics. Traditionally the medicinal chemist tackles the task of developing lead active pharmaceutical ingredients (API's) in an iterative design approach weighing up activity against parameters such as selectivity, solubility, absorption, distribution, metabolism, excretion, and toxicology (ADMET) – see the following recent example for a study which included determining the ADMET properties of silicon–nitrogen heterocycles.[6]

Currently, drug developers often look to known families of drugs to draw inspiration for the design of new biologically active compounds. Recent data would suggest that only about 3 dozen scaffolds exist which are routinely utilized and that they account for approximately 50% of all compounds which have been FDA approved.[7] These same studies have also demonstrated that most of the small bioactive molecule side-chains observed in modern drug structures have been designed by using a rather small number of different functional groups.[8] These observations has also led to the application of bioisosteres as a modern strategy in drug design which aims to utilize bioisosteres to improve the ADMET properties of small molecule drug-like entities or to obtain new subclasses of compounds with modified properties.[5,9]

During the 1970's the notion of using a "silicon switch", or effectively a silicon–carbon substitution to design novel analogues of bioactive molecules was developed by Tacke and colleagues. In this strategy, an existing molecule could be modified by replacing one or more carbon-atoms by silicon atoms (or silicon atom-containing functional/structural groups). It should be appreciated that a "silicon switch" of this type could be treated conceptually as a classical tetravalent bioisostere.[5] However, in our opinion, application of this approach still remains undervalued and therefore underutilized. For example, in 2001 it was estimated that less than 1% of all patent cooperation treaty (PCT) applications in the field of drug discovery referred to compounds that contained silicon or other less frequently used elements.[10] Recently, however, in addition to the aforementioned rapid growth in organosilicon chemistry there has been increased interest in the incorporation of silicon as a bioisostere of carbon into drug-like scaffolds in an effort to manipulate pharmacokinetically important parameters.

Impact of silicon on medicinal chemistry

Both carbon and silicon atoms possess four valence electrons and as such, similarities with respect to the chemistry of silicon and carbon are apparent. However, in terms of several chemical aspects the two elements differ substantially from one another.[5] A 2013 review by Franz and Wilson highlighted the fact that the different chemical properties of organosilicon-based compounds are of particular relevance to medicinal

Felix Hasenmaile

Felix studied Chemistry at the University of Freiburg and visited the Université Paris-Sud for a research stay working on Ca(II)-catalysed hydroaminations with Prof. Gandon and Prof. LeBoeuf. He obtained his Ph.D. in the group of Prof. Brückner, where he investigated the atropisomerism of macrocyclic biaryls and developed catalysts for asymmetric synthesis. He joined the group of Prof. van Otterlo as a post-doctoral fellow pursuing the atroposelective synthesis of naphthylisoquinoline alkaloids. He now works at the research department of Boehringer Ingelheim.

Willem A. L. van Otterlo

Willem van Otterlo received his PhD in 1999 from the University of the Witwatersrand (WITS), Johannesburg, South Africa, followed by a postdoctoral fellowship at the University of Montreal, Quebec, Canada. In 2001, he returned to WITS and progressed to the position of Associate Professor in 2008. In 2008/2009 he took up a von Humboldt Georg-Forster Research Fellowship at the Max Planck Institute, Dortmund, and in 2010 was appointed to the Chair of Organic Chemistry in the Department of Chemistry and Polymer Science at the University of Stellenbosch. His research interests are focused on the synthesis of small molecules with potential bioactivity.

chemistry.[11] Some of these fundamental differences can result in marked variations in the physico- and biochemical properties of silicon-containing analogues with respect to their carbon parent compounds. These differences can of course be rationally exploited in the drug design process, of which some concepts are described in Table 1.

Silicon has a high affinity towards oxygen and forms stronger bonds to oxygen and the halogens than carbon. On the other hand, bonds between silicon and carbon or hydrogen are weaker than the respective carbon–carbon or carbon–hydrogen bonds. The crux of modern organosilicon synthetic chemistry hinges on the generation of exceptionally stable bonds of silicon to oxygen or fluoride whilst at the same time cleaving weaker silicon bonds.[12]

The chemistry of Si–C and Si–O single bonds dominates the overall chemistry of silicon, and as such, its application as a tetrahedral bioisostere of carbon is therefore not unexpected. In contrast to the strength of some of the σ Si bonds, π Si bonds are generally weak.[12] For this reason, generally no stable sila-equivalents exist for alkenes and carbonyl functional groups even though compounds with sterically or electronically stabilised silicon–carbon[13] and silicon–oxygen[14] double bonds can be isolated. It should also be noted that whilst the carbonyl double bond is favoured over its hydrated form, the formation of a Si═O double bond is disfavoured over its hydrate (the silicon diol or silanediol).[15] It has also been observed that silicon cannot form physiologically stable Si–H-containing compounds. Not only is the Si–H bond weaker than its C–H comparator, it also experiences reversed polarity.[5] As such, the Si–H bond behaves quite differently to the C–H bond. For an example, the Si–H bond is readily cleaved with water under non-acidic conditions to afford the corresponding silanol featuring a Si–OH bond, conditions under which the C–H bond remains quite stable.[5] These crucial bond differences can therefore be used to synthesise sila-analogues where carbon counterparts are much more difficult to obtain, if not impossible to access under normal experimental conditions (see brief discussions of novel synthetic methodology concerning the synthesis of Si-containing molecules elsewhere in this review).

Silicon containing bonds are always longer than the corresponding carbon analogues – the C–C bond length is ~1.54 Å *versus* the C–Si bond length of ~1.87 Å.[16] A popular example demonstrating this is seen in that the trimethylsilyl (TMS) group is less sterically demanding than its carbon analogue, the *tert*-butyl arrangement – at least when measured in terms of *A*-values. The longer bond to the $SiMe_3$-group decreases steric interactions, even though the size of the whole group is indeed larger.[17] This bond length divergence leads to subtle but important changes in terms of the size and shape of silicon-containing compounds, when compared with their carbon-only parent compounds.[15] This in turn can result in changes in terms of how the silicon analogues interact with their biological targets to ultimately have a marked effect on the overall pharmacological profiles of the silyl-containing molecules.[5,15] Silicon is also more electropositive than carbon, and because of this carbon-silicon bonds are considerably polarized.[12] For the same reason, polarisations of bonds between and other elements will also be different when compared to the respective bonds to silicon.

A research area which has potential benefits for the "silicon switch" approach involves investigations into hydrogen-bond strengths and acidities.[5] It is important to note that the hydrogen-bond strength of a silanol makes it more favourable as a donor when compared to the corresponding carbinol.[15,18] As a result, in molecules where a carbon-bonded OH functions as a hydrogen-bond donor, the application of a silanol functional group can result in improved biochemical potency.[15] It should thus be stressed that due to the importance of hydrogen bond donors in drug discovery,[19] investigations into the physical properties of molecules like the silanols, including that of hydrogen bond acidity, are of significant value.[20]

Generally, silicon-containing compounds are more lipophilic (and in turn hydrophobic) than their corresponding carbon counterparts. When the lipophilicity of a molecule is modulated, this in turn can be expected to alter the *in vivo* effects due to the small molecule. For example, small increases in lipophilicity have been found to significantly increase molecular tissue penetration abilities.[15,21,22] As a result, silicon-containing molecules have proven to be less prone to hepatic metabolism resulting in subsequent higher molecular plasma half-lives (in comparison to the carbon-based parent molecules).[15] In addition, lipophilicity can play a crucial role in the ability of small molecule drug candidates to cross the blood–brain barrier (BBB).[15] Research has shown that many computational models predicting BBB permeation contain a lipophilicity criterion.[23]

Table 1 Properties and potential benefits of silicon in medicinal chemistry.[5]

Property	Difference	Potential benefit
Bonding	Altered bond strength and disfavoured multiple bonds	• Silane diol peptidomimetics • Access to bioisosteres not structurally available to carbon
Atomic size	Altered bond lengths and bond angles	• Altered *in vitro* potency • Modified selectivity • Altered rate of metabolism
Electronegativity	Increased H-bond strength and acidity of silanols	• Improved potency in pharmacophores where H-bonding is important
Lipophilicity	Increased lipophilicity of silicon-containing compounds	• Improved *in vivo* half-life • Enhanced tissue distribution • Enhanced cell penetration

The area of computational research involving small silicon-containing molecules has also seen recent attention, and *in silico* studies have regularly been utilized to support observed bond characteristics of silicon atoms in small molecules. Advances in this field include new Amber-compatible organosilane force fields[24] and other computational approaches to investigating molecules of this type.[25,26]

Another exciting area of research that will certainly impact the field of silicon-containing bioactive compounds is the development of enzymes capable of performing biocatalytic transformations of the silicon fragments contained in these compounds, as exemplified by the following reference.[27] Findings in this field may also be relevant in terms of evaluating the advantages of incorporating silicon into bioactive molecules. Care should also be taken to establish the broader implications of this switch in terms of biodegradability (or alternatively recyclability) of the new compounds, all with a view on responsible sustainability of utilizing the novel silicon-incorporated molecules (see for example the following reference).[28] Also of importance, in terms of the interaction of environmental microbes with silicon-containing molecules, is the recent research into the biodegradative formation[29] or cleavage[30] of Si–C bonds. These processes, which seem to occur under at least very mild environmental (natural) conditions, would appear yet to be proven in a satisfactory scientifically rigorous manner.

Silyl ethers as protecting groups

The major use of silicon in synthetic organic chemistry has to date been in the application of organosilyl protecting groups as parts of an essential synthetic strategy. Due to this use, there has been significant growth of Si-protecting group technology, to the point where they are now very often applied in any organic synthesis requiring the protection of an OH group.[31] The first group, that found larger application was the trimethylsilyl group (TMS) **1**. Since then sterically bulkier, and hence more stable groups, such as triethylsilyl (TES) **2**, triisopropyl (TIPS) **3**, *tert*-butyldimethylsilyl (TBDMS) **4**, *tert*-butyldiphenyl (TBDPS) **5** and *tert*-hexyldimethyl (TDS) **6**, have come into more regular use, as well as disiloxane protecting groups such as tetraisopropyldisoloxanediyl (TIPD) **7** (Fig. 1).

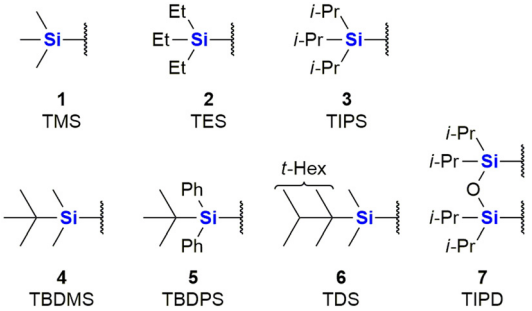

Fig. 1 Common organosilyl *O*-protecting groups.

Compounds containing organosilyl protecting groups are routinely deprotected under either acidic or basic conditions or by the application of reagents providing fluoride ions (as for example, by using the reagent, tetrabutylammonium fluoride which often is applied as the hydrate).[32] As a result of the deprotection, silanols (Si–OH), or, in the case of deprotection with fluoride ions, mixtures of silanols and silyl fluorides are obtained as side-products, which are usually considered waste.[31] The discarding of silicon protecting group waste occurs even on industrial scale, and is obviously still a significant issue in terms of the principles of Green Chemistry and reaction atom economy (AE). It is, however, possible to recycle the silanols by recovery from the aqueous waste and subsequently converting them back into their respective chlorosilanes, which can be used again for *O*-protection.[31]

Recent progress in organosilicon chemistry

The field of organosilicon chemistry has grown rapidly. Although not the focus of this review, the reader is referred to some recent highlights of the last decade in the area showcasing the large number of synthetic tools available for the synthesis of organosilicon compounds. A special emphasis is put on methods which are relevant for the synthesis of silicon containing scaffolds presented in this review (Fig. 2–6). In addition to the transformations shown in Fig. 2–6, the reader is further referred to several new reviews and perspectives (2020–2023) highlighting recent developments in electrochemistry,[33] C–H-activation,[34–37] cross-coupling reactions,[38–41] hydrosilylations,[42–46] carbosilylations,[47] construction of silicon stereogenic compounds,[48–50] silicon-containing small rings,[51,52] synthesis of silanols[53] and various other synthetic aspects.[54–60]

Incorporation of silicon in the scaffold of biologically active molecules necessarily requires the formation of Si–C-bonds. Significant advances have been made in this field and Fig. 2 presents some recent examples. Hydrosilylation of olefins,[61,79,95–113] strained rings[114,115] or Michael-acceptors[116–119] are popular methods for the construction of C–Si-bonds as a large variety of hydrosilanes are commercially available. Cheng *et al.* recently reported the asymmetric hydrosilylation of both styrenes and unactivated olefins by an earth-abundant Co-catalyst which proceeds under very mild conditions and with high stereoselectivity Fig. 2A).[61] Carbosilylations[120–130] of olefins are less common, yet Zheng *et al.* reported a photochemical procedure using arylnitriles and silanes as reaction partners (Fig. 2B).[62] Disilylations of olefins can be accomplished by an electrochemical process developed by Lu *et al.* using chlorosilanes as the silyl source (Fig. 2C).[63] Recently, also an electrochemical silyl-oxygenation[131] and a Ni-catalysed silyl-acylation[132] were reported. Among the numerous reports for the synthesis of vinylsilanes[133–137] or arylsilanes.[138–150] by cross-coupling, Lu *et al.* reported a particularly interesting method using photocatalysis and α-fluoroacrylic acids as

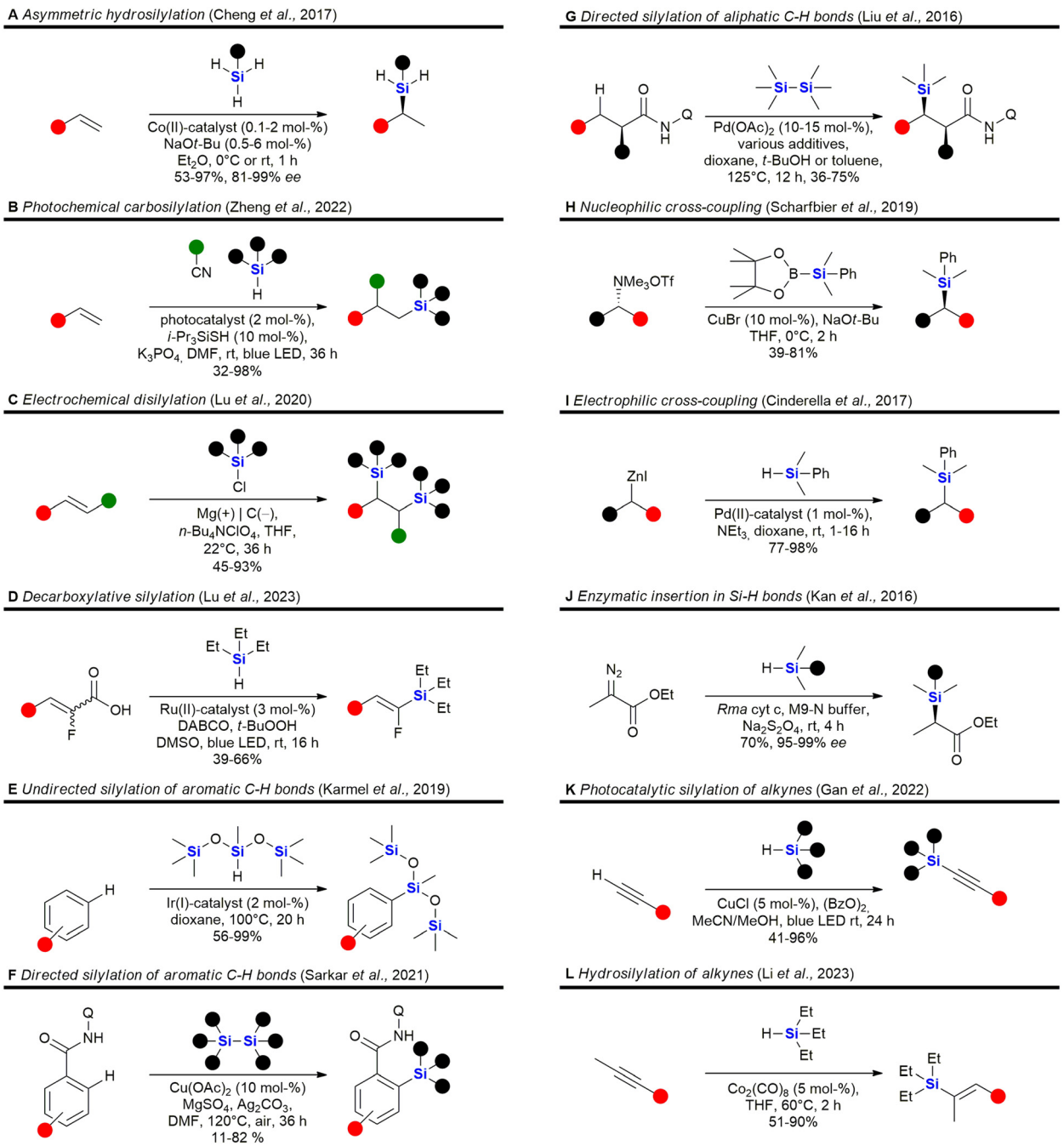

Fig. 2 Recent advances in the field of C–Si bond formation – examples A,[61] B,[62] C,[63] D,[64] E,[65] F,[66] G,[67] H,[68] I,[69] J,[70] K[71] and L.[72] Q = 8-aminoquinoline.

coupling partners (Fig. 2D).[64] Incorporation of silyl groups by C(sp^2)–H-activation has seen tremendous progress,[66,139,142,151–169] exemplified here by the undirected Ir-catalysed silylation reported by Karmel *et al.*[65] (Fig. 2E) or the directed silylation by Sarkar *et al.*[66] who employed an inexpensive Cu-catalyst (Fig. 2F). Silylation of aliphatic C–H bonds[80,157,170–178] is also rapidly developing. Recently Liu *et al.* reported the diastereoselective silylation of amides using Pd-catalysis and an aminoquinoline directing group (Fig. 2G).[67] Other means of C(sp^3)–Si bond formation[179] include processes in which the silyl group is introduced as a nucleophile[180–186] – see for example the work of Scharfbier *et al.* (Fig. 2H)[68] – or as an electrophile[187] – see for example Cinderella *et al.* (Fig. 2I).[69] A recent milestone in the field was the discovery of Kan *et al.* that enzymes are able to catalyse C–Si bond formation by the reaction of α-diazo esters with organsilanes (Fig. 2J)[70] – even though silicon is not naturally encountered in biomolecules. Terminal alkynes can be silylated[91,188–191] with organosilanes by a dehydrogenative photochemical reaction using a Cu-catalyst (Fig. 2K).[71]

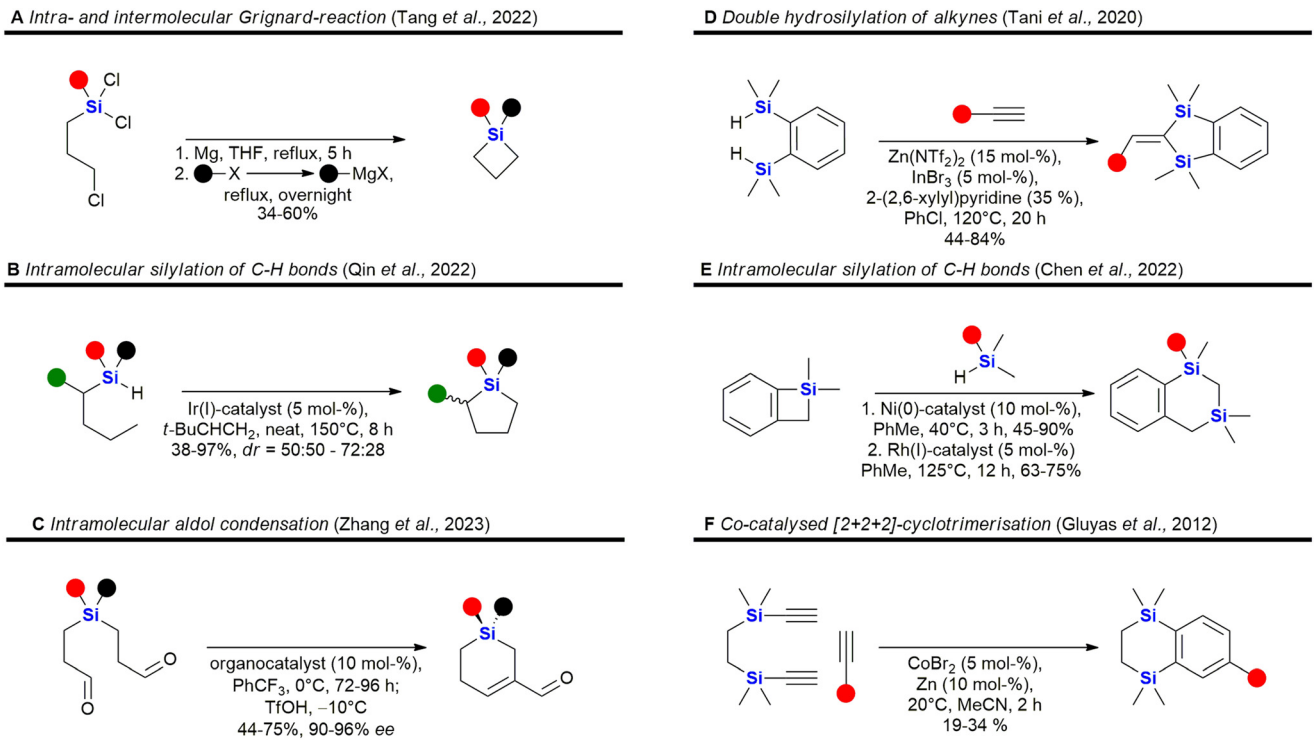

Fig. 3 Recent examples for the synthesis of silacycles – examples A,[73] B,[74] C,[75] D,[76] E[77] and F.[78]

Recently, a regioselective hydrosilylation of methylsubstituted internal alkynes was reported by Li *et al.* using Co-catalysis (Fig. 2L).[72] There has also been progress in the field of carbosilylation of alkynes:[192] and silylation of arynes.[193]

Some recent reports for the synthesis of 4–6 membered silacycles with one or two silicon atoms are shown in Fig. 3. The synthesis of silacyclobutanes is almost exclusively achieved by the intramolecular Grignard reaction of γ-haloalkylchlorosilanes (Fig. 3A). In this work, Tang *et al.* reported a convenient one-pot procedure in which a second substituent was also introduced (see ESI in ref. 73). Qin *et al.* reported the synthesis of silacyclopentanes[186,194–204] (Fig. 3B) by an iridium-catalysed C–H-activation followed by an intramolecular silylation.[74] Among the recent methods to construct 6-membered silacycles[82,198,200,205–212] the application of an organocatalysed intramolecular aldol condensation (Fig. 3C) stands out, as it provides a silicon centred stereocentre with high enantiomeric control.[75] See ref. 211, 213 and 214 for the synthesis of larger rings with one silicon atom. Five membered rings with two silicon atoms[215] may be obtained by a double hydrosilylation of terminal alkynes (Fig. 3D) by a Zn/In co-catalytic system.[76] Chen *et al.* reported the synthesis of benzannulated 1,3-disilacyclohexanes from silacyclobutanes by a nickel-catalysed silylative ring-opening, followed by a Rh-catalysed intramolecular C–H-silylation (Fig. 3E).[77] Synthetic methods to synthesise 1,4-disilycyclohexanes, which are incorporated in retinoid X receptor agonists (Fig. 15), seem to be less developed[78] and mostly rely on the Co-catalysed [2 + 2 + 2]-cyclotrimerisation reaction (Fig. 3F).[216]

Heterocycles, especially those containing nitrogen, are privileged structural motives in small molecule drugs.[217,218] Therefore, there is considerable interest in the synthesis of silicon-containing heterocycles (Fig. 4).[219] A recent highlight in the synthesis of 3-sila-pyrrolidines was the development of a Rh(I)-catalysed asymmetric intramolecular hydrosilylation for the synthesis of silaproline (Fig. 4A).[79] This unnatural amino acid [see ref. 220 and 221 for the synthesis of other unnatural silicon-containing amino acids] has been incorporated in several biologically active peptides (Fig. 59, 98, 117 and 119). 2-Sila-pyrrolidines are accessible by consecutive iridium-catalysed N–H and C–H silylations (Fig. 4B), but have not been reported as part of biologically active molecules so far.[80] 4-Sila-piperidines (Fig. 4C) are rather commonly used in small molecule drugs (Fig. 60 and 64–66). While traditionally prepared by double alkylation of a nitrogen-nucleophile,[222] Fang *et al.* recently reported their synthesis through a double dehydrogenative silylation of dialkylamines.[81] 3-Sila-piperidines are less frequently encountered (Fig. 108). They are accessible by the palladium-catalysed ring-opening of *in situ* prepared siletanes, followed by carbosilylation of terminal alkynes (Fig. 4D).[82] See also ref. 223 for the synthesis of silazepanes. There is also some interest in the synthesis of heterocycles containing both oxygen and silicon, yet these have not been incorporated into small molecule drugs so far. Benzannulated 3-silaoxolanes can be prepared by double lithiation of phenylbenzyl ethers, followed by addition of a dichlorosilane as an example (Fig. 4E).[83]

Recently, an interesting two-step procedure for the synthesis of 2-silafuranes was reported. It involved an

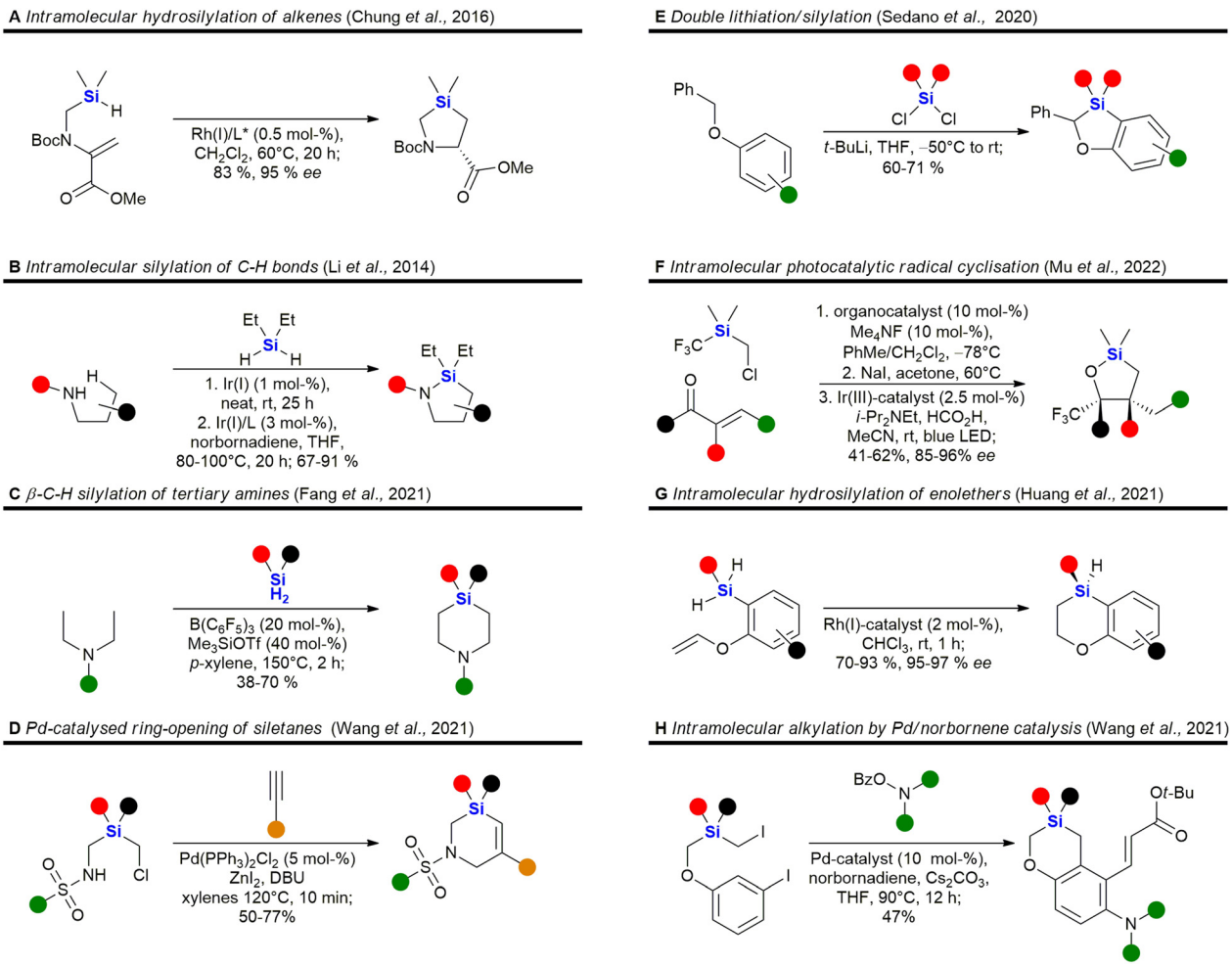

Fig. 4 Recent advances in the synthesis of sila-heterocycles – examples A,[79] B,[80] C,[81] D,[82] E,[83] F,[84] G[85] and H.[86]

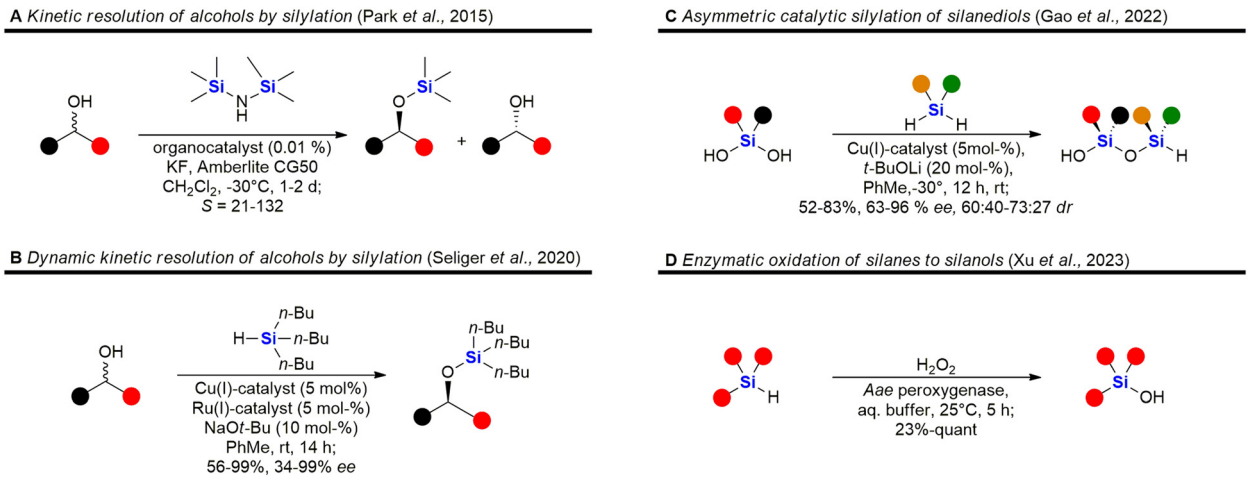

Fig. 5 Recent advances in the synthesis of silyl ethers, siloxanes and silanols – examples A,[87] B,[88] C[89] and D.[90]

organocatalytic 1,2-addition of a trifluoromethylsilane to an enone and a subsequent photocatalytic radical addition (Fig. 4F).[84] An asymmetric rhodium-catalysed intramolecular hydrosilylation of phenylvinyl ethers gave access to benzannulated 4-silatetrahydropyrans and also established a silicon stereocentre (Fig. 4G).[85] 3-Silatetrahydropyrans are less explored, but recently a palladium/norbornene cooperative catalysis approach provided one example of a

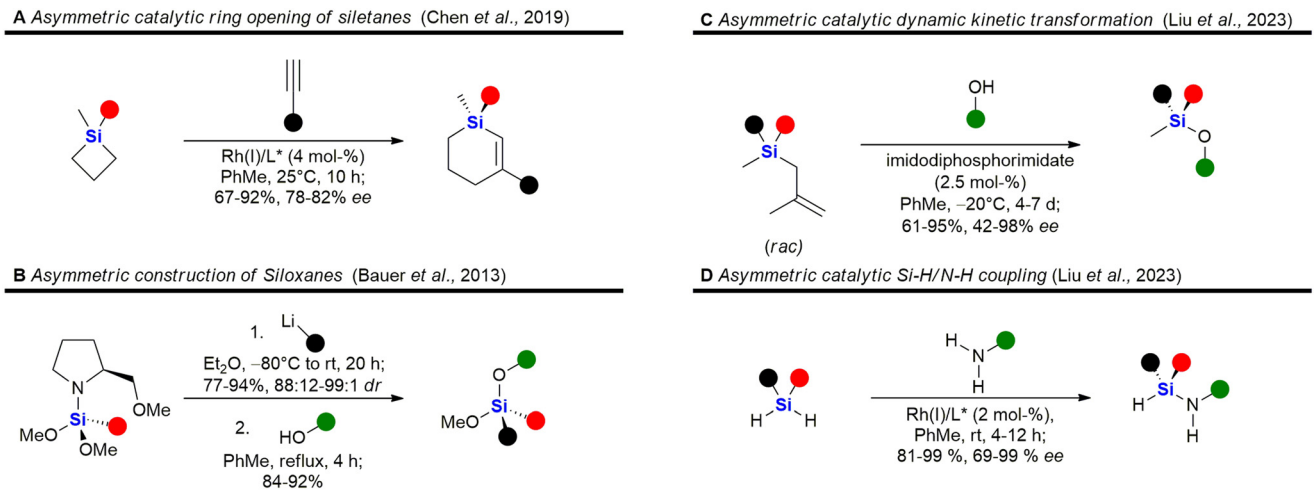

Fig. 6 Recent advances in the asymmetric synthesis of chiral silanes – examples A,[91] B,[92] C[93] and D.[94]

complex compound with such a structural motif (Fig. 4H).[86] In addition, see the following ref. 224 for the synthesis of siloxepanes by a Pd-catalysed ring-expansion of siletanes.

Fig. 5 shows some recent examples in the chemistry of silyl ethers, silanols and siloxanes. Derivatisation of natural products and known small molecule drugs by formation of silyl ethers is the most common approach to include silicon in biologically active molecules. Even though largely considered a standard procedure, new methods have been investigated.[195,196,225] A special focus has been laid on the asymmetric synthesis of silyl ethers. Park *et al.* reported the kinetic resolution of secondary alcohols by an organocatalytic silylation using hexamethylsilazane as a silyl source (Fig. 5A).[87] Later, a dynamic kinetic resolution was reported by Seliger *et al.* who employed a ruthenium-catalyst for the racemisation of secondary alcohols and a copper-catalyst for the asymmetric silylation (Fig. 5B).[88] Besides alcohols, silanediols can also be silylated in an asymmetric manner, as exemplified by Gao *et al.* who reported the desymmetrisation of silanediols with dihydrosilanes under Cu-catalysis (Fig. 5C).[89] This report also includes a few examples of a double desymmetrisation of both the silanediol and the dihydrosilane, resulting in disiloxanes with two silicon stereocentres. Disiloxanes are present in several biologically active molecules (*e.g.* Fig. 13 and 55). Numerous new methods for the oxidation of hydrosilanes to silanols, which possess interesting biological activities (*e.g.* Fig. 55, 63, 101, 104, 107 and 111), have been reported,[226–229] among these the enzymatic oxidation by Xu *et al.* under physiological conditions (Fig. 5D).[90]

A selection of recently developed methods for the asymmetric construction of silicon stereocentres[85,230–246] are shown in Fig. 6, yet only one example of a silicon-containing drug with a silicon stereocentre has been reported so far. Desymmetrisation of siletanes by a rhodium-catalysed sequence of ring-opening and carbosilylation of alkynes provides enantioenriched sila-cyclohexenes (Fig. 6A).[91] This methodology was later applied to the asymmetric synthesis of sila-mesembralon (Fig. 116). Prolinolmethyl ether was used as a chiral auxiliary in the desymmetrisation of dimethoxysilanes by nucleophilic attack of organolithium compounds (Fig. 6B). The auxiliary was cleaved by alcoholysis, which occurred under retention of configuration.[92] Very recently, a dynamic kinetic transformation of racemic methallylsilanes by an organocatalytic alcoholysis was disclosed (Fig. 6C).[93] Dihydrosilanes can also be desymmetrised by rhodium-catalysed dehydrosilylation of primary amines (Fig. 6D).[94]

The rest of this review summarises findings linked to the incorporation of silicon as a means of modifying both activity and pharmacokinetic parameters in drug-like molecules. These bioactive silicon-containing molecules will be briefly described in the specific fields of medicinal chemistry in which they have been applied, including cancer, anti-bacterial, anti-fungal, anti-viral, anti-inflammatory, cardiovascular and neurological diseases. Where appropriate, the presented organosilicon API's are contrasted against that of the non-silicon containing parent compounds which formed the basis for the silyl-derivation or carbon–silicon-switch, to allow the reader an understanding of how incorporation of silicon atom(s) has resulted in a modified molecule with new (and potentially improved) properties and/or bioactivity. The reader is further referred to earlier reviews and perspectives describing both the synthesis and biological evaluation of organosilicon compounds,[5,11,15,247–262] as well as some popular online science discussions that have highlighted the rather slow journey of silicon within the broader medicinal chemistry environment.[263–266] It should also be mentioned at this point that that focus of the rest of this review will be on medicinally-relevant "small molecules" and not on the broader area "silicon-based materials" which has also demonstrated significant value in modern medical therapeutics and devices.

Anti-cancer agents

The use of organosilicon compounds as anti-cancer agents can be traced back to the 1980's when Chiu *et al.* reported the use of silylated pro-drugs as potential anti-cancer agents.[267] These researchers examined the use of *N*- and

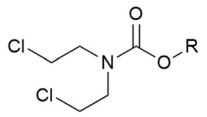

8

R = $SiMe_3$, $SiMe_2t$-Bu, $SiMe_2Ph$, $SiPh_2t$-Bu, $SiBn_3$, $Si(OEt)_3$

Fig. 7 *N*- and *O*-triorganosilylated compounds as potential pro-drugs for the treatment of cancer.

O-silylated compounds, that were related to various "mustard-like" anti-cancer drugs, as potential prodrugs (Fig. 7). In this research, several *O*-silylated carbamate derivatives **8** showed very good activity against P-388 lymphocytic leukaemia in mice.[267] Since then the carbon/silicon switch has received much attention as a means of designing compounds with high anti-tumour activity and low toxicity towards non-cancerous cells.

Bexarotene **9** is a retinoid X receptor (RXR)-selective retinoid agonist that is retailed under the brand name Targretin (Fig. 8). It is currently applied in therapies targeting cutaneous T-cell lymphoma and underwent phase III clinical trials for the treatment of non-small cell lung cancer,[268–270] albeit without broader success.[271] Retinoids are small molecule mimics of retinoic acid, a vitamin A metabolite. Retinoids have been demonstrated to function as retinoid X receptor agonists impacting the regulation of gene expression and thereby also cell differentiation and proliferation.[272] In comparison to carbon-based structural groups, the hydrophobic nature of silyl functional groups made them particularly useful for probing the chemical space associated with the hydrophobic retinoid pharmacophore.

In terms of an example, in 2005 Tacke and co-workers reported the agonist activity screening of a synthesized disila-substituted derivative **10**, in which a pair of carbon atoms of bexarotene **9** had been substituted with silicon.[273] Upon screening of **10** for agonist activity (involving a hRXR β cell-based luciferase assay), the researchers found that compound **10** had a comparable response when compared to bexarotene **9**. This research group have since also reported the synthesis of a structurally related disila-TTNPB analogue **11**, which was shown to act as a strong pan-RAR agonist. Compound **11** was also shown to display the same strong differentiation and apoptosis-inducing activity in NB4 promyelocytic leukaemia cells as its non-silyl source compound (Fig. 8)[274] (and other research involved the testing of these types of compounds against human pluripotent stem cells[275]). Interestingly, through *in silico* assessment of the electron densities of bexarotene **9** and disila-bexarotene **10**, Tacke and co-workers further showed in 2013 that the replacement of the carbon atoms with silicon atoms did not significantly influence the electronic structures of the molecules, or the RXR receptor activation.[26] Furthermore, the group also reported the synthesis and biological evaluation of disila-TTNN **12**, a powerful RARBγ-selective retinoid, where again, the carbon

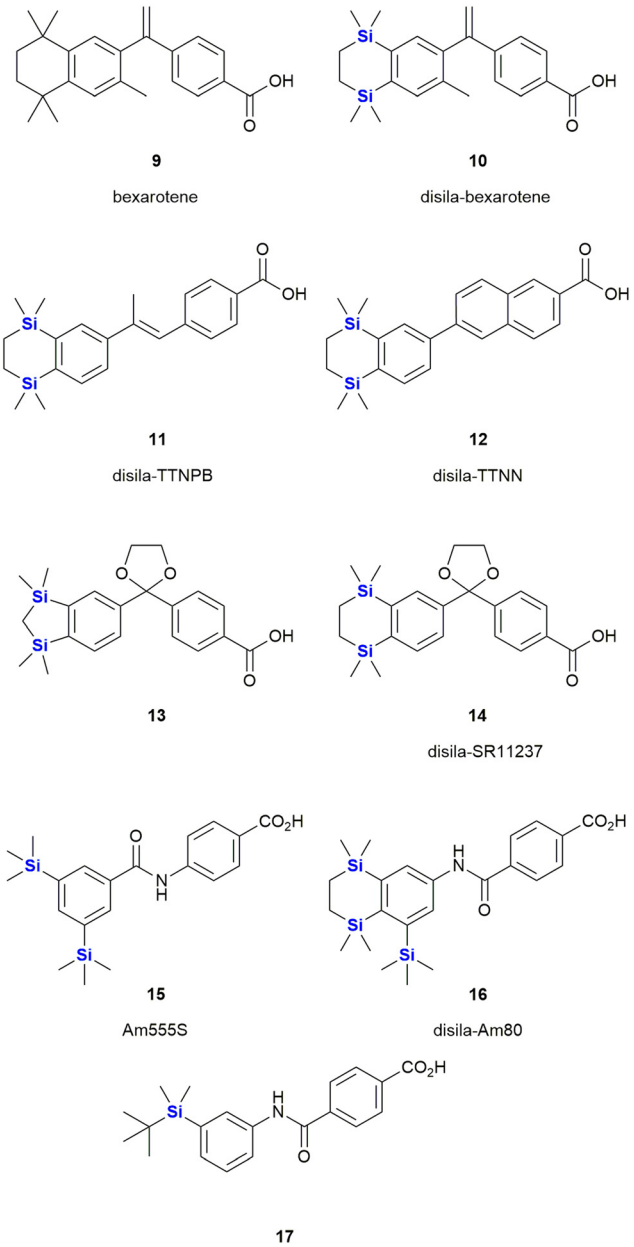

Fig. 8 Retinoid X receptor agonist bexarotene **9** and silicon-containing analogues.

silicon exchange afforded a novel compound with a significant increase in activity.[78]

In another report, the Tacke group reported the RXR agonists **13** and **14**. In both cases, there were slight, but reproducible improvements in the activity of these disila-compounds when compared to their respective carba-analogues.[276]

The Kagechika and Tacke groups further reported research on the retinoids Am555S **15** and disila-Am80 **16** respectively.[277,278] Am555S **15** had improved α-subunit activity and was evaluated in phase II clinical trials,[279] whilst disila-Am80 **16** had increased potency towards β- and γ-RAR relative to the analogous non-sila parent compound. Most

recently, Kagechika reported the synthesis and screening of several structurally related analogues. During this work the researchers also identified compound **17** which had an EC_{50} of 7.2 nM against the human acute promyelocytic leukaemia cell line HL-60 and which was 120 times more active than bexarotene **9** and showed strong selectivity towards RARγ.[280]

The Zablotskaya group have extensively studied the effect of modifying biologically active molecules through the incorporation of silicon groups.[281–292] Their research efforts have primarily focused on the development of neurological agents which are discussed later in this review; however, they have also reported the synthesis and biological evaluation of several potent anti-cancer agents. The Zablotskaya group's research has been driven by the hypothesis that the incorporation of silicon would potentially improve the biological properties of existing silicon-free active pharmaceutical ingredients (APIs) by increasing drug lipophilicity and therapeutic index, prolonging action, lowering toxicity and lowering therapeutic doses.

The group reported the positive influence of oxygen and nitrogen silylation, silyl alkylation, silyloxyalkylation and sila-substitution with regards to psychotropic and anti-tumour activity.[281] A review of the literature by the authors indicated that many synthetic anti-microbial APIs contain the structural ═N–C–C–O– sequence. The researchers thus undertook to study the structure activity relationships (SARs) of a range of trialkylsilyl substituents at the oxygen atom of various β-aminoethanol derivatives. The *in vitro* anti-tumour and anti-microbial properties of the novel compounds were studied and it was found that the silylmethiodide **18** showed high anti-tumour activity (IC_{50} 0.3 μg mL^{-1}) against HT-1080 (human fibrosarcoma) and NO-generation activity (IC_{50} 1 μg mL^{-1}) against MG-22A (mouse hepatoma) (Fig. 9) and also exhibited some anti-bacterial and anti-fungal activity.

In the same family, the silylmethiodid **19** showed comparable IC_{50} values of 3 μg mL^{-1} and 1 μg mL^{-1} against HT-1080 and MG22-A cell lines respectively (Fig. 9). In general, a more potent cytotoxic effect was observed with increasing bulk surrounding the silicon atom. In a subsequent report, these compounds were incorporated into novel water-soluble iron-oxide based magnetic nanoparticles which exhibited low to moderate cytotoxicity effects on tumour cell lines.[293]

In subsequent publications, the Zablotskaya group reported on the preparation and biological evaluation of a range of *N*-methyl-*N*-(2-triorganylsiloxyethyl)1,2,3,4-tetrahydro(iso)quinolinium iodide derivatives. The investigation of quinolone derivatives was driven by the fact that they commonly display a wide range of biological activities and are regarded as being "privileged" structures (Fig. 9).[282] Silylated derivatives showed improved cytotoxicity activity across the board when contrasted against the non-silylated parent analogues. The study also showed that the HT-1080 and MG-22A cell lines were highly responsive to the organosilicon substituents. Compound **20** displayed significant inhibition of HT-1080 and MG-22A cells when R_1, R_2, R_3 = C_2H_5, C_2H_5, C_2H_5 or CH_3, C_7H_{15}, C_7H_{15} with LC_{50} values of <1 and 1 μg mL^{-1} respectively and selective inhibition against MG-22A (LC_{50} 2 μg mL^{-1}) when R_1, R_2, R_3 = CH_3, CH_3, $C_{11}H_{23}$.

Zablotskaya and co-workers have continued with the development of silylated tetrahydroisoquinoline derivatives and most recently have reported the synthesis and biological evaluation of *O*-decyl substituted tetrahydroisoquinoline **21** and thiazolium organosilicon iodo salt **22**, which displayed LC_{50} values ranging from 0.1–0.2 μg mL^{-1} when screened against HT-1080, MG-22A and NIH 3T3 cell lines.[292] The silylated analogues possessed high NO generation abilities, which was absent in the unsilylated parent compounds; furthermore, the compounds were determined to be non-toxic, with LD_{50} values ranging from 200–1600 mg kg^{-1}.

Ignatovich and co-workers reported the synthesis of novel silicon-containing bisfuranes **23**, and their work included investigating the effect of the amine structure and the silicon atom's alkyl substituent with respect to the compounds' cytotoxicities (Fig. 10).[294] Cytotoxicity (IC_{50}) and toxicity (LC_{50}) were determined against two cancer cell lines, namely HT-1080 (human fibrosarcoma) and MG-22A (murine hepatocellular carcinoma), as well as normal NIH 3T3 (murine embryonic fibroblasts) cells, respectively. The researchers found that regardless of the amines utilized, the compounds exhibited moderate toxicity (174–360 mg kg^{-1}) and all derivatives with

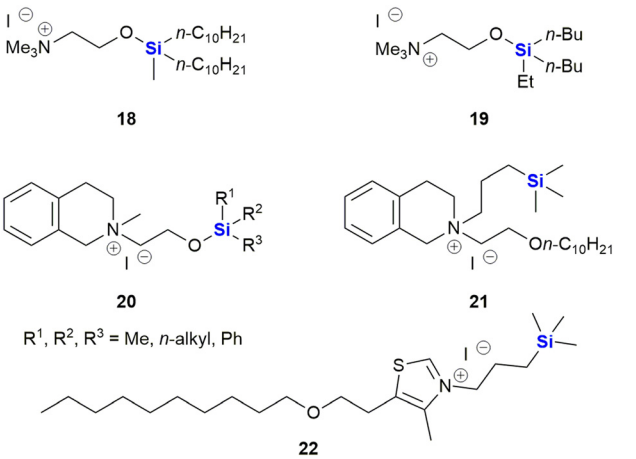

Fig. 9 Anti-cancer silyl ether derivatives of β-aminoethanols.

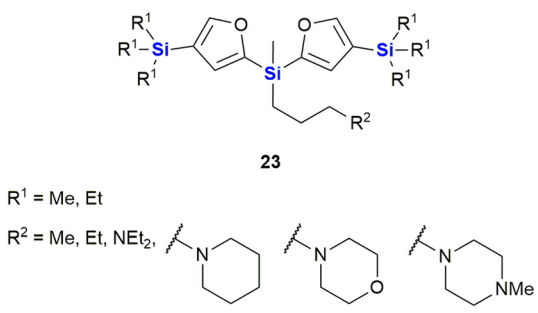

Fig. 10 Silicon containing bisfuranes **23** with anti-cancer properties.

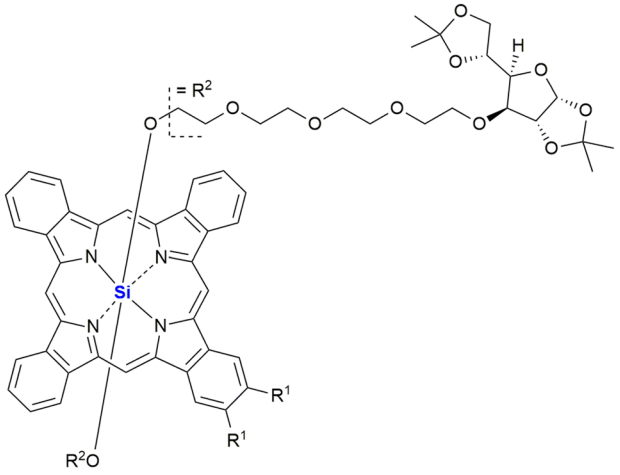

R^1 = H **24** or Cl **25**

Fig. 11 Novel glucoconjugated silicon(IV) phthalocyanines for photodynamic cancer therapy.

TMS substituents were more active than those with the corresponding TES substituents. The presence of an amine-containing group at position R_1 resulted in higher toxicity towards the normal NIH-3T3 cells, except for the morpholine group which showed low cytotoxicity across all three cell lines. Further studies on the morpholine-substituted derivative indicated that the introduction of the TMS group onto the furan ring greatly increased the cytotoxicity (3 μg mL^{-1} for HT-1080 and MG-22A cells). In contrast, examples with the TES group (no cytotoxic effect) or unsubstituted analogues were less active (100 μg mL^{-1} and 38 μg mL^{-1} for HT-1080 and MG-22A cell lines respectively).

In 2007, Lo and co-workers reported the synthesis of two novel glucoconjugated silicon(IV) phthalocyanines **24** and **25** (Fig. 11). Both compounds showed highly photocytotoxic activity against HT-29 (human colorectal carcinoma) and HepG2 (human hepatocarcinoma) cell lines, the most active being the non-chlorinated phthalocyanine **24** which demonstrated IC_{50} values as low as 6 nM.[295] It was proposed by the researchers that the chlorinated analogue **25** had reduced activity (IC_{50} 17–21 nM) due to a higher aggregation tendency in biological media, which in turn led to a decrease in the ability to form reactive oxygen species inside the cells. The non-chlorinated analogue **24** was also shown to have significant and selective affinity to lysosomes, but not mitochondria, of the HT-29 cells. The application of various thiophenic silicon phthalocyanines has received considerable interest as drug delivery systems for anti-cancer photodynamic therapy (PDT).[296–298] PDT allows the non-invasive treatment of malignant tumours through the employment of photochemical transformations which themselves are mediated by photosensitizers. Phthalocyanine derivatives are excellent photosensitizers; however, their planar geometry typically leads to molecular aggregation and often their hydrophobic nature prevents them from existing as monomeric dispersions in aqueous media.[299] In the latter case, strong collisional quenching of the molecules excited states

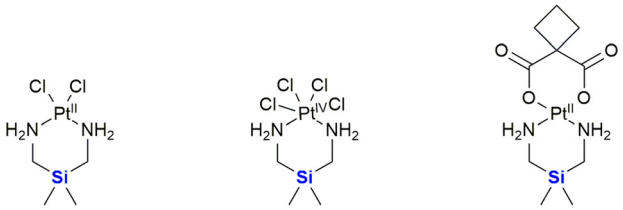

26 **27** **28**

Fig. 12 Silicon-containing-platin complexes of platinum(II) and platinum(IV) with anti-cancer activities.

occurs.[299] The use of silicon as a central atom helps overcome these issues as silicon can accommodate axial substituents preventing the formation of aggregates. Notably, Jaung, Jang and co-workers recently reported the development of non-aggregated photosensitisers for use as PDT agents.[299] In this instance the silicon-based photosensitisers were housed in carbohydrate-based block glycopolymer polymeric micelles, the use of polymeric micelles having been shown to enhance tumour localisation, permeation, and retention. For other representative examples of silicon phthalocyanines with biological application from the last decade, see the following references[300–312] and reviews.[313,314]

Following on from the clinical efficacy of *cis*-dichlorodiamineplatinum(II) (cisplatin), Anderson *et al.* prepared and assessed the anti-tumour activity of platinum(II) and platinum(IV) complexes with silicon containing diamines (Fig. 12).[315] Silaplatin **26** and the related platinum(IV) analogue **27** increased the life span of mice bearing intraperitoneally implanted murine L1210 leukaemia by 109–248% (**26**) and 115–214% (**27**) at doses of 10–40 mg kg^{-1}. Furthermore, the platinum(II) complex **26** showed high activity against a cisplatin-resistant L1210 cellular subline (35–98% at doses of 5–30 mg kg^{-1}) which compared favourably to the activity of cisplatin (8% at 10 mg kg^{-1}). A related cyclobutanedicarboxylic acid complex **28** showed activity against both cisplatin-sensitive (22–77% at doses of 10–40 mg kg^{-1}) and -resistant (7–41% at doses of 10–40 mg kg^{-1}) L1210, but was less potent than the dichloro analogue **26.**

SILA compounds 409 **29** and 421 **30** were patented in 1999 by Hegyes and co-workers and were shown to act as resistance modifiers against multidrug-resistant cancer cells through the

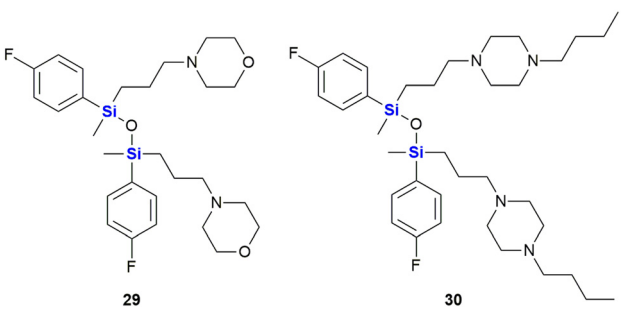

29 **30**

Fig. 13 Anti-proliferative SILA compounds 409 **29** and 421 **30**.

inhibition of cellular efflux pumps (Fig. 13).[316,317] These compounds were demonstrated to have anti-proliferative effects without the induction of apoptosis (although other researchers saw increased apoptotic activity)[318] and initial results indicated that these SILA derivatives specifically acted on the MDR1 p-glycoprotein 170 and subsequent investigations suggested further effects on cell-proliferation and viability.[319] Later, it was shown that the same compounds had moderate potential to prevent the formation of tumours caused by carcinogenic chemicals or the Epstein–Barr-virus[320] and increase the sensitivity of adenocarcinoma cells LoVo/Dx cells to doxorubicin.[321]

Thompson *et al.* described the isolation and structures of two potent anti-viral and anti-tumour compounds, mycalamides A **31** and B **32**, which were isolated from the New Zealand sponge *Mycale* sp.[322] Apart from acyl and alkyl derivatives, several silyl derivatives **33** were prepared to further explore the biological properties of these compounds (Fig. 14).

The TMS ethers were found to all be active against the murine leukaemia P388 cell line (IC_{50} = 0.1 to 1.3 ng mL^{-1}), though it is postulated that the TMS ethers were simply hydrolysing back to the active parent compounds (IC_{50} 0.07 to 0.5 ng mL^{-1}). The bulkier, less labile, TBDMS ethers showed a marked decrease in activity (IC_{50} = 23 to >12 500 ng mL^{-1}) relative to the parent compounds.

Members of the combretastatin family have been demonstrated to potently inhibit microtubule activity through tubulin-binding at the colchicine site, and in doing so interrupting cell growth and proliferation.[323] Combretastatin A-4 **34** showed the strongest anti-tumour cell growth-inhibition (IC_{50} = 0.004 μM) in an MCF-7 (breast cancer) cell proliferation assay. It also acted as a vascular disrupting agent (VDA) reducing blood flow and leading to tumour cell death (Fig. 15). Nakamura *et al.* reported the synthesis of silicon-containing combretastatin analogues **35** in which the ethene linker was replaced with a silicon bridge, thereby affording analogues in which the distance between the two ring systems remained almost unchanged (3.00 Å *vs.* 3.04 Å for the silyl-analogues). One of the compounds, **35**, which contains a $Si(CH_3)H$ linker, exhibited potent inhibition of tubulin polymerization, as well as significant cancer cell growth inhibition (IC_{50} = 0.007 μM) in an MCF-7 cell proliferation assay.[324]

In addition, this compound also prevented [^{3}H]colchicine binding (~91% inhibition at 3 μM) and the researchers surmised that these biochemical characteristics were comparable to that of combretastatin A-4 **34**. Furthermore, the silicon-containing analogue **35** showed improved physio-chemical stability. The authors therefore proposed that the silicon linker could thus act as a bioisostere of a *cis* alkene bond.

In a continuation of their work looking at diphenylsilanes as a *cis*-stilbene mimetics, Fujii and co-workers also turned their attention to investigating whether silyl groups could also mimic aliphatic *cis*-olefins (Fig. 16).[325] During this research, series of silylated oleoylethanolamide derivatives were prepared (which included compounds **37** and **38**), based upon a known endogenous *cis*-olefin-containing peroxisome proliferator-activated receptor PPARα agonist **36** (ref. 326) and evaluated in terms of their PPAR α/β/γ agonistic activities, as PPARγ agonists not only do they act as insulin sensitizers but they also possess anti-proliferative activity.[327] To this end, the design rationale revolved around the fact that the silicon-containing compound would mimic the *cis*-alkene functional arrangement. From molecular orbital calculations it was demonstrated that the distance between the carbons with a silicon bridge was similar to that of the two carbons in a *cis*-relationship (3.132 *vs.* 3.214 Å). In comparison, two carbons linked by a carbon bridging atom would according to the modelling have a significantly smaller distance between them of 2.579 Å. In terms of interesting

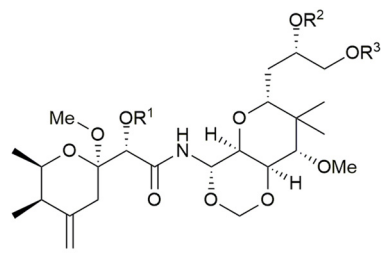

Fig. 14 Mycalamide A **29** and B **30** and silyl ether derivatives **31** with anti-cancer properties.

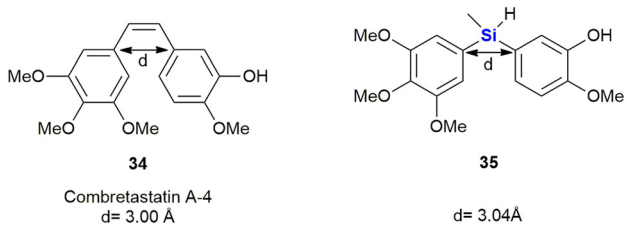

Fig. 15 Combretastatin A-4 **34** and silicon analogues **35**.

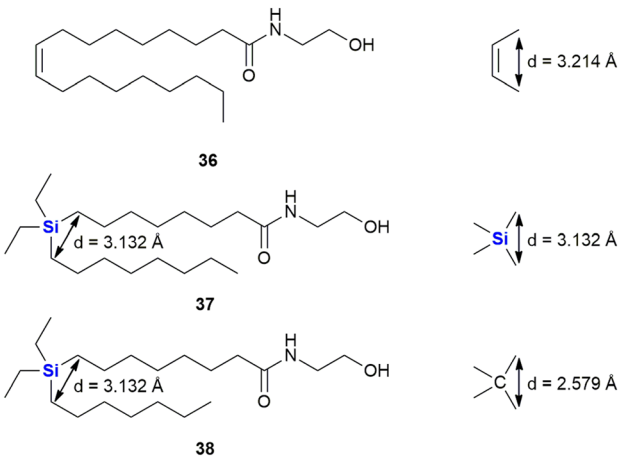

Fig. 16 The use of silyl groups as mimics of aliphatic *cis*-olefins.

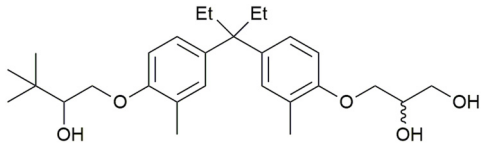

39

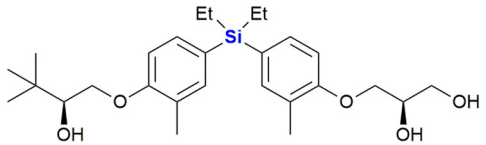

40

Fig. 17 Non-secosteroidal vitamin D mimic LG190178 **39** and sila-analogue **40**.

outcomes, the diethylsilyl derivative **37** was found to exhibit PPAR α/δ agonistic activity while the related compound **38** was demonstrated to be a PPARδ-selective agonist.

The same researchers further reported the synthesis of bisphenol analogues possessing vitamin D receptor (VDR) agonistic activity and androgen receptor (AR) antagonistic activity (Fig. 17).[328] The researchers observed that the replacement of the quaternary carbon linker in the known non-secosteroidal vitamin D mimic LG190178 **39** (ref. 329) with silicon, increased the compound's AR antagonistic activity, but reduced its VDR-agonistic ability. The results thus represented the first example of a nuclear receptor (NR) selectivity switch by carbon–silicon substitution. Of note was that the most potent AR-selective analogue **40** inhibited the testosterone-induced growth of murine mammary carcinoma cell line SC-3 cells more efficiently (IC_{50} = 0.072 μM) than the well-known androgen antagonist hydroxyflutamide (IC_{50} = 1.4 μM).[328,330]

In another study, Maruyama *et al.* investigated the SARs of bisphenol analogues as oestrogen receptor antagonists, potential drug candidates for the treatment of oestrogen-sensitive breast cancer (Fig. 18). The bisphenol **41** was identified as a potent antagonist of oestrogen receptor ERα (IC_{50} = 25 nM) and less so of ERβ (IC_{50} = 260 nM). Its sila-analogue **42** however was less potent against both ERα (IC_{50} = 72 nM) and ERβ (IC_{50} = 800 nM).[328]

Steroidsulphatase (STS) plays a crucial role in the oestrogen synthesis of postmenopausal women and is therefore a possible target for postmenopausal hormone-dependent breast cancer therapy. Although several steroid-based STS inhibitors are now known, these compounds have been found difficult to optimize and have the potential to

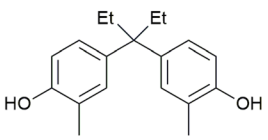

41

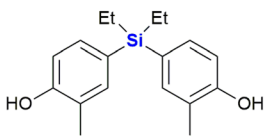

42

Fig. 18 Bisphenol **41** and sila-analogue **42** as oestrogen receptor antagonists.

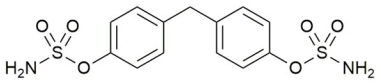

43

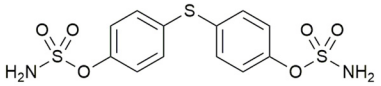

44

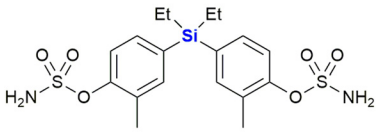

45

Fig. 19 Bis-phenol sulphonamides **43**, **44** and **45** as STS inhibitors.

interact with other targets. While investigating this challenge, Kajita *et al.* postulated that diphenylmethanebisphenol derivatives would potentially bind to the ligand-binding domain (LBD) of oestrogen receptors like attributed to oestradiol, thereby acting as a steroid proxy molecule (Fig. 19). The silicon linked bisphenol **45** showed an inhibitory activity of STS (IC_{50} = 170 nM) between that of the carbon analogue **43** (IC_{50} = 1024 nM) and the sulphur analogue **44** (IC_{50} = 88 nM). Upon hydrolysis of the sulphonamide moiety, these inhibitors would liberate bisphenol metabolites which might possess oestrogen receptor antagonistic properties (*vide supra*). Hydrolysis of the sulphonamide groups of **45** by STS generates the metabolite **42** (Fig. 18) which possess antagonistic properties against oestrogen receptor ERα, thus adding to the anti-proliferative properties of **45** against breast cancer cells. In contrast, the metabolites of carbon analogue **43** and sulphur analogue **44** possessed weak agonistic properties against ERα, which is unwanted as it might promote the growth of breast cancer cells.[331]

In 2014, Trindade and co-workers reported an NHC-catalysed umpolung reaction between 5-hydroxymethyl furfural (HMF) derivatives and diazo compounds affording a set of HMF-substituted acylhydrazones which exhibit anti-tumour activity (Fig. 20).[332] Upon screening of various HMF derivatives to determine their anti-proliferative activities

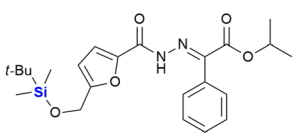

46

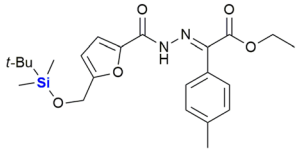

47

Fig. 20 Silicon-containing acylhydrazones displaying anti-tumour activity.

against HT-29 (colon), MCF-7 (breast), NCI-H460 (lung) cancer cell lines, it was observed that the hydroxyl and *O*-benzyl derivatives displayed insignificant activity. However, the respective TBDMS derivatives were shown to be active against MCF-7 cell lines with IC_{50} values as low as 3.5–7.29 μM. It was postulated that the TBDMS group increased the lipophilicity of the compound, and that this aided in the biological activity. Interestingly, the two most active compounds, **46** (IC_{50} 3.60–6.37 μM) and **47** (IC_{50} 3.50–7.29 μM), displayed the lowest toxicities towards differentiated CaCo-2 (colon cancer) monolayer cells at IC_{50} values of 40.12 and 27.90 μM respectively.

In 2005, Padrón and co-workers described research in which it was demonstrated that incorporation of the TBDMS group onto small molecules could positively modulate their cytotoxicity against human-based tumour cells.[333] In this work, the researchers synthesized a set of enantiomerically pure (2*R*,3*S*)-disubstituted tetrahydropyrans **48** and **49** bearing a variety of diverse functionalities (Fig. 21). In addition to the TBDMS group, other common hydroxyl functionality protecting groups were utilized (including allyl, acetate and benzoate groups – not shown). The compounds were subsequently screened *in vitro* against HL-60 human leukaemia cells and MCF-7 human breast cancer cells. Significant observations included that the synthetic derivatives bearing the TBDMS group at tetrahydropyran ring position 3 elicited considerable cancer cell cytotoxicity.[333] When the SAR of the set of molecules was evaluated, the results indicated that the TBDMS group should not only be seen as a functional protecting group for organic synthesis, but that it could also be utilized as part of a plausible strategy to introduce lipophilicity in drug-like molecules.

This increased lipophilicity was anticipated to aid in the cellular uptake of the TBDMS-containing molecules and thus to potentially modulate their cytotoxic activity. The Padrón group furthermore investigated this enhanced drug cytotoxicity by further *in vitro* screening of the aforementioned compounds and some other derivatives against a range of solid tumour cell lines, namely: T-47D

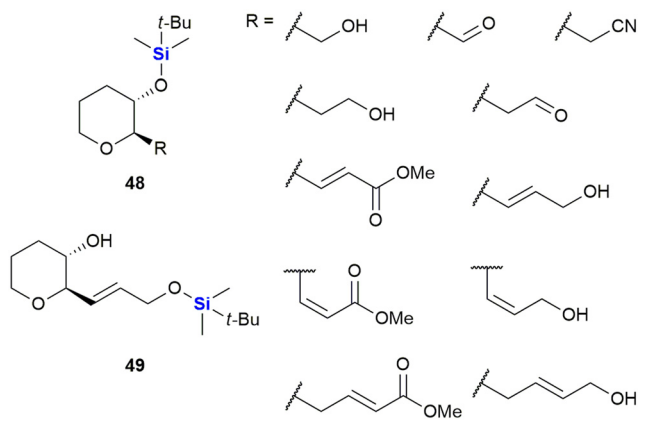

Fig. 21 Silyl-(2*R*,3*S*)-disubstituted tetrahydropyrans with anti-cancer properties.

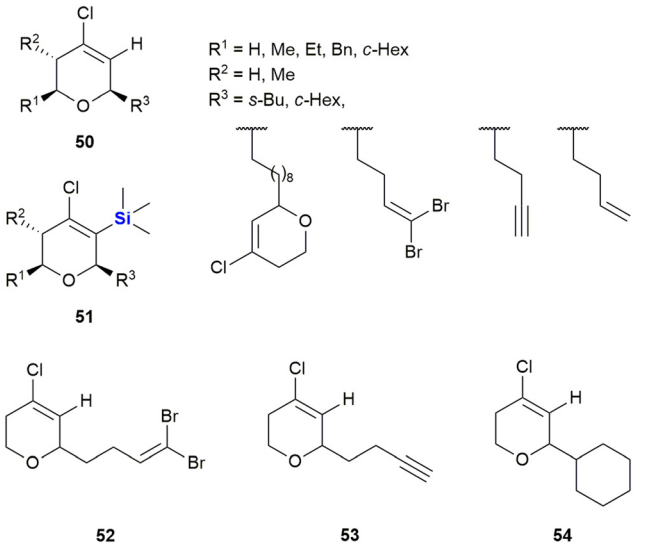

Fig. 22 Chlorovinyl-TMS dihydropyrans displaying anti-proliferative activity against human solid tumour cell lines.

(breast cancer), HeLa (cervix cancer), SW-1573 (non-small cell lung cancer), WiDr (colon cancer) and A-2780 (ovarian cancer) cells. The results obtained were published the following year (2006) and supported the conclusions from the original paper.[334]

In 2007, the same authors extended the tetrahydropyran scaffolds to structurally similar chlorovinyl-TMS containing dihydropyrans which were prepared and assessed for anti-proliferative activity against human solid tumour cell lines A-2780 (ovarian cancer), SW-1573 (non-small cell lung cancer) and WiDr (colon cancer).[335] The non-sila parent compound **50** showed no growth inhibition against the human solid tumour cell lines; however, in general the silylated analogues **51** showed an enhancement in cytotoxicity (Fig. 22). The introduction of the TMS group at position 3 of the oxacyclic ring system in general improved activity against all the cell lines screened. When compared against previously reported cytotoxic non-sila alkyl chloro dihydropyrans (**52**, **53** and **54**) the sila analogues showed improved activity when R^3 was a cyclohexyl or but-3-ynyl group.

Growth inhibition against A-2780 and SW-1573 cell lines was generally better (17–34 μM) than that of WiDr cells (15–67 μM). Notably, in the case of the non-sila analogues **53** and **54** no inhibition was observed against the WiDr cells.

Saeeng and co-workers have reported the synthesis of novel C-19-analogues of andrographolide **55**, a major diterpenoid from *Andrographis paniculata* with potent cytotoxic activities.[336] SAR studies showed that the incorporation of a silyl ether or triphenylmethyl ether group at the C-19 position increased toxicity against various cancer cells such as P-388 (leukaemia), KB (oral), COL-2 (colon), MCF-7 (breast), LU-1 (lung) and ASK (rat glioma) (Fig. 23). Seven of the ten sila-analogues showed improved activity across all cells lines relative to the parent compound **55**. The most potent sila-analogues **56** and **57** displayed effective

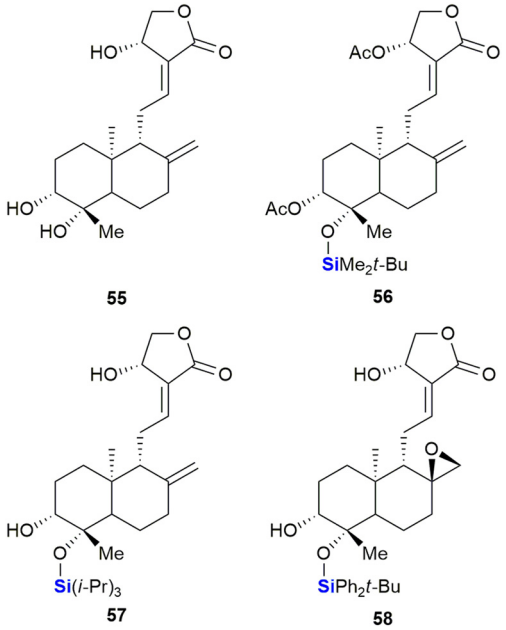

Fig. 23 Andrographolide **51** and silyl ether derivatives with potent cytotoxic activities.

inhibitory doses ranging from 0.34–3.62 μM and 0.88–3.01 μM respectively. The activities against P-388 (0.34–0.88 μM) and ASK (1.22–2.85 μM) cells were better than that of the potent anti-cancer drug ellipticine which gave values of 2.44 and 3.56 μM. Against the remaining cell lines activities were comparable. The authors hypothesized that the improved activity of the silylated compounds was potentially due to the bulky silyl groups at the C-19 position aiding in transport across cellular membranes.

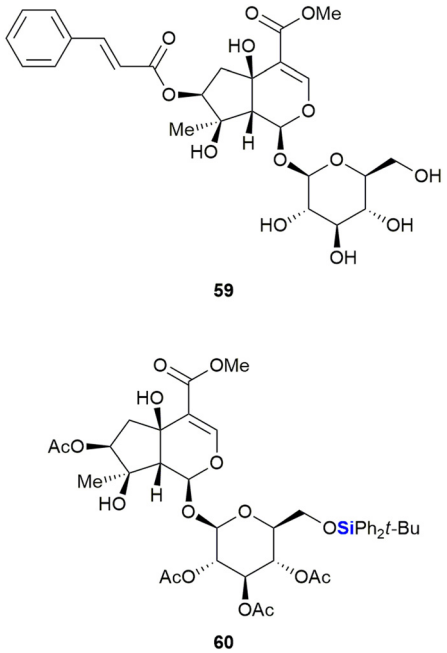

Fig. 24 Durantoside I **59** and silyl ether derivative **60**.

Thereafter, the group reported the identification of exo-epoxide-containing **58**, which was shown to be highly cytotoxic against CHO (Chinese hamster ovary), HepG2 (liver), UISO-BCA1 (breast) and HeLa (cervix) cancer cells,[337] by inhibiting the activity of Topo-IIα.[336,338] In further studies, compound **58** was shown to function by targeting the Wnt/β-catenin/GSK-3β pathway in HT-29 colorectal cancer cells.[339]

The Saeeng group also reported the isolation and derivatisation of durantoside I **59** from *Citharexylum spinosum* L. (Fig. 24).[340] During their studies it was noted that removal of the cinnamate group at position C-7 and silylation of the sugar group afforded the most active compounds. The TBDPS ether **60** proved most active of the compounds synthesized, with an ED_{50} of 8.2–9.19 μM against the MCF-7 (breast), A-549 (lung) and ASK (rat glioma) cancer cell lines. In contrast, durantoside I **59** showed no appreciable activity against the cancer cell lines.

The iridoids, catalpol **61** and 6-epi-catalpol **66** (Fig. 25), showed significant inhibition of *Taq* DNA polymerase, with

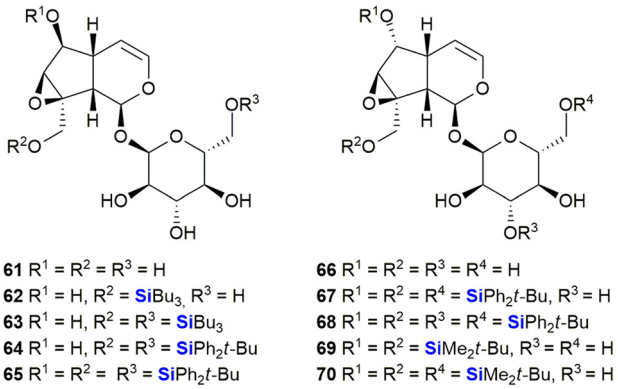

Fig. 25 Catalpol and 6-epi-catalpol silyl ethers.

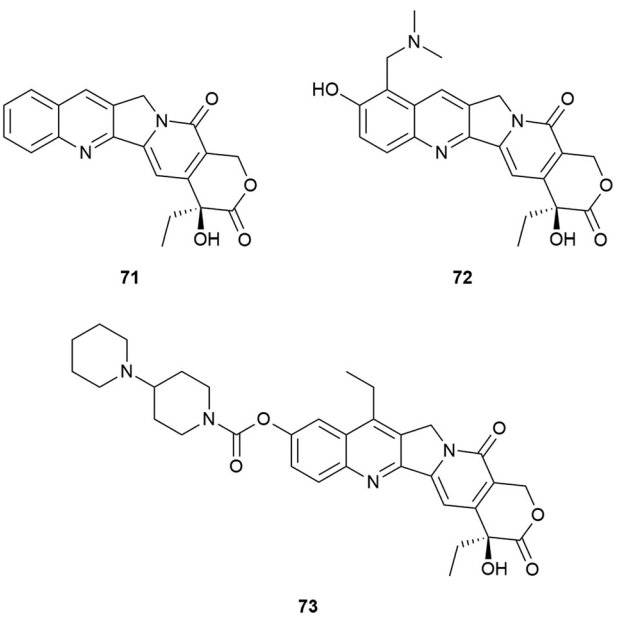

Fig. 26 Camptothecin **71**, topotecan **72** and irinotecan **73**.

IC_{50} values of 48 μM and 22 μM, respectively. Padrón *et al.* subsequently synthesised catalpol silyl ether derivatives **62–65** and investigated their anti-proliferative activity against several solid tumour cell lines.[341] The bioactivity results indicated that all the silyl ethers were significantly more active than the parent compound or related ester derivatives. As an example, compound **65** inhibited the growth of tumours by 50% at concentrations of 1.8–2.7 μM. Later, Garro, Pungitore *et al.* investigated the silyl ether derivatives **67–70** of 6-epi-catalpol.[342] In terms of this set of compounds, **67–68** showed no inhibition of *Taq* DNA polymerase, while **69** was slightly active. Of interest was that only TBDMS-derivative **70** showed promising activity (IC_{50} = 5.57 μM).

Camptothecin (20*S*)-**71** is the forerunner of a set of well-known anti-tumour therapeutics that has been the focus of new cancer treatments. The closely related topotecan **72** was approved for curative use in the USA whilst the prodrug irinotecan **73** was similarly approved as parts of anti-cancer therapy in the USA, France and Japan.[343,344] In addition, a number of other camptothecin-related drugs have provided promising *in vivo* results and have been in various stages of clinical trials (Fig. 26).[345,346]

With respect to the synthesis of camptothecin derivatives and analogues, the Curran research group developed an innovative cascade radical annulation route, in order to obtain a range of novel substituted (20*S*)-7-silylcamptothecins (which were given the general name of the "silatecans").[347] During the same research, a series of unsubstituted 7-silylcamptothecins were also prepared using established Friedlander synthetic methods. A selection of these derivatives (**74–78**), all containing one or more TMS substituents on the camptothecin skeleton, are depicted in Fig. 27. The synthetic camptothecin derivatives were all tested in terms of their abilities to inhibit the growth of HL-60 (human promyelocyticleukaemia), 833 K (human teratorcarcinoma) and DC-3F (hamster lung) cells *in vitro*. The researchers observed that the newly synthesized compounds were at least equipotent, with some eliciting even more impressive growth inhibitory activity than camptothecin **71**. This outcome was particularly impressive because even by current standards, the anti-cancer activity of camptothecin **71** is still regarded as a challenging benchmark, not easy to eclipse.

Of interest was that the cellular results demonstrated that the TMS-camptothecin derivatives are also highly active. TMS-bearing **74** showed surprising *in vivo* chemotherapeutic outcomes (demonstrated by way of tumour volume reduction against sarcoma-180 in B6D2F1 mice) compared to camptothecin **71**.[347] Compound **75** showed a comparable anti-tumour effect to camptothecin **71**, when evaluated on Lewis lung carcinoma, albeit at a four-fold lower dose. These *in vitro* results indicated the significant promise this class of compounds was expected to have in terms of *in vivo* activity, though only limited *in vivo* data has been published. Compounds **74** and **75** were superior to camptothecin **71** when tested against Lewis lung carcinoma and sarcoma-180 tumour models in murine xenografts.[348]

The Burke group introduced the camptothecin derivative silatecan **79**, which showed potent activity in the National Cancer Institute (NCI) cytotoxicity screen with an average tumour growth inhibition of GI_{50} = 21 nM (Fig. 28).[349] While the activity of camptothecin against MDA-MB-435 S human breast cancer cells dropped significantly in the presence of humane serum albumin (from IC_{50} = 15 nM to IC_{50} = 375 nM), **79** largely retained much of its activity (with a change from IC_{50} = 14 nM to IC_{50} = 90 nM). The *in vivo* potency of **79** was subsequently proven by the successful treatment of U87

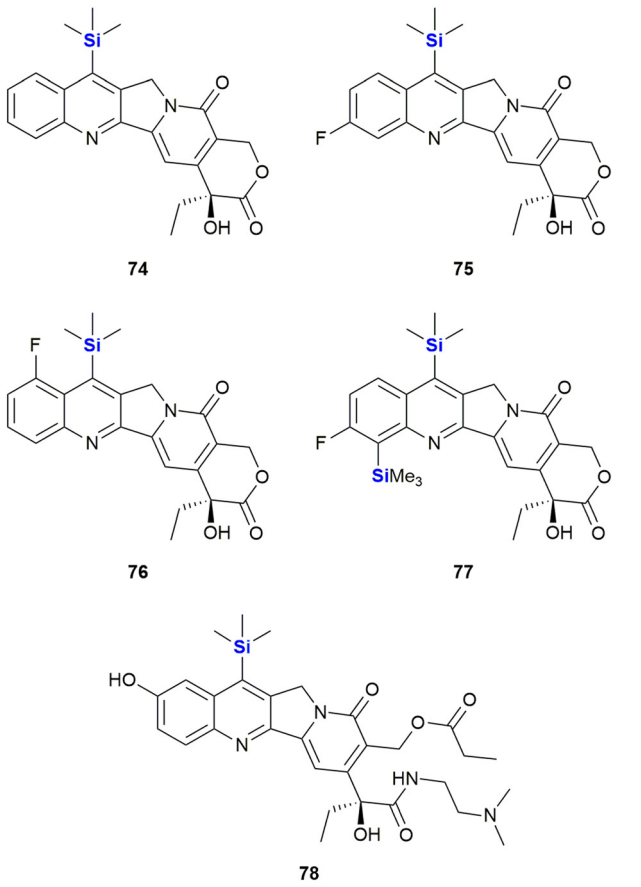

Fig. 27 A selection of further silylcamptothecins.

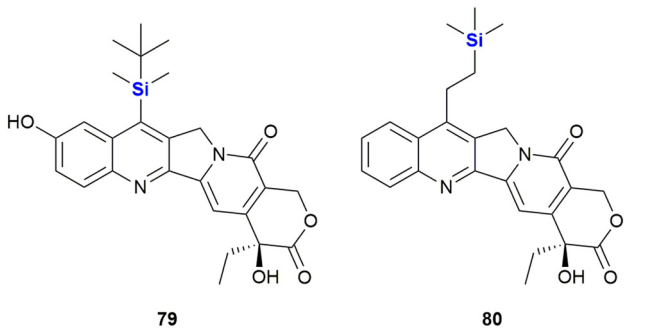

Fig. 28 Silatecan **79** and karenitecin **80**.

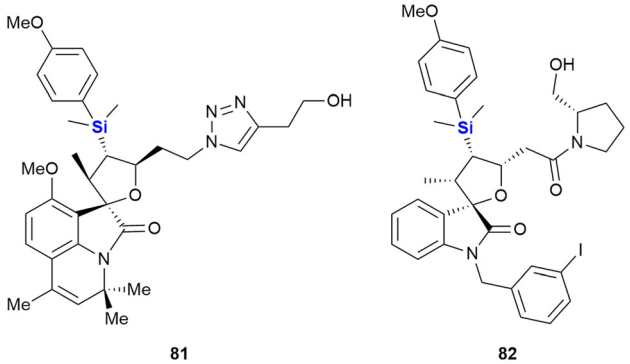

Fig. 29 Anti-cancer spiro-oxindoles with silyl groups.

subcutaneous glioma and intracranial glioma in murine xenografts at a dose of 30 mg kg^{-1}.

During the investigation of more effective camptothecin derivatives, van Hattum *et al.* synthesized and investigated karenitecin **80** (Fig. 28).[350,351] It was determined that the lipophilic silylated side chain increased oral bioavailability and stability of the active lactone form, probably due to stabilisation by alpha-1 acid glycoprotein,.[352] In addition, the structural modification provided resistance to metabolic conversion. Karenitecin was shown to be less susceptible to tumour-mediated drug resistance mechanisms and showed potent activity against ovarian (IC_{50} = 1.8–2.2 nM) and colon cancer cell lines (IC_{50} = 1.5–3.2 nM). It also showed promising results in phase I and II clinical trials for the treatment of refractory melanoma.[353,354] Finally, for a review on the important topic of silylated analogues of camptothecin and their value as anti-cancer agents. See the following ref. 355.

Schreiber and co-workers performed the synthesis of a diverse range of small organosilicon molecules and then evaluated their cellular activity profiles. As part of this research the authors developed a general method for the annulation of isatins allowing for the preparation of a range of spiro-oxindoles (Fig. 29).[356] As an outcome, the results of ninety representative compounds from 41 diverse assays were profiled, all with the goal of evaluating the potential of organosilicon-containing compounds as cellular process modulators. A wide range of activities for organosilicon-containing small molecules was demonstrated and representative examples were subjected to secondary screens for dose-dependent activity and EC_{50} determination. Activities of selected examples against lung adenocarcinoma (A-549) and hepatocellular carcinoma (HepG2) included EC_{50} inhibition of 42.8 μM and 32.5 μM for silyl-containing triazole **81** and 16.6 μM for the HepG2 assay in the case of pyrrolidine **82.**

Indomethacin **83**, a non-steroidal anti-inflammatory drug (NSAID) has been utilized in treatments for rheumatoid arthritis, ankylosing spondylitis and osteoarthritis (Fig. 30). Indomethacin **83** has also shown promise in the treatment and prevention of human cancers;[357–360] however, the observance of severe side-effects unfortunately limited its application in the treatment of cancer patients. In research performed by West and co-workers, aimed at improving the safety profile and biocellular activity of indomethacin **83**,[361] the design, synthesis and testing of a series of sila-substituted indomethacin derivatives **84–86** was performed.

In terms of cellular testing against the human MiaPaCa-2 pancreatic cell line, it was found that the cell growth inhibitory activity for the sila-indomethacin derivatives **84–86**

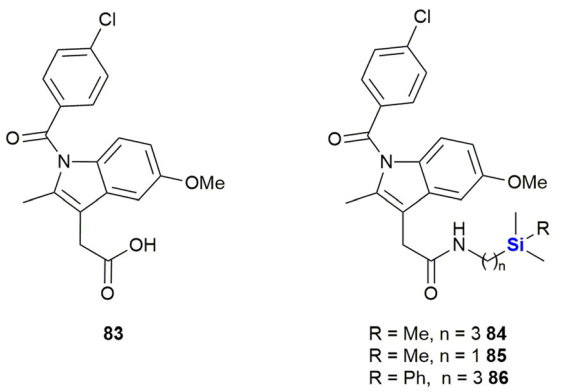

Fig. 30 Indomethacin **83** and silicon containing derivatives.

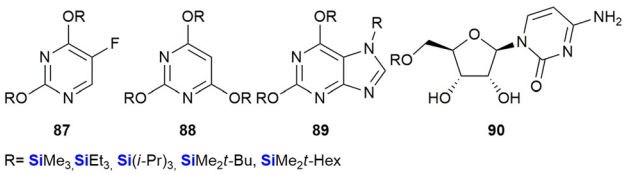

Fig. 31 Anti-cancer silyl ether derivatives of heterocyclic bases and uridine.

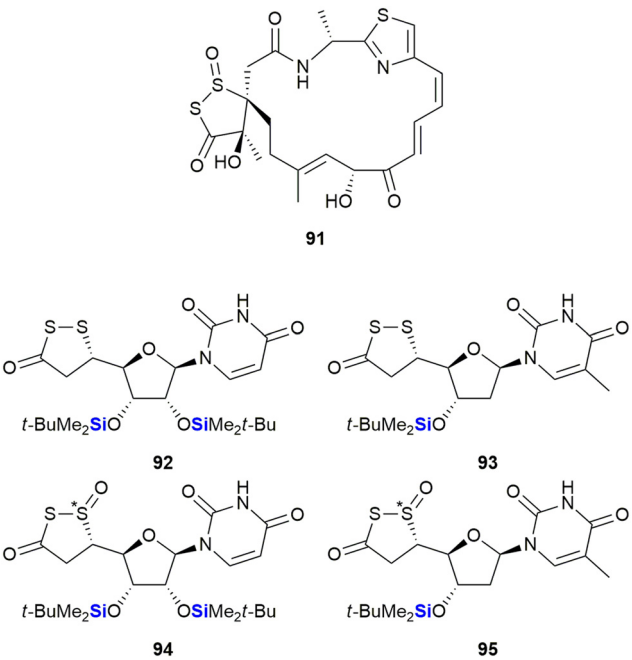

Fig. 32 Leinamycin **91** and sila-leinamycin mimetics (note that the stereochemistry of the silatrane unit was not given in the original publication).

was indeed significant (indomethacin **83** was previously shown to have an IC_{50} value of 170 μM against the same cell line). The West research group demonstrated that their novel sila-indomethacin derivatives had IC_{50} values of 4.78–20.0 μM in the *in vitro* assays.[361] Further *in vitro* pharmacology enzyme assays determined that the sila-indomethacin derivatives **84** and **86** were selective COX-2 inhibitors that were in essence superior to indomethacin **83** in this regard.

In a paper by Lukevits and co-workers the biological implications of *in vitro* silyl-removal processes involving triorganosilyl derivatives of some biologically active heterocyclic bases (including 5-fluorouracil **87**, barbituric acid **88** and xanthine **89** and uridine **90** derivatives), was investigated.[362] The researchers found that temporarily masking hydrophilic functional groups on small molecules appeared to have a significant effect on their biological activities. For example, in contrast to the pyrimidine nucleoside uridine, TBDMS-protected uridine **90** (R = $SiMe_2t$-Bu) inhibited the development and proliferation of HT-1080 (fibrosarcoma in human lungs – 96% inhibition at 100 μg mL^{-1}) and NiH 3T3 cells (fibroblasts in mice – 95% inhibition at 100 μg mL^{-1}) in cell culture experiments (Fig. 31).

This type of impact was also recognized in research performed by Herczegh and co-workers who synthesised a series of leinamycin mimetics (**92–95**) by introducing the biologically active 1,2-dithiolan-3-one-1-oxide moiety of leinamycin **91** onto an aldehyde-D-arabinose coupled to a uridine or methyluridine fragment (Fig. 32).[363] In doing so the researchers noted that the lipophilic silyl group derivatives **92** and **94** demonstrated improved cytotoxic activities against HeLa3 cervix tumour cells (IC_{50} = 3.68–10.04 μM) when compared to the analogues without the silyl groups (IC_{50} = 50.71–62.23 μM). The desoxythymidine derivatives **93** (no IC_{50} determined) and **95** (IC_{50} = 43.12 μM) were less active.

A further example of a silyl nucleoside derivative demonstrating anti-cancer activity was reported by Fenlon and colleagues in 2002.[364] This research involved the synthesis and anti-cancer screening of a set of 3′-*O*-silatranylthymidines (Fig. 33). The diastereomeric mixture of 3′-*O*-(trimethylsilatranyl)thymidine **96** was evaluated *versus* human breast (MDA-MB-435) and central nervous system (CNS) (SNB-19 and U251) cancer cell lines at a concentration of 0.1 mM over 48 hours. The researchers found that the growth percentages of cells treated with compound **96** were as follows: (i) breast cells 54% and (ii) CNS cells 83%, when compared to untreated control cells (where growth was taken to equal 100%). When compared to the closely related silatranylthymidine **97**, activity was absent in the CNS and lung cells, while 81% growth was observed in the breast cell line (correlating to 19% inhibition). It should be noted that **96** is a mixture of four diastereomers, and it would thus be expected that each diastereoisomer would have a unique activity, given that stereochemistry influences pharmacological activity.[364] The researchers thus reported that work on the synthesis and screening of each of the individual diastereomers was ongoing. More recently, Ye and co-workers reported structurally similar analogues wherein the sugar moiety was replaced with a γ-amino group.[365] The 5-fluorouracil derivative **98** was the most active silatrane derivative of a nucleobase identified in this study and was assayed against human breast (MDA-MB-435, IC_{50} = 17.1 μM), cervix (HeLa, IC_{50} = 18.3 μM) and intestinal (HT-29, IC_{50} = 11.6 μM)) cancer cell lines.

In 2016, van Otterlo and co-workers evaluated the application of novel nucleoside derivatives to induce apoptosis and cell death in two colorectal adeno-carcinoma cell lines, namely Caco-2 and HT-29.[366] As part of this

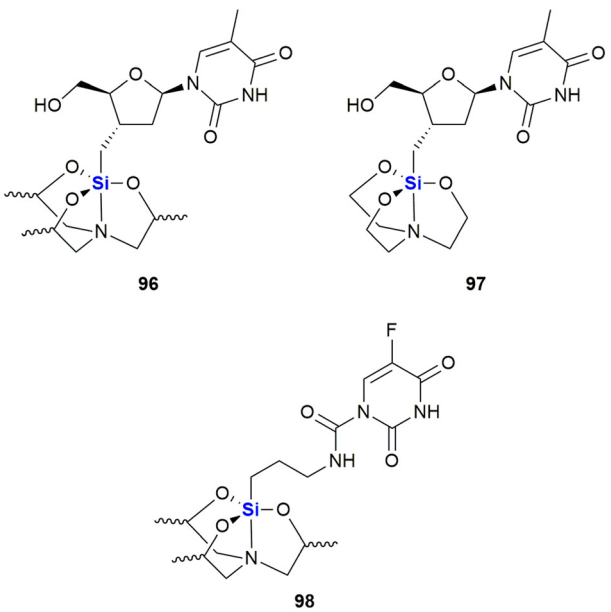

Fig. 33 Silatrane modified thymidines which possess anti-cancer activity (note that the stereochemistry of the silatrane unit was not given in the original publication).

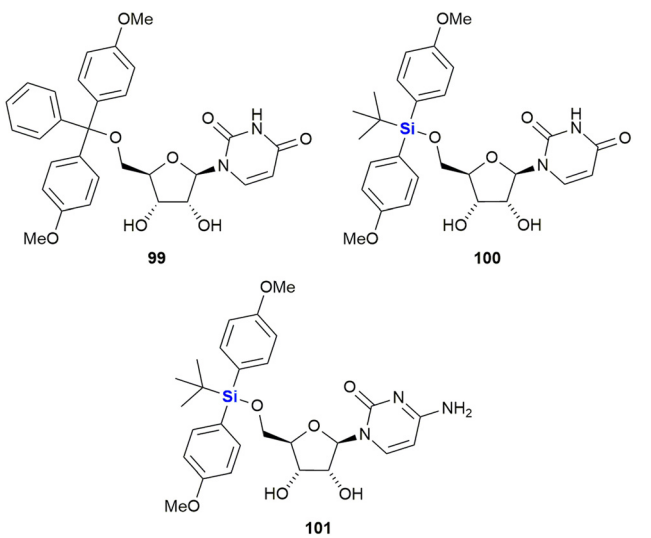

Fig. 34 Nucleoside silyl ether derivatives displaying activity against Caco-2 and HT-29 cell lines.

research, three novel nucleosides **99–101** were prepared and shown to have cytotoxic activities against both cell lines with IC_{50} values ranging from 3–37 μM, with the Caco-2 cells being more sensitive to the compounds (Fig. 34). The nucleoside analogues proved to be significantly less toxic to normal, unstimulated leukocytes when compared to camptothecin **71**. In addition, it was demonstrated that the induction of apoptosis was promoted by an increase of caspase 8 and caspase 3 activities. The group also reported the synthesis of novel silyl- and trityl-modified nucleosides **102–109**, followed by biological screening of the compounds against several tumour lines: HL-60 (leukaemia), K562 (leukaemia), Jurkat (T-cell leukaemia), Caco-2 and HT-29. In addition, the small library of compounds was tested at varying concentrations against two human glioma lines (U373 and Hs683) to obtain GI_{50} values (Fig. 35).[366]

The effect of a selection of the compounds on the growth of cancer cell lines and white blood cells is shown in Table 2. TBDPS-containing compounds showed activity with the best being the uridine derivative **105a** which demonstrated slight inhibition of the leukaemia suspension cell line (<10%), but was better against the adherent cell lines as the colorectal Caco-2 and HT-29 cell proliferation were inhibited to below 40 and 35% respectively.[366] Interestingly, a non-silyl trityl-nucleoside **99** also displayed comparable activity to the TBDMPS-containing systems and acetylation of the carbohydrate rings in both the silyl and non-silyl cases resulted in a loss of activity. When cell viability was determined against freshly isolated leucocytes it was noted that all the synthetic derivatives showed reduced *in vitro* growth inhibition when compared to the 100 μM camptothecin control **71**, suggesting that they may be less impactful on non-cancerous cells.

Finally, **105a** and **107** were also shown to induce apoptosis (in combination with extensive cytoplasmic vacuole formation) in both HT-29 and Caco-2 cell lines, demonstrating comparable or better activity than the camptothecin **71** reference.[367]

Further investigations into the effect of silyl-decorated nucleoside derivatives on cancer cell population growth revealed 8 compounds showing GI_{50} values in the range of 25–40 μM. Five of these compounds contained TBDPS-groups (namely **105b**, **106**, **8107**, **108a** and **108b**), one contained the TIPD-protecting group (**88a**) and the remainder were the non-silyl trityl derivatives (see Fig. 35).[366] Alog*P* calculations suggested that there was a trend wherein the more lipophilic molecules showed improved GI_{50} values, thus suggesting that bulkier non-polar silyl groups could be improving cell membrane permeation, or could be causing activity by disrupting cell membranes.[366]

Cutler and co-workers also reported on the anti-proliferative activity of nucleoside derivatives in the form of N^6,5′-bis-ureidoadenosine analogues (Fig. 36).[368] In this research, the prepared compounds were screened against the NCI60 panel of human cancers. The presence of a 2′-OTBS group proved necessary for activity; however, acceptable anti-proliferative effects also required the presence of a N^6,5′-bis-ureido group. In a follow-up manuscript, Peterson and co-workers investigated if the 3′C-carboxymethyl moiety in **110**, which was synthetically challenging to install, was in fact necessary for activity.[369] The studies showed that replacement of this moiety with a second-OTBS group afforded a lead compound **111** with improved potency. Notably, the new analogue afforded IC_{50}'s in the range of 6–10 μM for five of the six human colon cancer lines, with three of the renal cancer lines displaying similar activities.[369] The researchers attempted thereafter to improve

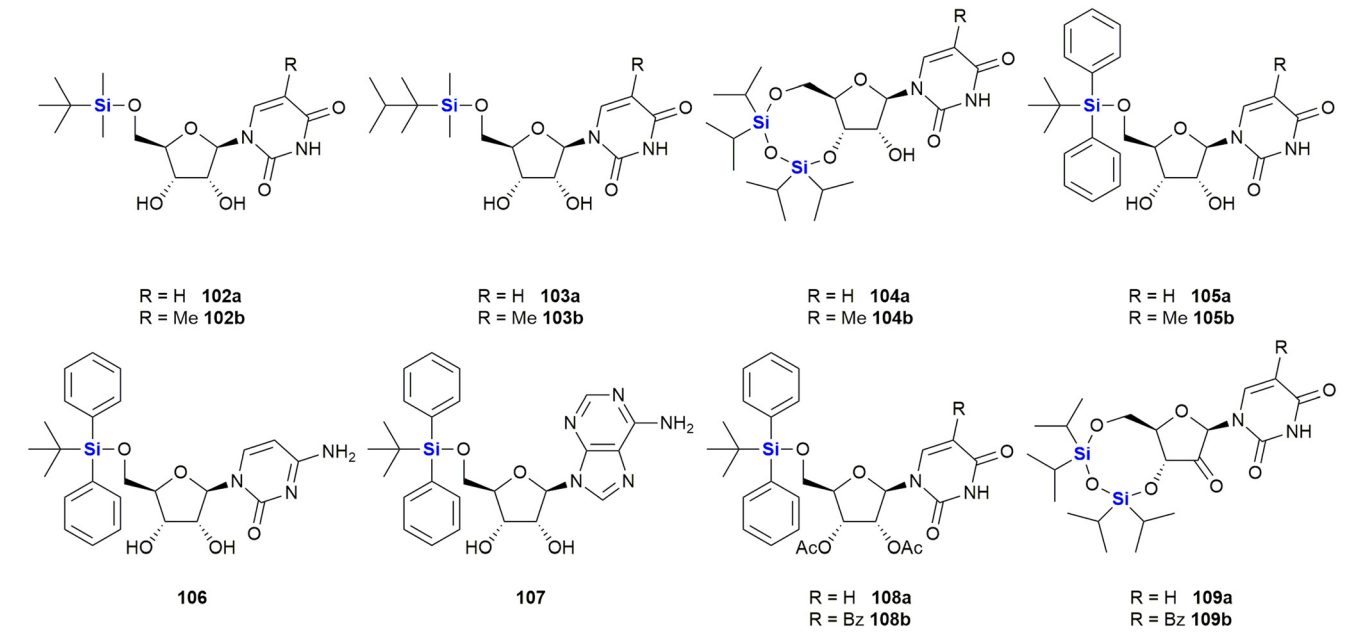

Fig. 35 Nucleoside silyl ether derivatives displaying activity against Caco-2 and HT-29 cell lines.

Table 2 Anti-cancer activity of selected nucleoside silyl ether derivatives against several cell lines (for structures see Fig. 35)

	Cell viability (% surviving at 100 μM as compared to control (100%))					
Compound	HL-60	Jurkat	K-562	Caco-2	HT-29	WBC
105a	5.6 ± 0.3	6.3 ± 0.6	9.4 ± 0.1	37.4 ± 1.0	29.4 ± 0.6	61.5 ± 4.5
106	26.0 ± 0.6	16.0 ± 1.3	35.6 ± 0.9	37.2 ± 0.4	25.6 ± 0.7	NI
107	27.9 ± 0.5	18.3 ± 1.2	45.5 ± 0.7	NA	NA	59.3 ± 2.0
108b	11.2 ± 0.5	NA	35.5 ± 2.4	NA	NA	NI
71	Camptothecin	8.9 ± 0.7	39.6 ± 0.9	12.8 ± 0.2	11.4 ± 0.2	34.6 ± 2.0

NA = not active, NI = no inhibition (cell viability >50% for cell lines, cell viability 100% for WBC).

the activity of **111** by preparing a library of analogues wherein the TBDPS groups were replaced by other silyl or acyl groups; however, biological assessment showed no improvement over lead compound **111**. Interestingly, the desilylated derivative of **111** was screened for binding affinity to the bone morphogenetic protein receptor, together with representative examples from the silyl and acyl derivatives, and it was only the desilylated compound that showed appreciable activity (K_d = 11.7 ± 0.5 μM). These results, together with computational docking studies, suggested that **111** was in fact a prodrug of the active (desilylated) derivative.[370,371] Finally, modification of the 5′-bis-ureido group to give **112**, afforded a compound which demonstrated potent inhibition of the NCl-H522 lung adenocarcinoma cell line at nanomolar concentrations (GI_{50} = 9.7 nM).[372]

Staying with the theme of silylated nucleosides, Lanver and Schmalz reported the synthesis of silyl ethers of carbocyclic nucleoside analogues (CNAs) involving a Pauson–Khand reaction. The-CNA analogues were synthesised based upon a CNA scaffold known to be apoptosis-inducing (Fig. 37).[373] In a subsequent study by the same team, an enantioselective synthesis of further CNA analogues was developed and the compounds were assessed in terms of their anti-tumour activity against a Burkitt-like lymphoma cell line model. Activities for the compounds were observed to be in the low micro-molar range. Generally, TBDMS ethers were more active than TDS ethers, with the silyl ether CNA **114** being the most active compound of the whole series (LD_{50} = 46 μM **113**, LD_{50} = 9 μM **114**).[374]

Schmalz and co-workers also reported the synthesis and biological evaluation of iron-containing nucleoside analogues (**115–120**) characterised by the presence of a 1,3-butadiene-$Fe(CO)_3$ sub-scaffold (Fig. 38).[375,376] A lead silyl-containing compound **115** was identified displaying potent apoptosis with an LD_{50} of 10 μM when screened against Burkitt-like lymphoma BJAB cancer cells. A further three silyl-compounds (**106–108**) displayed LD_{50} values of 18 μM (**106**), 30 μM (**107**) and 14 μM (**108**). In a more recent paper, silylated metal-containing nucleosides (**119–120**) were reported to show selective cytotoxicity against CLL leukaemia cells. Equal activity was also observed in cells from high-risk disease groups (*e.g.*, del11q/del17p cytogenetic and fludarabine resistant cells).[377]

In their synthesis of C1,C2 functional group derivatives of the *Amaryllidaceae* alkaloid lycorine, Kornienko and co-workers demonstrated that there was a strong correlation between compound lipophilicity and anti-cancer activity. These results thus suggested that their compound design

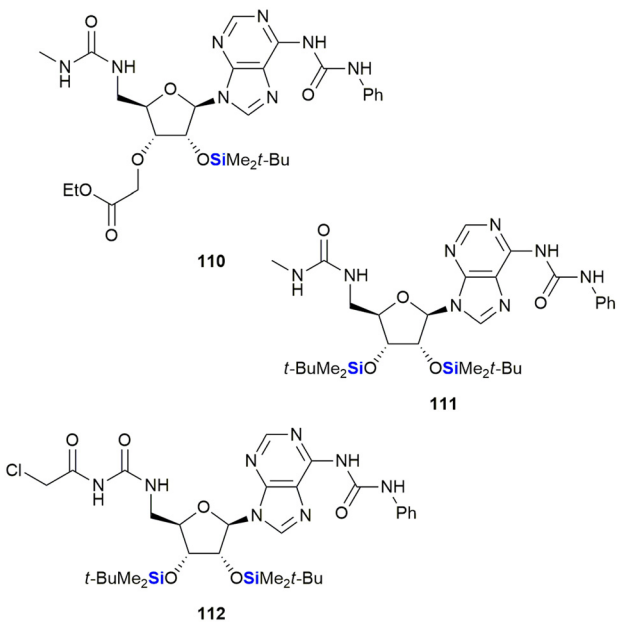

Fig. 36 Anti-proliferative nucleoside silyl ether derivatives.

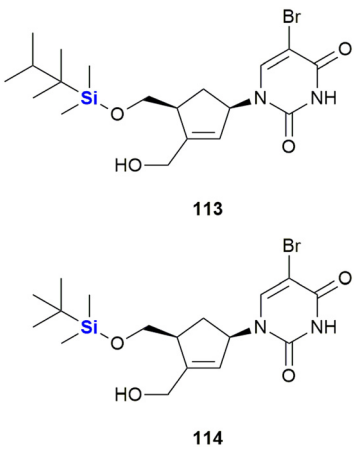

Fig. 37 Carbocyclic nucleoside analogues shown to induce apoptosis.

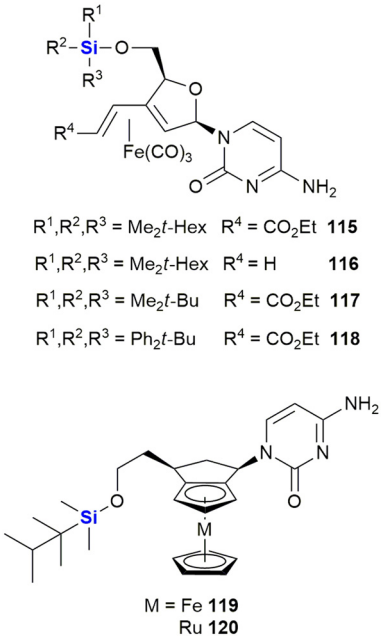

Fig. 38 Iron-containing nucleoside analogues which show activity against BJAB and CLL cell lines.

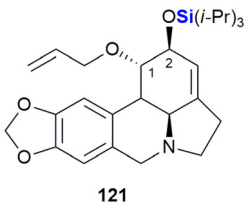

Fig. 39 Silyl ether lycorine derivative with anti-cancer properties.

needed to take cell permeability into account (Fig. 39).[378] To this end, the use of silyl groups afforded increased lipophilicity. This was showcased by the TIPS-silyl ether derivative **121** which was shown to be equipotent to lycorine when tested against A-549 (lung), MCF-7 (breast), T98-G (glioblastoma), HS-683 (human glioma), SK-MEL (melanoma) and B16 (melanoma) cancer cell lines.

Recently, Nelson *et al.* reported the development of novel silyl cyanocinnamic acid derivatives as metabolic plasticity inhibitors for potential anti-cancer treatment (Fig. 40).[379] The

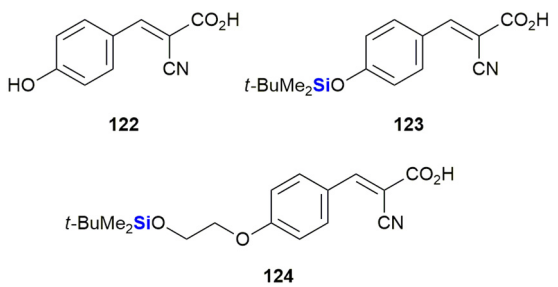

Fig. 40 Anti-proliferative cyanohydroxycinnamic acid **122** and related sila-analogues.

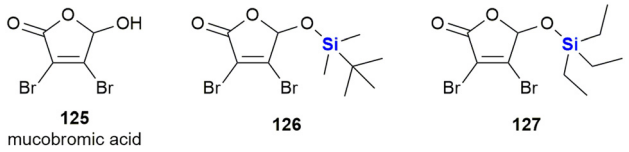

Fig. 41 Anti-proliferative sila-analogues of mucobromic acid.

researchers rationalised that insertion of a bulky, acid stable TBDPS ether on the phenolic hydroxy of the monocarboxylate transporter cyanohydroxycinnamic acid **122** would increase lipophilicity, metabolic stability and the ability of the small molecule to influence the mitochondrial function, all the while retaining the activity of **122**. With this objective in mind, silylated analogues **123** and **124** were synthesized and demonstrated to show enhanced inhibition of proliferation in cancer cells through glycolysis and mitochondrial dysfunction. When applied in *in vivo* studies against a colorectal cancer cell WiDr (colon cancer) tumour xenograft, the silylated derivatives were also well tolerated.

In 2021, Walczak and co-workers reported the outcomes of an investigation into the effects of adding silicon groups to mucobromic acid **125**, a molecule containing the furan-2(5*H*)-one core (Fig. 41).[380] In previous studies, the authors had shown that the incorporation of aliphatic groups at the C-5 position of mucobromic acid increased the compound's anti-proliferative activity and improved its selectivity towards the non-small cell lung cancer A-549 cell line.[381] The researchers then investigated the effect of introducing silyl ethers at the same position, thus allowing them to control both the hydrophobicity and selectivity of the new compounds. Three of the four silyl derivatives screened showed increased activity relative to the parent compound **125**, with compounds **126** and **127** showing selective anti-proliferative activity for the HCT-116 colon cancer cell line (IC_{50} = 1.3 and 1.6 μM respectively). Critically, the compounds were shown to be most active against colorectal cancer cell lines.

In the last decade, Bazzocchi and co-workers have explored the chemical space surrounding withaferin A **128** which has included the synthesis of silyl ether-containing withaferin A derivatives (Fig. 42). These investigations resulted in derivatives with increased cytotoxicity against HeLa (cervical carcinoma), A-549 (lung carcinoma) and MCF-

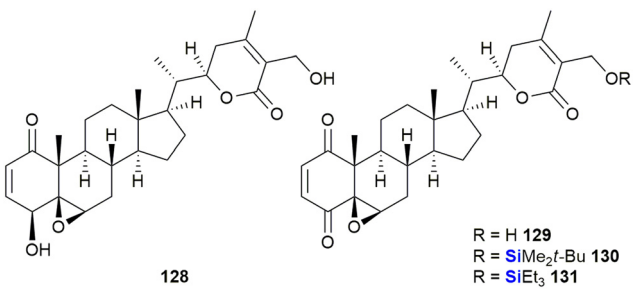

Fig. 42 Withaferin A-based silyl ether analogues with anti-cancer properties.

7 (breast adenocarcinoma) cell lines.[382–384] In an effort to improve on their initial findings, a library of thirty analogues was prepared leading to the identification of eight analogues with activities ranging from 1–32 nM when screened against human epithelial ovarian carcinoma cisplatin-sensitive and -resistant cell lines. From these experiments, silyl-containing compounds **129–131** were identified by the researchers as potential candidates for clinical translation in individuals suffering from relapsed ovarian cancer.

Zhao *et al.* designed dipeptides with a silicon-containing alkyl chain for the treatment of prostate cancer resistant to androgen-deprivation therapy and conventional chemotherapeutics (Fig. 43).[385] The dipeptides **132** exhibited potent cytotoxicity against multiple cancer cell lines from the NCI-60 cell line panel at low micromolar or even nanomolar concentrations. They were further evaluated against resistant prostate cancer cell lines and showed an average IC_{50} value of 1.50 μM. The authors determined the mode of action of these compounds to be comprised of the promotion of androgen receptor AR protein degradation, its variant Ar-v7 and survivin, a protein essential for cell division and which also inhibits cell death.

Garro *et al.* investigated the anti-proliferative activity of the silyl ether derivatives **133** and **134** (Fig. 44) against human solid tumour cell lines.[386] Experiments determined that while **134** was inactive, **133** showed moderate activity against cervix, breast and colon tumour cell lines (HeLa: GI_{50} 24,1 μL mL^{-1}, T-47D: GI_{50} 26.6 μL mL^{-1}, WiDr: GI_{50} 32.2 μL mL^{-1}).

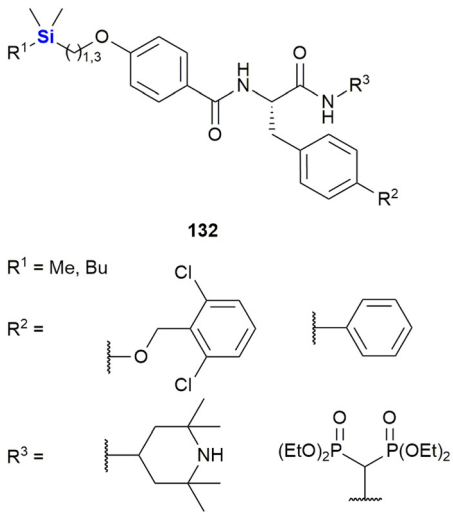

132

Fig. 43 Silyl modified dipeptides against prostate cancer.

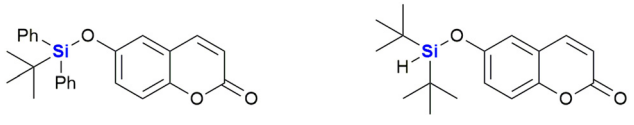

133 134

Fig. 44 Anti-proliferative silyl ether derivatives of 6-hydroxycoumarins.

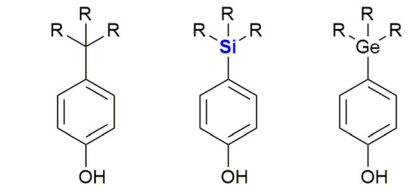

R = Me	135	136	137
R = Et	138	139	140

Fig. 45 Carbon, silicon and germanium containing phenols with oestrogenic activity.

While silicon-containing drugs are well investigated, reports of biologically active germanium compounds are less common. Kagechika *et al.* synthesised a series of *para*-substituted phenols with either a carbon-, silicon- or germanium-containing substituent (Fig. 45).[387] While the hydrophobicity of the compounds increased significantly by the incorporation of a silicon instead of a carbon atom (clog P = 3.50 (**135**) and 4.12 (**136**)), switching from silicon to germanium did not to have a profound impact (clog P = 4.11 (**137**)). This effect, however, was less pronounced in the case of ethyl instead of methyl substituents. The authors also determined that these synthetic phenols promoted the proliferation of the breast cancer cell line MCF-7 by binding to the oestrogen receptor. Both the silicon (EC_{50} = 63 nM (**136**) and 3.4 nM (**139**)) and germanium (EC_{50} = 100 nM (**137**) and 2.1 nM (**140**)) compounds were significantly more active than their carbon counterparts (EC_{50} = 870 nM (**135**) and 23 nM (**138**)). For a computational study on Si/Ge isosterism in the fungicide flusilazole see the following ref. 388.

Mousazadeh *et al.* reported the triazoles **141** and **142** with a unique combination of sulphur- and silicon-containing functional groups (Fig. 46). These compounds possessed potent cytotoxic activity against the human breast cancer cell line MCF-7 with an IC_{50} = 30.3 μg mL^{-1} for the most potent derivative, which is close to the activity of doxorubicin (IC_{50} =

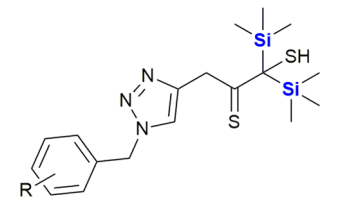

141

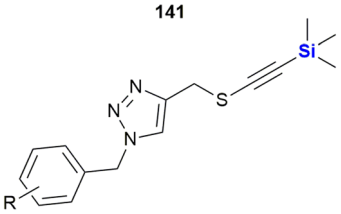

142

R = H, Cl, Br, NO2

Fig. 46 Sulphur- and silicon-containing cytotoxic triazoles.

28.89 μg mL^{-1}). The silylalkynes **141** also showed promising activities against both Gram-positive and Gram-negative bacteria, while the disilyl derivatives **142** were only active against Gram-positive strains.[389] See the following references for related synthetic work from the same group.[390,391]

In a computational study, Eryilmaz investigated the pharmacological properties of all FDA approved drugs for the treatment of acute lymphoblastic leukaemia.[392] Among these, nelarabine **143** (Fig. 47) was predicted to exhibit the most promising activity against four out of six possible target proteins. Further modelling investigations involving the nelarabine scaffold suggested that the disilylated analogue **144** might not only possess improved molecular properties, but also more potent bioactivity against even five out of six target proteins. These predictions must still be borne out by the actual synthesis and testing of the disylated nelarabine compound.

The neurotensin receptor NTS_1 is over-expressed in several cancer cell lines and therefore is an attractive target for tumour diagnostics and therapy.[393] In 2020, Morgat, Cavelier and co-workers investigated neurotensin derivatives for tumour imaging (Fig. 48).[394] In this research, the shortest functional pentapeptide fragment of neurotensin was connected to a ^{68}Ga-labeled complex. The researchers found that the exchange of the C-terminal leucine found in natural neurotensin by the non-natural amino acid TMS-alanine shown in **145** improved binding affinity towards NTS_1 (K_D = 6.29 nM), increased stability in human plasma ($t_{1/2}$ = 7.17–24.63 min) and lowered efflux.

Vorinostat **146** (Fig. 49) is an inhibitor of Zn(II) dependent histone deacetylases (HDACs) and is approved by the FDA for the treatment of cutaneous T-cell lymphoma.[395,396] Olsen *et al.* synthesised and investigated **147**, in which the Zn(II) chelating hydroxamic acid group of **146** was exchanged for a silanediol group,[397] as it was proposed that silanediols should possess a similar affinity for Zn(II) ions as hydroxamic acids.[398] When tested, **147** showed inhibitory activity against 6 out of 10 tested HDACs at micromolar concentrations (IC_{50} = 0.6–28 μM), but was generally less active than vorinostat **146** (IC_{50} = 0.021–70 μM). For a patent detailing the description of Si-containing HDACS, see the following ref. 399.

Very recently (2022), Zaltrariov *et al.* investigated the activity of the silatrane **148** and its imine derivative **149** (Fig. 50) against hepatocarcinoma (HepG2) and breast adenocarcinoma (MCF-7) cell lines.[400] The silatrane **148**, with a free amine functional group, was determined to be inactive even at a high concentration of 300 μg mL^{-1}. Its imine derivative **149**, however, showed dose dependant activity

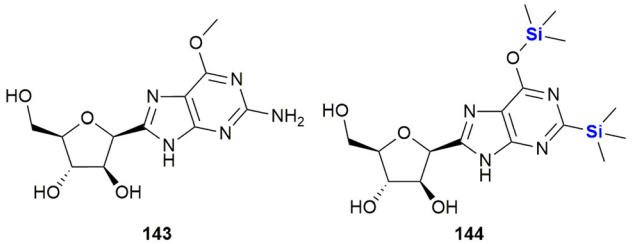

Fig. 47 Nelarabine **143** and siliyl-containing analogue **144**.

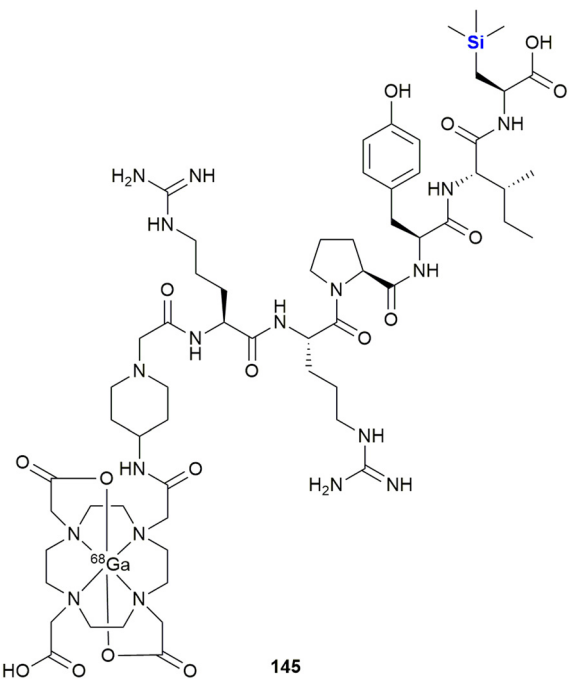

Fig. 48 ^{68}Ga-radiolabeled silicon-containing neurotensin analogue.

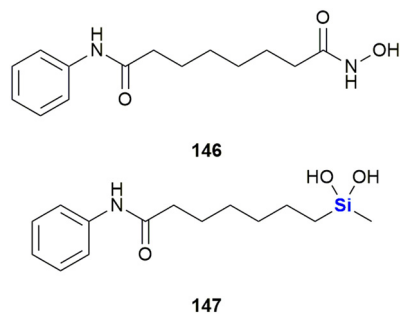

Fig. 49 Vorinostat (**146**) and silanediol analogue **147**.

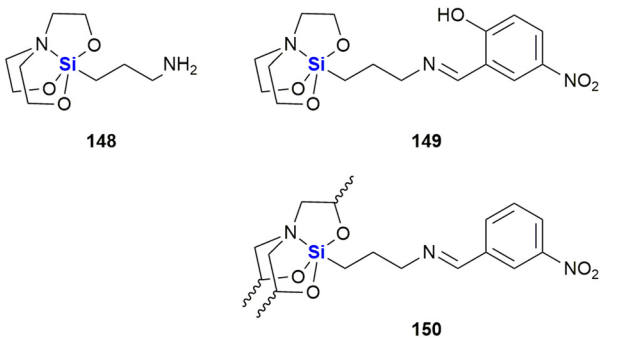

Fig. 50 Anti-cancer silatrane containing amine **148** and its imine derivatives **149** and **150** (note that the stereochemistry of the silatrane unit was not given in the original publication).

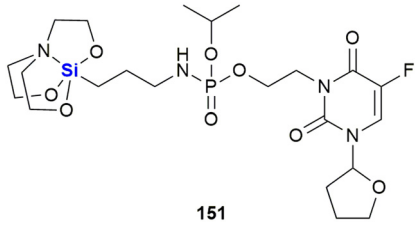

Fig. 51 Silatrane modified 5-fluorouracil with anti-cancer properties.

against both cancer cell lines with IC_{50} values of 150 μg mL^{-1} (HepG2) and 65 μg mL^{-1} (MCF-7) respectively. The cytotoxic properties were therefore linked to the aldimine moiety and not to the silatrane structure. On the other hand, the free amine group enhanced the activity of **148** against several fungal and bacterial strains, where **149** showed MICs in the range of 1.20–2.90 μg mL^{-1}.

Within the broader silatrane topic, Ping *et al.* investigated amide, carbamate, imine and 5-fluoruracil derivatives of γ-aminopropylsilatrane. Among the tested compounds, **150** showed the highest activity and inhibited the growth of melanoma (MDA-MB-435, IC_{50} = 12.5 μg mL^{-1}), cervix (HeLa, IC_{50} = 11.8 μg mL^{-1}) and colon cancer cell lines (HT-29, IC_{50} = 12.3 μg mL^{-1}).[401]

Staying with silatranes, Shi *et al.* reported the synthesis of a silatrane modified 5-fluoro uracil and its bioactivity (Fig. 51). The compound **151** showed some inhibition effect against colon (HCT-8, 29.33%) and liver (Bel7402, 29.26%) cancer cell lines at 5 μg mL^{-1}.[402]

El-Hussieny *et al.* presented the synthesis of a range of silicon-containing heterocycles **152–158** by condensation of silylated isocyanates or isothiocyanates with phosphorous ylids (Fig. 52).[403] The resulting compounds were tested as inhibitors of the Zn(II) dependent matrix metalloprotease MMP-2, a prospective target for the prevention of tumour growth.[404] In the biochemical evaluations, the compounds showed significant activity at low concentrations (IC_{50} = ~41–429 nM) with the thiolactam **157** being the most potent. Molecular docking studies revealed that **157** could be inhibiting MMP-2 by binding of the sulphur atom to the Zn(II) cofactor in the active centre.

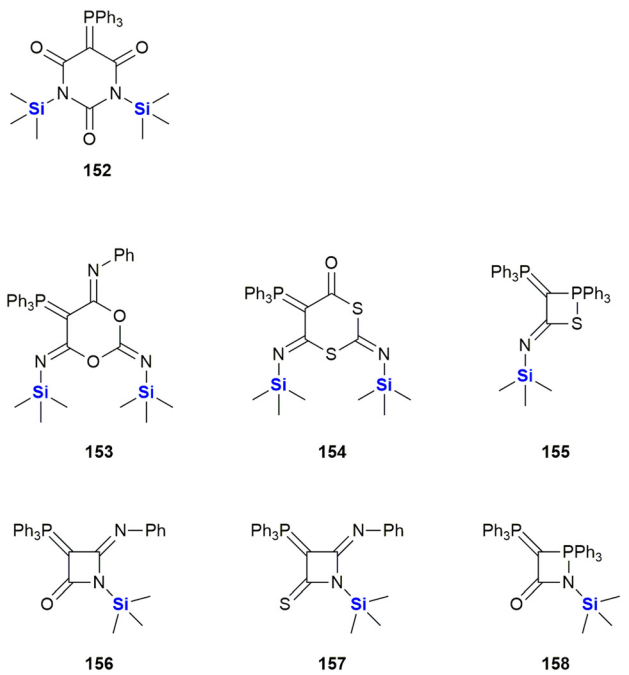

Fig. 52 Silicon-containing MMP2 inhibitors.

Anti-viral agents

Interest in the use of organosilicon regents as anti-viral agents can be traced back to the 1990's when Camarasa and co-workers reported the synthesis and testing of a new class of 3′-spiro nucleosides as HIV inhibitors (Fig. 53).[405] In this particular research, a number of xylo- and ribo-nucleoside analogues (**159–161**) decorated with TBDMS groups were evaluated for their anti-HIV-1 activity. It was found that compounds **160a–c** with a 3′-spiro moiety in the *R* configuration and which contained silyl groups at the C-2′ and C-5′ positions showed strong anti-HIV activity while the *S*-configured spirocycles **159a–c** were significantly less active.

The thymine derivative (**160a**) showed an EC_{50} of 0.034 μg mL^{-1} against HIV-1 induced cytopathicity in MT-4 cells, whilst the analogous uracil **160b** (EC_{50} = 0.114 μg mL^{-1}) and 4-*N*-cytosine **160c** (EC_{50} = 0.097 μg mL^{-1}) compounds being three-fold less active. Removal of one or both silyl groups at either position, like in **161a** (EC_{50} > 100 μg mL^{-1}) caused a complete loss of activity, suggesting a critical role of the *O*-trialkylsilicon moieties. Eventually, the pharmacological profile of these molecules found them to be unfavourable for further clinical development. These compounds have however been shown to be highly useful for studying certain biological aspects of RT in HIV-1 and they have thus been used to study the importance of the p51 subunit in RT

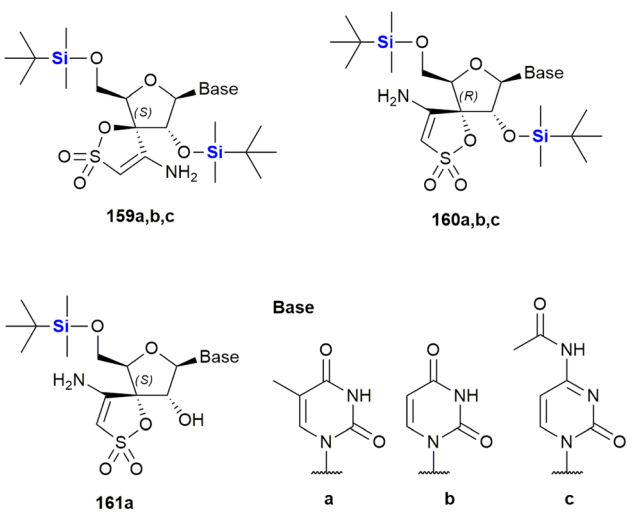

Fig. 53 Silicon containing 3′-spiro nucleosides displaying strong anti-HIV activity.

inhibition, showing non-peptide molecular interaction at the p66/p51 subunits and proving that the β7–β8 loop of p51 is required for RT dimerization.[406]

During the same time period, Sieburth and co-workers reported the development of silanediol peptidomimetics wherein the tetrahedral diol core **163**, normally formed as result of the hydrolysis of a peptide bond **162** by a protease enzyme, was replaced with the nonhydrolyzable silanediol **164** (Fig. 54).[407] These derivatives are neutral and cell-permeable and were shown to be active within an order of magnitude of the HIV protease inhibitor indinavir. In addition, for a recent manuscript disclosing approaches to late-stage site-selective modifications of activated synthetic peptides in complex structures through the application of photoredox catalysis, see the following ref. 408, and for a book chapter review covering silylated amino acids, peptides and peptidomimetics see ref. 409.

The Déléris group synthesised novel *C*-alkylated heterocyclic derivatives (**165–166**) as leads for reverse-transcriptase-mediated anti-HIV-1 activity (Fig. 55).[410] The synthesised nucleobases were designed to specifically interact with the catalytic site of HIV-1 reverse transcriptase (RT). Compound **165** was identified as being both a good inhibitor of HIV-1 replication (IC_{50} 10–15 μM) and of recombinant HIV-1 RT (IC_{50} 6–14 μM) with insignificant cytotoxicity. The compound was shown to be a non-competitive inhibitor selective for HIV-1 with no activity against other DNA and RNA viruses being observed. The degree of inhibition was dependent on the template primer used and the compound's selectivity for HIV-1 over HIV-2 was also established.

More recently, Miller and co-workers reported on the ω-functionalisation of prodrugs of the gold standard HIV nucleotide reverse transcriptase inhibitor, tenofovir **167** (Fig. 56).[411] Tenovofir **167** unfortunately suffers from poor cell permeability and oral bioavailability and must be administered in a pro-drug form to be therapeutically effective. The pro-drug forms in turn are facilely and prematurely metabolized in the liver and as a result significant research has focussed on the development of derivatives with better pharmacokinetic properties. Of specific interest to this review was the phospholipid-based pro-drug TXL **168** which was developed to address this issue; however, the molecule unfortunately suffered from substantial hepatic extraction ($t_{1/2}$ = 42 min). In response, the research team involved in this work, reported the synthesis of two pro-drugs, **169** and **170**, which had increased half-lives of 8.66 h and 2.49 h respectively in human liver microsomes, potent anti-HIV activity (49 nM and 69 nM, respectively) and enhanced pharmacokinetic properties.

Last year (2023), Chen *et al.* published an investigation of HEPTe derivatives for the inhibition of HIV-1 reverse transcriptase (Fig. 57).[412] These researchers exchanged the thioether linker for either a CHOH or a CHOTMS group. While generally compounds with a free alcohol showed higher activity

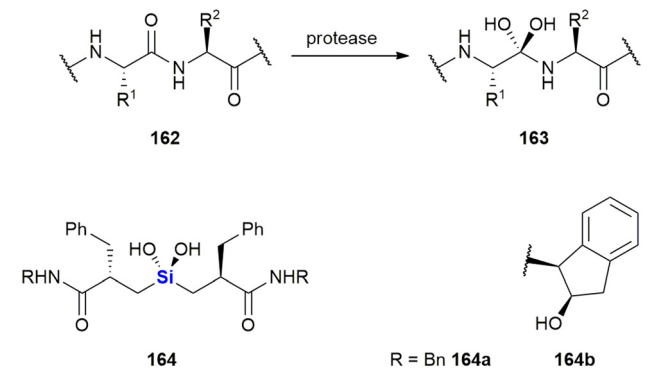

Fig. 54 Silanediol peptidomimetics targeting HIV protease.

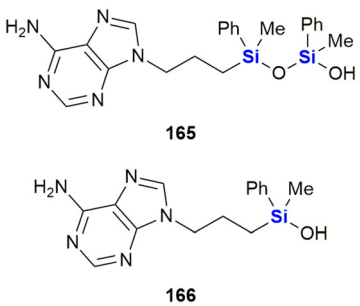

Fig. 55 Silanols as HIV-1 reverse transcriptase inhibitors.

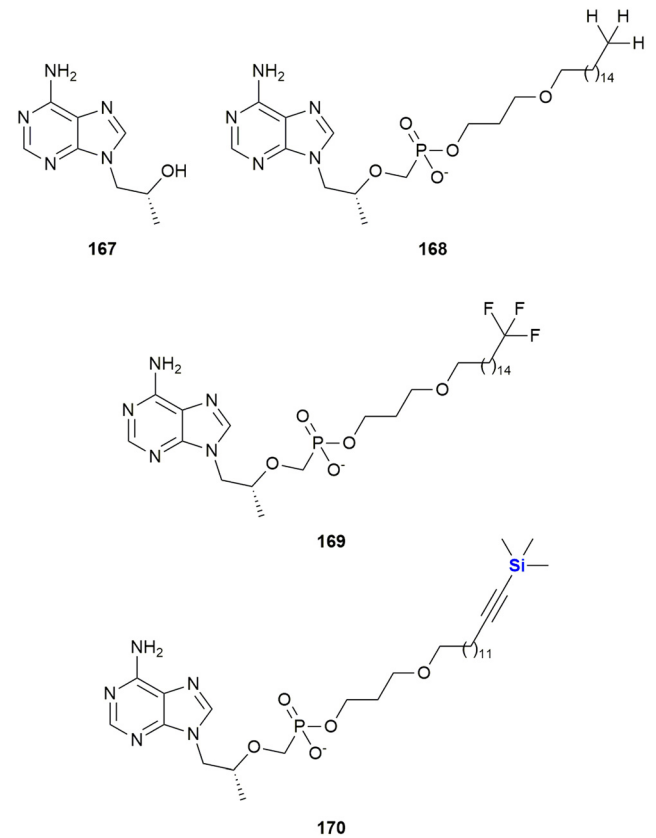

Fig. 56 HIV reverse transcribase inhibitor tenofovir **167** and prodrug forms **168–170**.

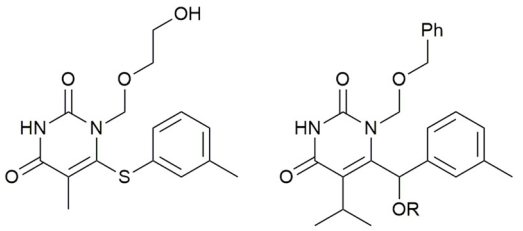

Fig. 57 HEPT (**171**) derived non-nucleosidic HIV-1 reverse transcriptase inhibitors.

against wild type HIV-1 than their silylated counterparts, the silyl ether **173** (EC_{50} = 0.20 μM) showed the second highest activity of all compounds tested and even slightly surpassed its unsilylated analogue **172** (EC_{50} = 0.20 μM). Compound **173** also showed moderate activity against clinically relevant mutant strains and exhibited nanomolar inhibition of HIV-1 reverse transcriptase (IC_{50} = 0.65 μmol L^{-1}).

Ye *et al.* investigated a series of acyclovir (**174**) derivatives in which the drug was attached to a silatrane by a linker chain (Fig. 58). The silatrane unit was expected to stimulate the immune response, while the acyclovir part was supposed to inhibit virus replication. Indeed, **175** increased proliferation of splenic lymphocytes and upregulated the expression of interferone IF-γ, interleukine IL-2 and T-cell CD markers, while it maintained the anti-viral activity of acyclovir **174** against herpes simplex viruses HSV-1 and HSV-2.[413] In another study, **176** showed similar immunomodulatory effects and decreased secretion of hepatitis B virus antigens HBsAg and HBeAg with IC_{50} = 34.5 μM and 89.8 μM, respectively.[414]

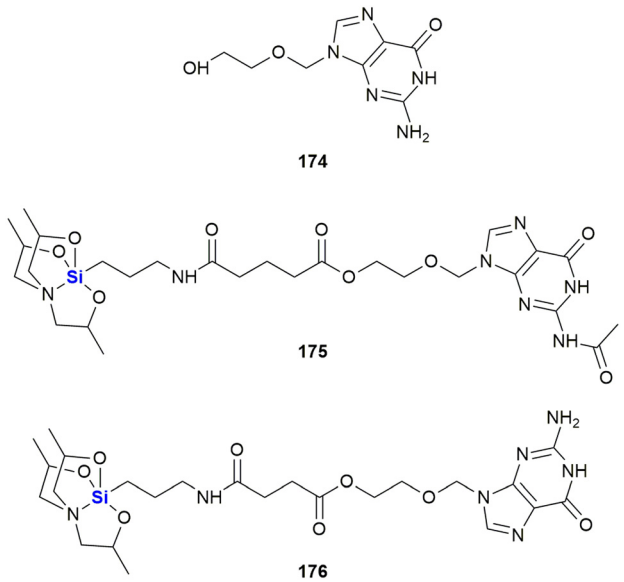

Fig. 58 Acyclovir **174** and silatrane modified acyclovir derivatives **175** and **176** (note that the stereochemistry of the silatrane unit was not given in the original publication).

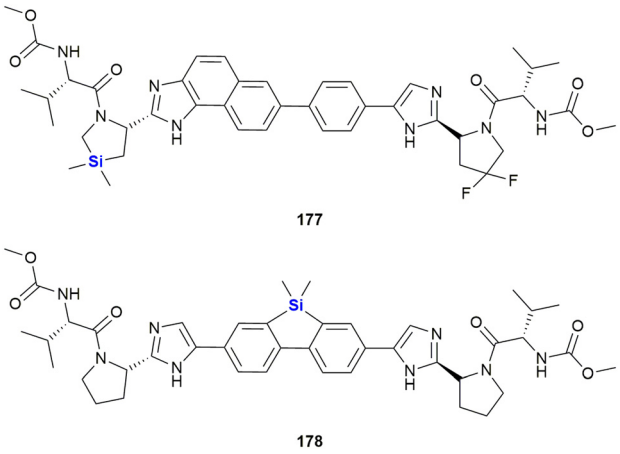

Fig. 59 Anti-viral silyl-containing compounds against HCV.

In 2012, the Merck Sharpe and Dohme Corporation filed a patent detailing the preparation of silyl-containing compounds for the treatment of viral diseases, and in particular the hepatitis C virus (HCV) (Fig. 59).[415–417] NS5A RCI **177**, which contains a silaproline moiety,[418] inhibited GT-1a and GT-1b replicons (EC_{50} 16 and 3 pM respectively) and inhibited chimeric GT-2a (JFH), GT-3 and GT-4a (EC_{50} 27, 350 and 20 pM respectively).

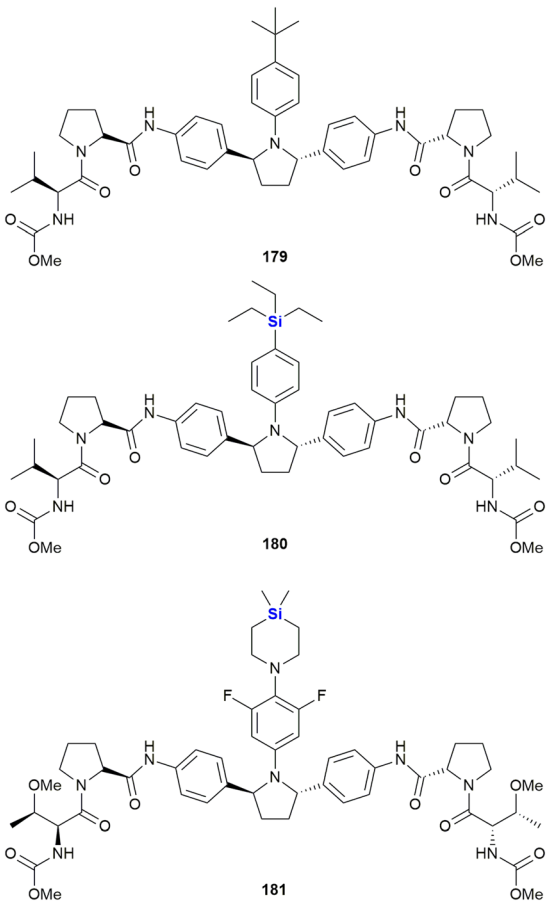

Fig. 60 Ombitasvir **179** and sila-analogues **180** and **181**.

In the related compound **178** the utility of a bridging silicon group was investigated; potent anti-viral activity was observed in the GT-1a and GT-1b (EC_{90} 76 and 43 pM respectively). The compound was however found to be sensitive to the Y93H mutation in the GT-1a replicon with anEC_{50} of 811 nM.

In 2018, Zhang and co-workers reported the synthesis and biological evaluation of a series of silicon-containing HCV NS5A inhibitors based upon ombitasvir **179**, a compound which displays pan-genotype activity (Fig. 60).[419] The compounds were prepared by the bioisosteric replacement of a quaternary carbon with a silicon atom. The most promising analogue **180** displayed improved pan genotype NS5A inhibition with picomolar potency against GT1a (7 pM), GT1b (3 pM), GT2a (0.8 pM), GT3a (10 pM), GT4a (0.1 pM), GT5a (1 pM) and GT6a (445 pM). In all cases, the sila-analogues were more potent than ombitasvir **179**. Pharmokinetic evaluations revealed that **180** had similar plasma protein binding and liver distribution patterns to ombitasvir **170**, and no cytotoxicity or inhibition of hERG and CYP 450. More recently (2020), the same researchers reported the identification of compound **181** based on the same core, this time incorporating a 4-silapiperidine group in place of the triethylsilyl group. Again, this compound had excellent potency against genotype 1 subtype a, GT1a, GT1b, GT2a, GT3a, GT4a, GT5a and GT6a, with EC_{50} values in the range of 0.33–17 pM.[420] Compound **181** also had good pharmacokinetic parameters and high liver distribution in preclinical animal models.

Wang and co-workers prepared 5′-silyated 3′-1,2,3,3-triazolyl thymidine analogues **182** and **183** which act as inhibitors of the tropical diseases West Nile virus (WNV) and Dengue virus (DENV) (Fig. 61).[421] 5′-Silylated analogues of 3′ aziothymidine (AZT) were prepared which were able to selectively inhibit WNV and DENV. SAR studies indicated that this activity was heavily dependent on the 5′-silyl group and the 3′-triazole. The activity appeared highly selective, with compound **182** showing potent anti-HIV-1 activity (EC_{50} = 67 nM) with no appreciable WNV or DENV activity (7.4% and 0% inhibition respectively at 10 μM concentration). In contrast, the TBDMS ether analogue **183** showed potent WNV and DENV activity (97% and 85% inhibition respectively at 10 μM concentration), but insignificant anti-HIV-1 activity. Assessment of the SAR studies performed indicated that large bulky silyl groups (*e.g.*, TBS, TIPS and TBDMS) all inhibited

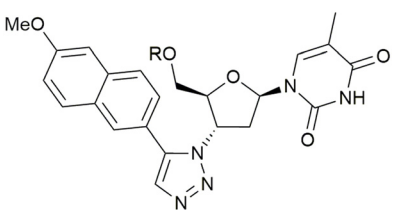

R = H **182**, SiMe$_2$*t*-Bu **183**

Fig. 61 Anti-viral silyated thymidine analogues against West Nile virus (WNV) and Dengue virus (DENV).

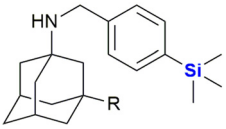

R = H **184**
R = OH **185**

Fig. 62 Organosilanes against multi-drug resistant influenza-A.

both WNV and DENV with 85–100% inhibition at 10 μM; conversely, small non-silyl groups, such as acetyl, methyl, ethoxymethyl and tetrahydropyran, elicited poor activity. When large non-silyl groups were used (such as DMTr), only moderate activity was observed, with 23% and 46% inhibition at 10 μM being measured for WNV and DENV respectively. The SAR also highlighted that in addition to a bulky silylated substituent at the 5′ position, the triazole at the 3′ position needed a bulky aromatic ring system(s), although bulky alkyl groups also conferred some activity. Within the libraries of silylated analogues there was also some selectivity observed between the viruses WNV and DENV.

Wang and co-workers further reported on the development of organosilanes as potent anti-virals targeting multi-drug resistant influenza-A viruses (Fig. 62).[422,423] The research was conducted in response to the growing resistance to the only oral FDA-approved treatment oseltamivir (Tamiflu) and targeted the AM2-S31N mutant proton channel present in 95% of the current circulating influenza virus. In this work, organosilanes **184–185** were designed as potent channel blockers and silane **185** showed improved activity in inhibiting the A/WSN/33 (H1N1) virus over the related carbon analogue (EC_{50} 0.4 μM *vs.* 2.5 μM). The compound was also highly active against oseltamivir-sensitive (EC_{50} 0.6–1.2 μM) and -resistant (EC_{50} 0.6–3.0 μM) influenza A viruses.

Anti-bacterial agents

In 2006 (ref. 424) and 2007,[425] Kim, Baney and co-workers published articles outlining research involving the possible application of trialkylsilanols (**186–194**) as a novel class of anti-microbials. These research outputs described the discovery of an unexpected class of powerful biocides based on fairly straightforward-to-synthesize silanols.[424] Anti-

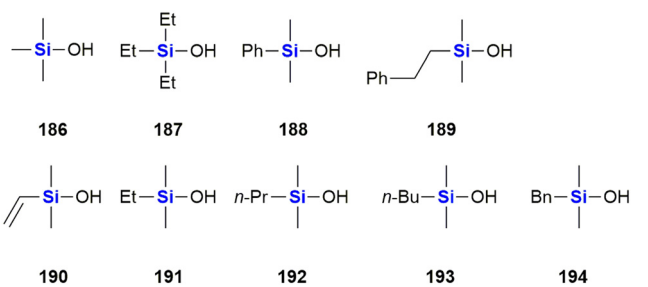

186 **187** **188** **189**
190 **191** **192** **193** **194**

Fig. 63 Representative examples of silanols showing anti-bacterial activity.

microbial screens with the synthetic silanols, *tert*-butanol and siloxanes were subsequently conducted against Gram-negative (*Escherichia coli*) and Gram-positive (*Staphylococcus aureus*) bacteria. The researchers found that when the silanol treatments were used, the number of viable bacteria were reduced by more than eight orders of magnitude when compared to the application of the corresponding alcohols. Of note was that in particular, triethylsilanol **187** exhibited a potent biocidal effect at a very low concentration and within ten minutes of application. A subsequent study of the SAR for these silanols revealed that the increased O–H bond acidity, as well as the increased lipophilicity, were the primary factors governing the anti-bacterial properties of the compounds.[426] Examples of the compounds tested are provided in Fig. 63.

In 2014, Reddy and co-workers patented a number of silicon analogues of piperine **195**, an alkaloid originally isolated from black pepper as this compound possessed respectable anti-tubercular activity (Fig. 64).[427,428] Two of the compounds developed, **196** and **197**, displayed MIC values of 50 μg L^{-1} when screened against *Mycobacterium tuberculosis* (H37Rv). In comparison, piperine **195** showed no observable activity under the same conditions.

The researchers further patented silicon analogues of the diarylpyrrole compound BM212 **198**.[428] Compounds **199** and **200** showed improved activity when screened against $H_{37}R_v$, with MIC values ranging from 0.2–1.5 μM in the case of scaffold **199**, while **198** showed a MIC of 1.7 μM. Interestingly, when the position of the silyl containing group was moved to the adjacent position on the pyrrole ring system, as in compound **199** (MIC = 3.6–23.1 μM), a significant decrease in activity was noted (Fig. 65). More recently, the mechanism of action of these compounds was investigated by docking studies.[429] The authors suggest that diarylpyrroles **199** bind to mycolic acid transporter MmpL3.

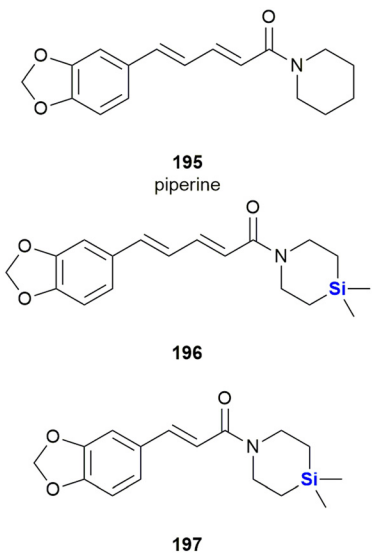

Fig. 64 Silicon analogues of a piperine alkaloid originally isolated from black pepper possessing anti-tubercular activity.

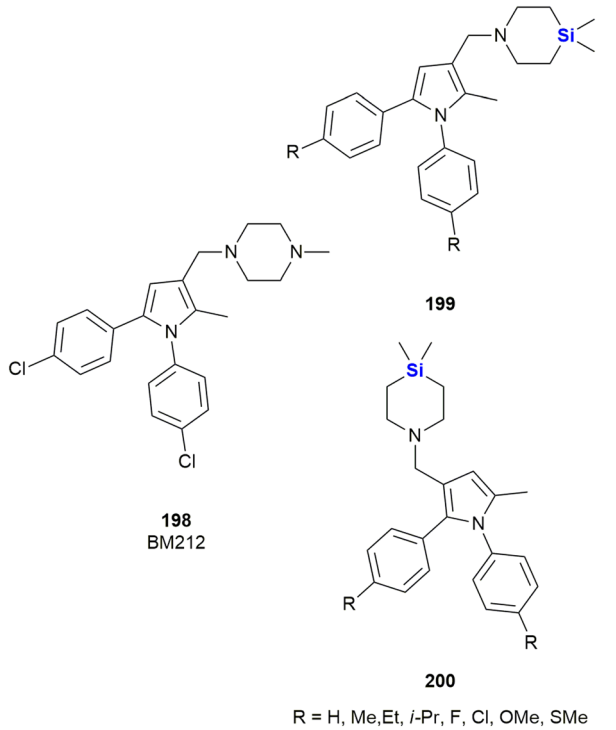

Fig. 65 Anti-tubercular silicon containing pyrroles.

As hydrophobic interactions between the ligand and MmpL3 are dominant, it is easily understood why the incorporation of silicon increases the binding affinity compared to the parent compounds **198**. The position of the amino group is crucial for the interaction with Asp256 and Tyr257, thus explaining the lower affinity of arylpyrroles **200**.

More recently (2016), the Reddy group has reported the identification of further novel sila analogues of rimonabant **201** as anti-tubercular agents. The most potent of these was compound **202**, which displayed an MIC of 31 ng mL^{-1} when screened against *M. tuberculosis* (H37Rv).[430] The researchers found that inclusion of the silicon atom showed greatly improved potency over the non-sila derivatives (Fig. 66).

The potency of the disiloxan **30** (Fig. 13) to inhibit efflux pumps in cancer cells (*vide supra*) raised attention to its use in

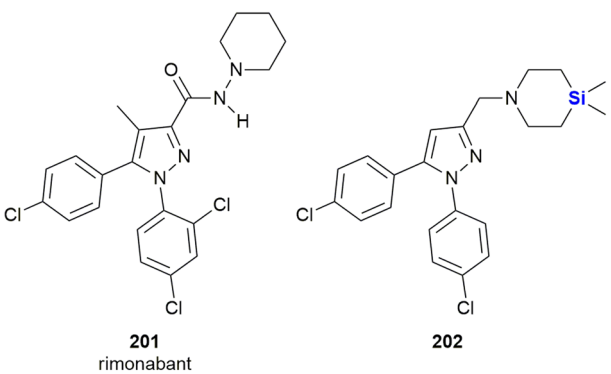

Fig. 66 Rimobant **201** and sila-analogue **202**.

the treatment of multidrug resistant tuberculosis. Initial investigations by Martins *et al.* showed that compound **30** (but not the related compound SILA 409 **29**, Fig. 13) enhanced the intracellular killing activity of human macrophages infected with extensively drug-resistant tuberculosis XDR-TB and possessed *in vitro* activity against XDR-TB (MIC = 3.125 mg L^{-1}).[431] **30** thus transformed non-killing macrophages into killers of phagocytosed bacteria with no observable cytotoxicity. Furthermore, Simons *et al.* showed that **30** possessed inhibitory activity against 21 clinical *Mycobacterium tuberculosis* isolates,[432] some of them drug and multidrug resistant, with MIC_{50} values in the range of 2–16 mg L^{-1}.[431,433] Later, Knegt *et al.* demonstrated *in vitro* that **30** significantly enhanced the susceptibility of *M. tuberculosis* against isoniazid and especially against rifampicin. While the therapy of tuberculosis-infected mice with a combination of **30** and isoniazid, rifampicin and pyrazinamide proved to be beneficial in the short term, it did not prevent relapse of TB after treatment was curtailed after 13 weeks.[432]

The development of neurologically active agents is often hampered by poor brain penetration across the BBB, Reddy and co-workers reported that silicon analogues of the marketed oxazolidinone broad spectrum anti-biotic linezolid afforded dramatic improvements in the ability to cross the BBB, brain/plasma ratio and brain exposure (Fig. 67).[434] As part of their investigations, the researchers replaced the morpholine or thiomorpholine groups of linezolid **203** or sutezolid **204** (phase II clinical candidate for treating TB) giving silicon analogue **203**, a compound for which solubility clog*P* increased from 0.17 (**203**) and 1.00 (**204**) to 4.15 (**205**). Silicon analogue **205** also demonstrated up to a 30-fold improvement in the brain/plasma ratio when compared to linezolid **203**. However, anti-bacterial activity against several

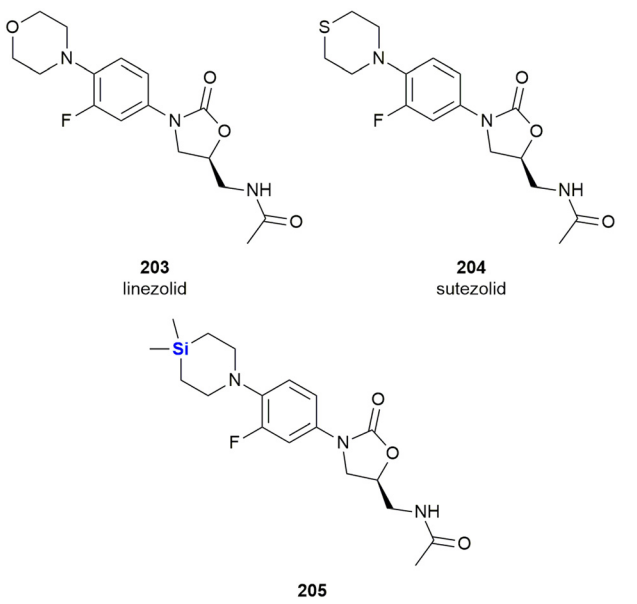

Fig. 67 Oxazolidinone anti-biotics linezolid **203** and sutezolid **204** and silicon analogue **205**.

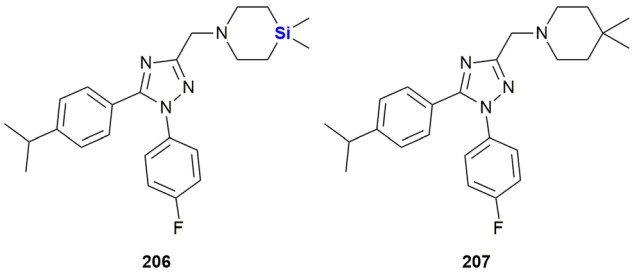

Fig. 68 Anti-tuberculosis 1,2,4-triazoles with (**206**) and without (**207**) silicon.

bacteria, including *Streptococcus pneumoniae* (4 to 16 μg L^{-1}) and *Neisseria meningitidis* (32 μg L^{-1}) was less than that of linezolid **203** which had anti-bacterial activities of 0.5 to 8 μg L^{-1}. This would indicate that although there was increased ability of **205** to cross the blood–brain barrier, the incorporation of the silicon had an adverse effect on the ability of the compound to induce anti-bacterial activity.

The choline and colamine derivatives **18** and **19** developed by the Zablotskaya group shown previously in this review (Fig. 9) also displayed good anti-bacterial activity when screened against two Gram-positive (*Bacillus cereus* ATCC 11778 and *Staphylococcus aureus* ATCC 25923) and two Gram-negative (*Proteus mirabilis* NCIM 2241 and *Escherichia coli* ATCC 25922) bacteria using the agar dish diffusion method.[281] The results showed that the non-silylated parent compound showed no activity, whereas the silylated analogues displayed comparable or improved activities when compared to the standard anti-microbials, gentamicin and piperacillin. Furthermore, *O*-decyl substituted derivatives of tetrahydroisoquinoline and thiazolium organosilicon salts (Fig. 9) have been reported by the same group. These, in addition to having good anti-tumour activity, displayed good anti-bacterial and anti-fungal properties, suggesting their potential as monotherapeutic agents for the treatment of bacterial and/or fungal infections in cancer patients.

In 2023, Bishai, Yu and co-workers, investigated triazole derivatives as inhibitors of mycobacterial membrane protein large 3 (MmpL3) for the treatment of *Mycobacterium tuberculosis*.[435] The silicon-containing **206** (Fig. 68) emerged as the most promising drug candidate from 37 compounds synthesized and showed >90% inhibition at concentrations as low as 0.03125 μg mL^{-1}, while showing negligible cytotoxicity. Furthermore, compound **206** was eight times more potent than its unsilylated analogue **207**, an observation which the researchers explained was probably due to increased hydrophobic interactions of **206** with the target protein.

In 2022, Cebrián, Kuipers, Morales *et al.* investigated modifications of the well-known natural product resveratrol by converting this molecule into its respective silyl ethers (Fig. 69).[436] In terms of activity, the resveratrol silyl ethers **208** showed inhibitory activity against several strains of Gram-positive bacteria at micromolar concentrations (MIC 4–128 μM). Their mode of action involved membrane

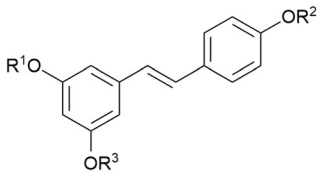

208

R^1, R^2, R^3 = H, SiEt$_3$, Si(*i*-Pr)$_3$, SiMe$_2$*t*-Bu, SO_3^-

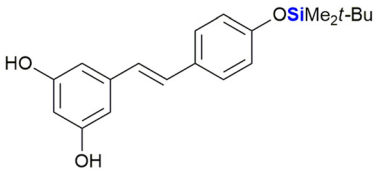

209

Fig. 69 Anti-bacterial silyl ether derivatives of resveratrol.

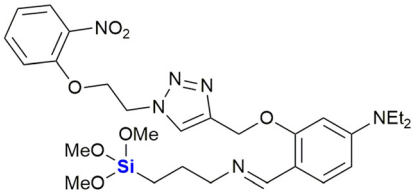

211

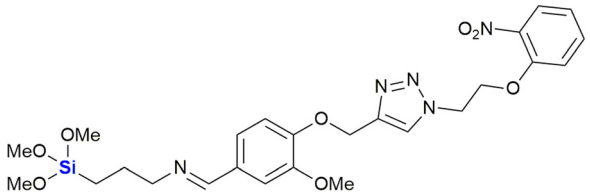

212

Fig. 71 Anti-bacterial silicon-containing 1,2,3-trizoles.

permeability and ionophore-related activities. While some of the silyl ethers were also quite cytotoxic, with IC_{50} values against MRC5 cells of up to 1.8 μM, the silyl ether **209** showed low cytotoxicity, all the while maintaining high bactericidal activity. Furthermore, some synergistic effects with traditional antibiotics were observed. In 2022, Choudary and co-workers reported the design of novel zinc ionophores **210** (Fig. 70).[437] The researchers determined that introduction of a lipophilic silyl group *ortho* to the phenol shielded the hydrophilic part of the complex and thus increased cellular membrane permeability.

The silyl group also lowered the binding affinity to Zn(II) ions which improved the compounds' ability to release Zn(II) ions after transporting them across a cell membrane. In bioactivity assays, the silylated zinc ionophores **210** showed anti-bacterial activity against various Gram-positive bacteria strains, for example *Straphylococcus epidermidis*, showed growth inhibition at concentrations as low as 1.2–8.4 μg mL^{-1}. In terms of other characteristics, while commercial pyrithione showed comparable activity, the silylated zinc ionophores **210** showed much lower cytotoxicity against human cells.

Very recently (2023), the silicon-containing triazoles **211** and **212** (Fig. 71) were evaluated for their anti-bacterial properties.[438] In this research, it was demonstrated by Singh *et al.* that the triazoles showed weak activity against *Escherichia coli* and *Pseudomonas aeruginosa* (**211:** 6.3 mg mL^{-1}; **212:** 15 mg L^{-1}), yet moderate activity against *Straphylococcus aureus* (**211:** 0.195 mg mL^{-1}; **212:** 1.87 mg mL^{-1}). Finally, **211** was indicated to be a potential inhibitor of the DNA gyrase from *S. aureus* by molecular docking predictions.

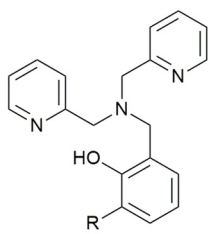

210

R = SiMe$_3$, SiEt$_3$, Si(*i*-Pr)$_3$, SiMe$_2$*t*-Bu, SiPh$_2$*t*-Bu

Fig. 70 Silylated zinc ionophores with anti-bacterial properties.

Dhingra *et al.* studied the anti-bacterial properties of silicon complexes with imine ligands (Fig. 72).[439] While both complexes **213** and **214** inhibited the growth of several Gram-positive and Gram-negative bacteria strains, **214** was generally more active and even surpassed the activity of streptomycin against *Staphylococcus aureus* (MIC 1.56 μL mL^{-1}). The researchers also determined that complex **214** possessed anti-fungal activity comparable to fluconazole. In another study, Singh *et al.* investigated the anti-bacterial effects of silicon complexes with amino acid-derived imine ligands. The zone of inhibition against Gram-positive and Gram-negative bacteria were measured and quantitative SARs were investigated. Generally, complexes **215** were more active than **216** and the serine derived ligands were more potent than ligands derived from other amino acids.[440]

Adamovich and coworkers reported the synthesis and anti-bacterial properties of silatrane pyrrole-2-carboxamide hybrids which were linked by an amide bond (Fig. 73). Generally, these compounds were more active against Gram-positive bacteria than Gram-negative bacteria. Compound **217** showed high activity against Gram-positive *Enterococcus durans* (MIC = 3.1 μg mL^{-1}) and *Bacillus subtilis* (MIC = 6.2 μg mL^{-1}), whereas **218** showed the highest activity against Gram-negative *Escherichia coli* (MIC = 62.5 μg mL^{-1}).[441]

Adamovich and co-workers furthermore investigated the anti-bacterial properties of a series of isoxazole derivatives of γ-aminopropylsilatranes (Fig. 74). Among these compounds, **219** showed high activity against *Enterococcus durans* (MIC = 12.5 μg mL^{-1}) and *Bacillus subtilis* (MIC = 6.2 μg mL^{-1}).[442]

Singh *et al.* reported the synthesis of silatrane dithiocarbamate **220** and investigated its anti-bacterial

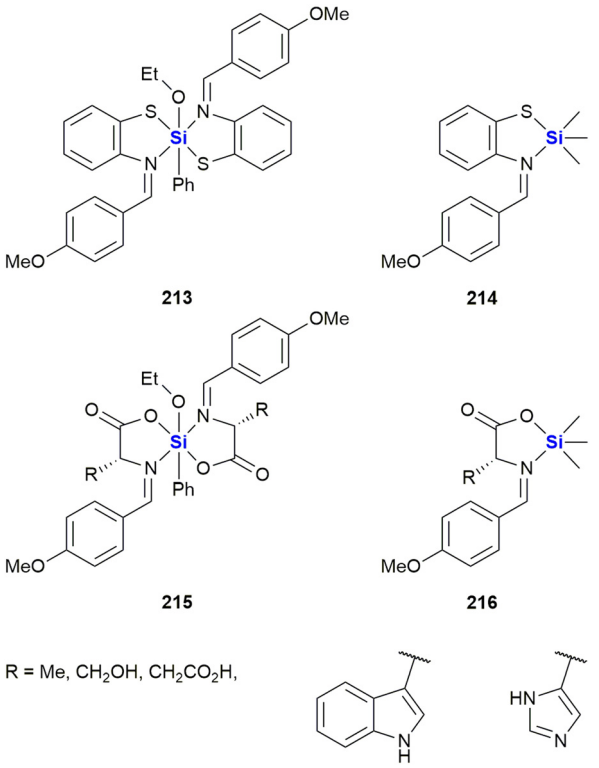

Fig. 72 Anti-bacterial silicon complexes with imine ligands.

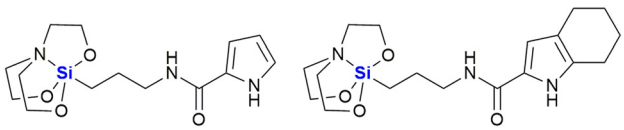

Fig. 73 Anti-bacterial silatrane pyrrole-2-carboxamide hybrids.

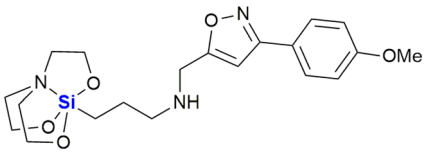

Fig. 74 Anti-bacterial isooxazol derivatives of γ-aminopropylsilatrane.

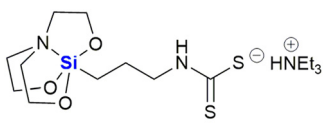

Fig. 75 Anti-bacterial silatrane dithiocarbamate **220**.

properties (Fig. 75). Compound **220** weakly inhibited the growth of *Bacillus subtillus* (MIC 0.8–3.94 mg mL^{-1}) and *Escherichia coli* (MIC = 0.765–3.62 mg mL^{-1}).[443]

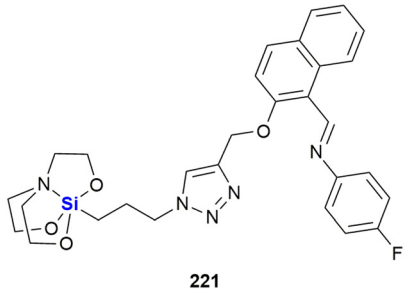

Fig. 76 Anti-bacterial silatrane-containing imines.

In 2018, Singh *et al.* connected a series of imines to a silatrane group by forming a triazole linker using click-chemistry (Fig. 76). Compound **221** showed the most potent anti-bacterial activity and inhibited the growth of both Gram-negative (MIC = 13.25–26.5 μg mL^{-1}) and Gram-positive (MIC = 3.25 μg mL^{-1}) bacteria.[444]

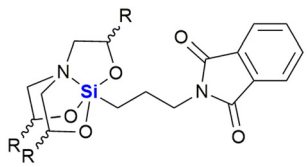

Fig. 77 Anti-bacterial silatrane containing phthalimides (note that the stereochemistry of the silatrane unit was not given in the original publication).

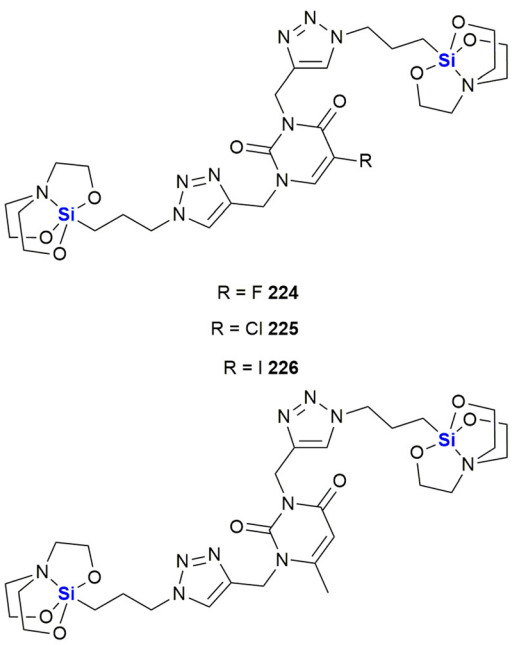

Fig. 78 Anti-bacterial silatrane containing thymine and 5-halo uracil derivatives.

Singh *et al.* also investigated the anti-bacterial properties of silatrane-containing phthalimides (Fig. 77). Compounds **222** and **223** showed similar but moderate activity against *Staphylococcus aureus*, *Acinetobacter baumannii*, *Pseudomonas aeruginosa* and *Escherichia coli* with MICs in the range of 0.20–0.25 mg mL^{-1}.[445] For the anti-cancer activity of structurally related amino derivatives of trimethylsilyl-containing 4-azatricyclo-[5.2.1.02,6]dec-8-ene-3,5-diones see the research of Napiórkowska *et al.*[446]

In another study, Singh *et al.* synthesised derivatives of 5-halo uracils (**224–226**) and thymine (**227**) containing two silatrane moieties (Fig. 78). These compounds were tested against *Escherichia coli*, *Bacillus subtillus*, *Staphylococcus aureus* and *Vibrio cholera* using a microbroth dilution assay and MIC_{50} values were in the range of 0.18–0.33 mg mL^{-1}.[447]

In 2023, Adamovich *et al.* reported the Michael addition of 3-aminopropyl-silatrane to several unsaturated nitriles, esters and amides yielding the silatranes **228–230** (Fig. 79).[448] While these compounds inhibited the growth of several Gram-positive and Gram-negative bacterial strains at high concentrations of >100 μg mL^{-1}, they stimulated bacterial growth at lower concentrations of <12 μg mL^{-1}. Further *in silico* investigations predicted anti-neoplastic and macrophage colony stimulating activity of these silatranes.

Baghershiroudi *et al.* reported the synthesis of the sulphur- and silyl-containing tetrazoles **231–233** and the evaluation of their anti-bacterial properties against several Gram-positive and Gram-negative strains (Fig. 80). Thiones **231** showed promising activities with MICs in the range of 3.91–31.25 μg mL^{-1} for the most potent derivative. The thioalkynes **232** showed lower activity, whereas the tris(trimethylsilyl) compounds **233** showed no anti-bacterial activity at all.[449]

Anti-fungal agents

The Zablotskaya's group's choline and colamine derivatives **18** and **19** also displayed anti-fungal activity when screened against two fungi strains, *Candida tropicalis* ATCC 4563 and *Candida albicans* ATCC 2091 (Fig. 9).[281] When compared to the standard anti-fungals, nystatin and fluconazole, both the silylated and non-silylated parent compounds displayed comparable activity to nystatin, but in all but one case were not as potent as fluconazole.

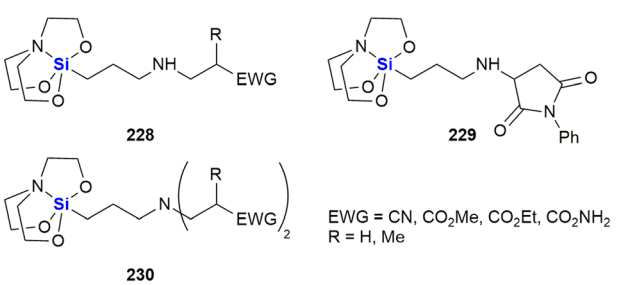

Fig. 79 Bioactive Michael adducts of 3-aminopropylsilatranes.

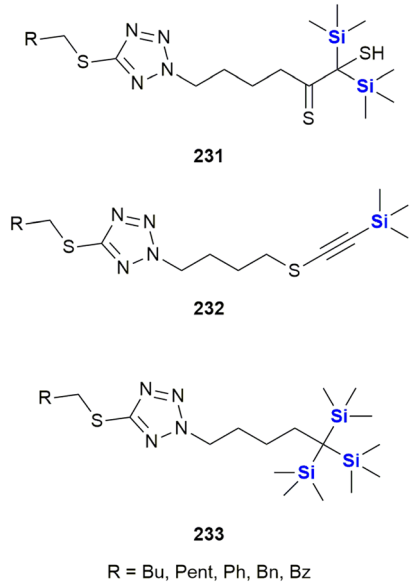

Fig. 80 Sulphur- and silicon-containing anti-bacterial tetrazoles.

In 2015, Reddy and co-workers reported the development and anti-fungal screening of a series of silicon analogues of the known anti-fungals, fenpropimorph **234**, amarolfine **235** and fenpropodin **236** (Fig. 81).[450] A small library of 15 sila-analogues were prepared of which 12 (**237–248**) showed potent activity against *C. albicans*, *Candida glabrata*, *C. tropicalis*, *Cryptococcus neoformans*, and *Aspergillus niger*. The most potent candidate of the new silicon-containing molecules was compound **245**, which displayed better anti-fungal activity than fluconazole, fenpropimorph and fenpropodin across all five pathogen lines. In addition, the MIC values for **245** were comparable or better than those of amorolfine, as it elicited the most potent fungicidal effect against all of the tested strains.

Fu, Liao and co-workers have reported the development of an octahedral silicon complex as a potent anti-fungal agent. Their study involved an effort to prepare silicon complexes as template-analogues of ruthenium complexes which had previously been shown to display a range of biological activities.[451]

The use of silicon was anticipated to allow the formation of more stable and less toxic complexes. To this end, complex **249** was prepared and shown to exhibit significant inhibition of the growth of the fungus, *C. neoformans* with MIC and MFC of 4.5 and 11.3 μM respectively. Compound **249** was also shown to act in a fungicidal manner against both the proliferative and quiescent *Cryptococcus* cells (Fig. 82).

Bargan *et al.* reported the synthesis the anti-bacterial and anti-fungal properties of imine derivatives of

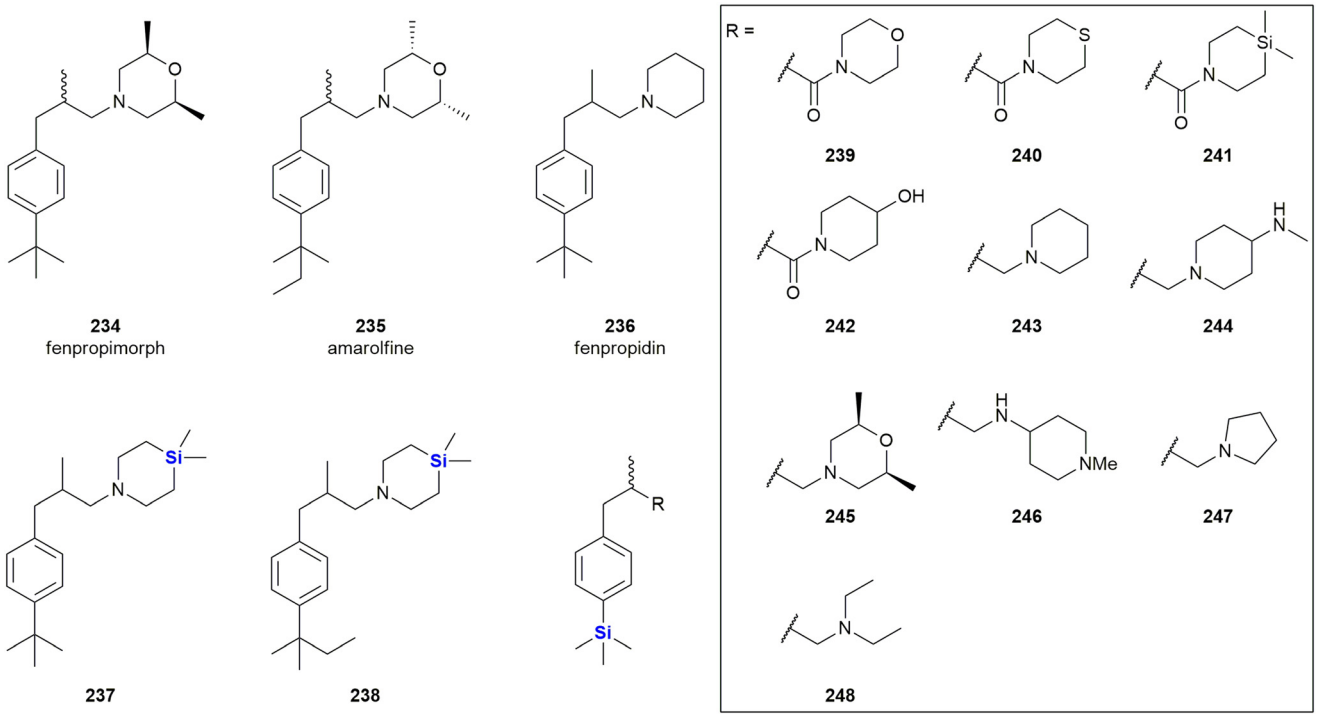

Fig. 81 Anti-fungal fenpropimorph **234**, amarolfine **235** and fenpropodin **236** and silicon-containing analogues **237**–**248**.

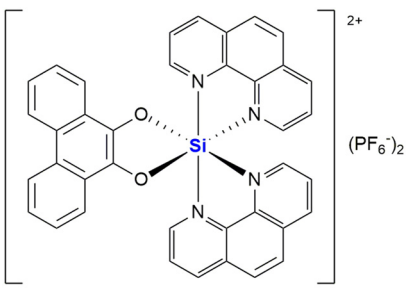

Fig. 82 Anti-fungal silicon arenediolate complex **249**.

γ-aminopropylsilatranes **250**–**252** (Fig. 83). **250** showed high anti-fungal activity against *Aspergillus fumigatus*, *Penicillium chrysogenum* and *Fusarium* (MIC = 0.08 μg mL^{-1}) while no anti-bacterial activity was reported. Compounds **251** and **252** were inactive.[452]

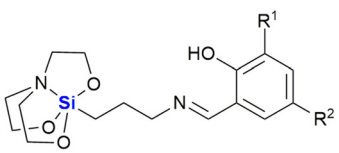

250 R^1 = H, R^2 = OMe
251 R^1 = R^2 = Cl
252 R^1 = R^2 = *t*-Bu

Fig. 83 Anti-fungal γ-aminopropylsilatrane-coupled imines.

Anti-parasitic agents

Smith and co-workers described the preparation and anti-parasitic activity of ferrocenyl- and aryl-functionalised organosilanethiosemicarbazones which were converted into half-sandwich ruthenium(II) and rhodium(III) complexes (**253**–**262**) (Table 3).[453] The complexes were assessed for activity against chloroquine-sensitive (NF54) and resistant (Dd2) *Plasmodium falciparum* strains and found to have activities in the range of 2.92–7.81 μM and 1.01–6.66 μM respectively. Although marginally less active than the non-silicon analogues (2.57–3.41 μM and 1.01–2.29 μM for NF54 and Dd2 respectively), the inclusion of the silicon atoms reduced cytotoxicity towards a Chinese hamster ovarian cell line. Limited additional screening against the G3 strain of *Trichomonas vaginalis* suggested that the silicon-containing compounds were more effective than the non-silicon ones.

Smith and co-workers also synthesised two silicon-containing chloroquine analogues **263** and **264** and derived a series of transition metal complexes **269**–**278** of these scaffolds (Fig. 84).[454] Both the free quinolines and their ruthenium and rhodium complexes showed potent activity against a chloroquine-sensitive strain of *Plasmodium falciparum* (NF54), but only lower activity against the chloroquine-resistant strain Dd2. Generally, it was found that a longer alkyl chain increased anti-plasmodial activity. Of additional interest was that although the compounds showed weak anti-mycobacterial activity against *Mycobacterium tuberculosis* $H_{37}R_v$ they demonstrated fairly potent anti-

Table 3 Ferrocenyl- and aryl-functionalised organosilanethio-semicarbazones (**253**–**262**)

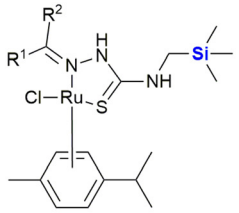

253 R^1 = Ferrocene, R^2 = H
254 R^1 = Ferrocene, R^2 = Me
255 R^1 = 3,4-dichlorobenzene, R^2 = H
256 R^1 = 3,4-dichlorobenzene, R^2 = Me

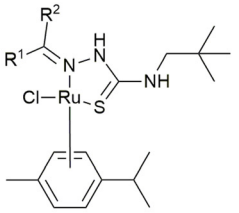

257 R^1 = 3,4-dichlorobenzene, R^2 = Me

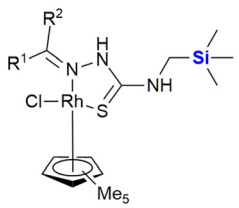

258 R^1 = Ferrocene, R^2 = H
259 R^1 = Ferrocene, R^2 = Me
260 R^1 = 3,4-dichlorobenzene, R^2 = H
261 R^1 = 3,4-dichlorobenzene, R^2 = Me

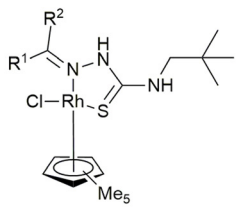

262 R^1 = 3,4-dichlorobenzene, R^2 = Me

	253	254	255	256	257
IC_{50} (μM) NF54	—	7.81	2.92	4.19	2.57
IC_{50} (μM) Dd2	—	—	4.28	6.66	2.29

	258	259	260	261	262
IC_{50} (μM) NF54	1.80	—	3.73	1.31	3.41
IC_{50} (μM) Dd2	2.27	—	3.11	1.18	1.01

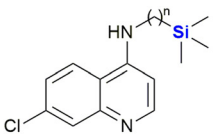

	263 n = 1	**264** n = 3
NF54	248.08 nM	97.65 nM
Dd2	524.74 nM	269.74 nM

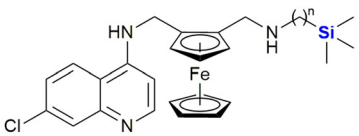

	265 n = 1	**266** n = 3
NF54	13.32 nM	31.37 nM
Dd2	13.40 nM	27.13 nM

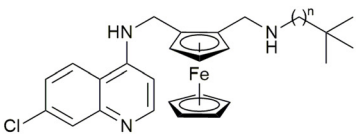

	267 n = 1	**268** n = 3
NF54	6.90 nM	11.45 nM
Dd2	13.87 nM	35.57 nM

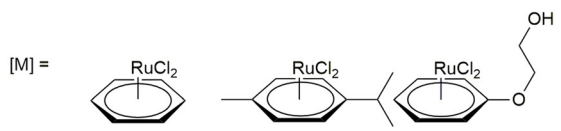

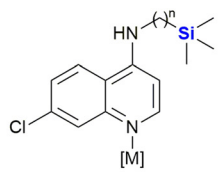

	269 n = 1	**270** n = 1	**271** n = 1	**272** n = 1	**273** R = H, n = 1
NF54	61.40 nM	276.83 nM	270.23 nM	459.54 nM	306.69 nM
Dd2	>1749 nM	526.56 nM	835.09 nM	>1955 nM	>1742 nM

	274 n = 3	**275** n = 3	**276** n = 3	**277** n = 3	**278** R = H, n = 3
NF54	71.70 nM	81.61 nM	151.92 nM	101.22 nM	134.73 nM
Dd2	211.77 nM	228.96 nM	385.61 nM	721.13 nM	294.62 nM

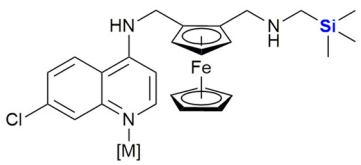

	279	**280**	**281**	**282**	**283** R = Me
NF54	30.73 nM	8.27 nM	4.96 nM	28.03 nM	10.36 nM
Dd2	42.99 nM	42.73 nM	36.64 nM	77.19 nM	34.33 nM

Fig. 84 Anti-plasmodial quinolines with an organosilane side chain.

tumour activity against the oesophageal WHCO1 cancer cell line (IC_{50} = 4.41–51.92 μM).

The same group reported the synthesis of ferrrocenyl-functionalised quinolines **265** and **266** with a silylated side chain (Fig. 84). These compounds were evaluated for their anti-plasmodial properties.[455] The compounds were found to be less active than their carbon analogues **267** and **268** against the chloroquine-sensitive strain of *Plasmodium falciparum* NF54 (IC_{50} = 13.32–31.37 nM), but, in contrast to the carbon analogues, did not lose activity when tested against the chloroquine-resistant strain Dd2 (IC_{50} = 13.4–27.1 nM). Furthermore, compounds **265** and **266** also inhibited

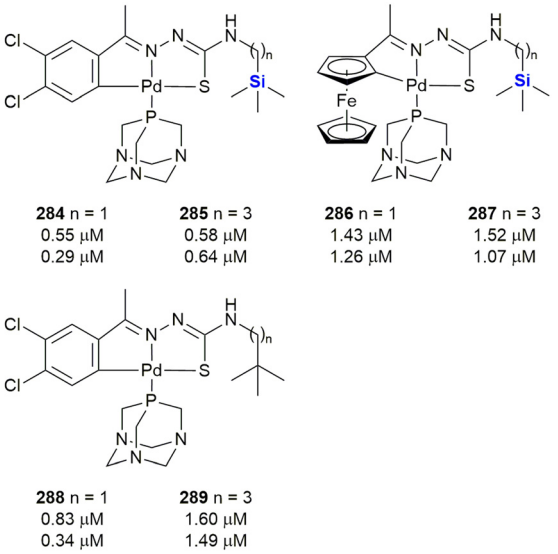

Fig. 85 Thiosemicarbazone palladium complexes with an organosilane side chain.

the growth of *Trichomonas vaginalis* by 24% and 77%, respectively, at a concentration of 50 μM.

In a subsequent study, ruthenium and rhodium complexes **279–283** were investigated, some of which displayed even higher activity than the parent quinoline **265**.[456]

Adams *et al.* reported the synthesis and anti-plasmodial properties of palladacycles **284–289** with thiosemicarbazone ligands (Fig. 85). The compounds were again tested against a chloroquine sensitive (NF54) and a chloroquine resistant strain (NFDd2) of *Plasmodium falciparum* and showed similar activity against both strains at micromolar concentrations. The free ligands were also tested, but showed much lower activity than their corresponding palladacyclic complexes, especially against the chloroquine resistant strain.[457]

In 2016, Singh and co-workers published their efforts in the design and synthesis of molecules based on chalcones

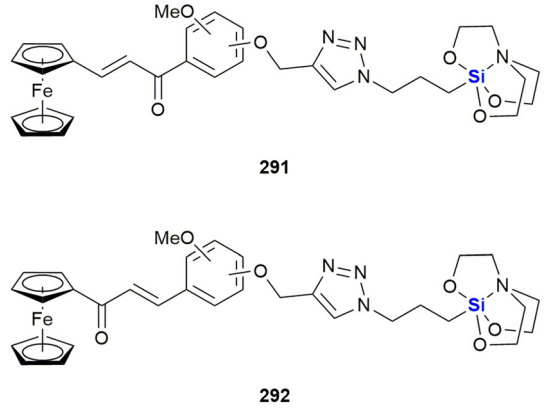

Fig. 86 Anti-parasitic silatranes.

connected *via* triazole linker to silatranes, such as generalized example **290**, as anti-parasitics targeting giardicidal and trichomonacidal unicellular paraites (Table 4).[458] The compound libraries prepared all showed potent activity against *Giardia lamblia* and *Trichomonas vaginalis* with IC_{50} value ranges from 19.58–131.2 μM and 18.24–101.26 μM respectively. Almost the entire library displayed better activity than the current therapeutic treatment involving the drug metronidazole. The group further published data on related anti-parasitic and anti-oxidative pyrene-functionalised silatranes showing activity against *Giardia lamblia* and *Entamoeba histolytica*.[459,460]

Singh *et al.* reported the synthesis of a series of hybrid molecules **291** and **292** with a chalcone and a silatrane group (Fig. 86). While the anti-bacterial and anti-fungal activity was low, they showed potent activity against *Giardia lamblia* (up to IC_{50} = 0.57 μM after 24 h) and *Trichomonas vaginalis* (up to IC_{50} = 57.72 μM after 24 h).[461]

Singh *et al.* also reported the synthesis of pyrene functionalised silatranes **293** and **294** (Fig. 87). Compound **293** showed slightly lower anti-parasitic activity than the methylated silatrane **294** against *Giardia*

Table 4 Anti-plasmodial activity of chalcone containing silatranes **290**

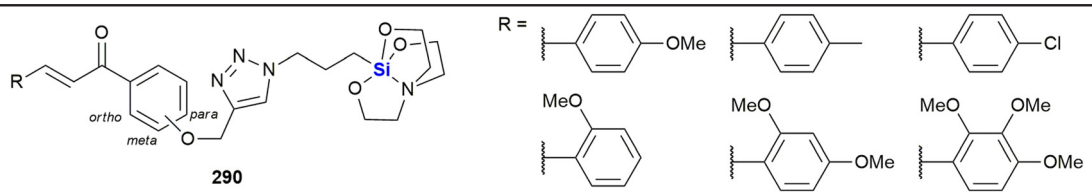

	ortho		*meta*		*para*	
R	*G. lamblia*	*T. vaginalis*	*G. lamblia*	*T. vaginalis*	*G. lamblia*	*T. vaginalis*
Ph	59.695	27.24	28.08	23.26	80.96	65.595
4-MeOPh	54.855	21.605	32.16	26.69	NS	30.275
2-MeOPh	40.94	22.69	NS	23.81	43.73	43.125
2,4-MeOPh	31.945	22.855	35.395	22.125	43.885	43.805
2,3,4-MeOPh	30.175	18.245	NS	21.265	19.58	42.095
4-MePh	33.245	24.82	47.995	50.025	131.2	101.265
4-ClPh	33.08	21.925	33.935	22.27	78.45	55.68
Metronidazole	62.48 μM (for *G. lamblia*) 55.85 μM (for *T. vaginalis*)					

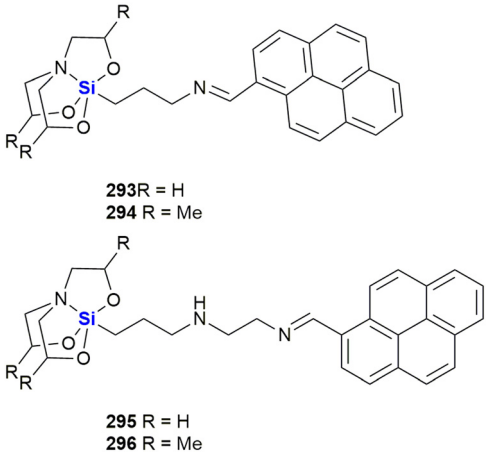

Fig. 87 Anti-parasitic pyrene functionalised silatranes.

lamblia (IC_{50} = 53.27–63.06 μM) and *Tryposomas vaginalis* (IC_{50} = 1.75–3.40 μM).[459]

Later, the same group reported the synthesis of the closely related pyrene functionalised silatranes **295** and **296** with an additional ethylenediamine linker (Fig. 87). Interestingly, the **295** showed higher activity than its methylated counterpart **296** against *Giardia lamblia* (IC_{50} = 0.56 μM and 44.55 μM, respectively) but lower activity against *Entamoeba histolytica* (IC_{50} = 56.91 μM and 1.14 μM, respectively).[460]

In 2023, San Nicolás-Hernández *et al.* investigated 24 silylated derivatives of the known leishmanicidal and trypanocidal drug. Withaferin A **297** and its 4-dehydro congener **298**, in order to optimize their respective ADMET profiles (Fig. 88).[462] Most of the silyl ethers showed higher anti-parasitic activity than the established reference drugs, miltefosine and benznidazole.

Anti-inflammatory agents

Geronikaki *et al.* have reported the synthesis of silicon-containing thiazole derivatives **299** as both lipoxygenase and anti-inflammatory agents (Fig. 89).[463] The class of compounds was found to possess good anti-inflammatory action (55% CPE inhibition at a dose of 0.01 mmol kg^{-1} for **299**), mild protection against edema formation and inhibition against soybean lipoxygenase. The substituent at the 4-position of the

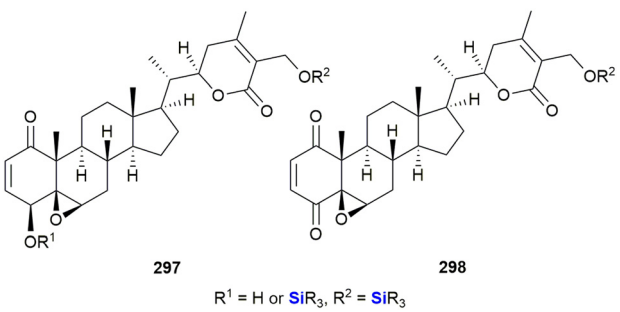

Fig. 88 Silyl ether derivatives of withaferin A (**297**) and 4-dehydrowithaferin A (**298**).

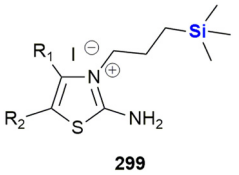

Fig. 89 Silicon-containing thiazole derivatives with anti-inflammatory activity.

thiazole ring was linked to lipoxygenase inhibition and cytotoxicity, with the most potent inhibitor (IC_{50} LOX 0.01 mM) containing a bulky *p*-MeOPh-group at this position. It was further shown that increasing the distance between the thiazole ring and the piperidyl ring in both the silyl- and non-silyl compounds was linked to an increase in cytotoxicity.

Ibuprofen **300** is the gold standard NSAID used for pain management (Fig. 90),[464,465] and recently Beckmann, Grabowsky and co-workers reported the synthesis and bioevaluation of sila-ibuprofen **301**. In this research the sila-analogue was designed to contain a $SiHMe_2$ group as a bioisostere for the isobutyl group in ibuprofen. Furthermore, the sila-analogue **301** displayed a similar inhibitory profile to ibuprofen when screen against COX-I and COX-II, but with improved solubility characteristics. Pérez *et al.* prepared esters and amides **302** from ibuprofen with a silicon containing alkyl chain.[466] These derivatives were tested for their anti-inflammatory properties by testing them against nuclear factor κβ, a transcription factor which is involved in inflammation response and chronic inflammatory diseases. While the esters did not inhibit NF-κβ, the amides showed potent activity (IC_{50} = 45.5–92.0 μM) and performed even better than ibuprofen (IC_{50} = 241.5 μM). Further work performed by these researchers included *in vivo* and *in silico* studies on the novel silicon-containing ibuprofen derivatives synthesized.[467]

In 2007, Barnes *et al.* reported the synthesis of two silylated derivatives (**304** and **305**) of the p38 mitogen-activated protein (MAP) kinase inhibitor BIRP-796 (**303**) and investigated their anti-inflammatory activity (Fig. 91).[468] The researchers demonstrated that **304** (IC_{50} = 64 nM) showed similar activity to **303** (IC_{50} = 55 nM), but was more stable in human liver microsomes. Compound **305** was only briefly investigated and showed low nanomolar activity.

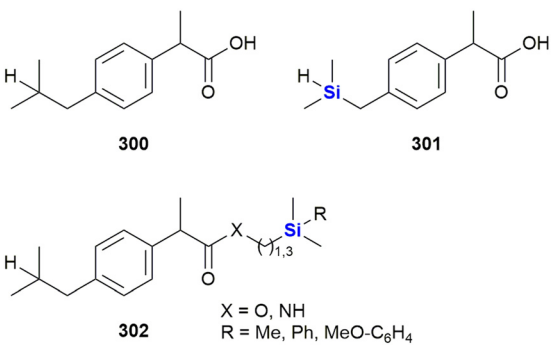

Fig. 90 Ibuprofen **300** and sila-analogues **301** and **302**.

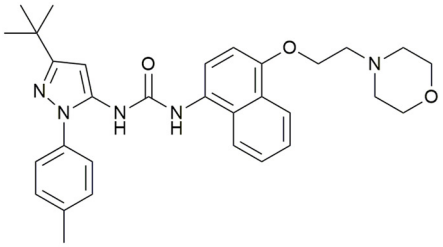

303

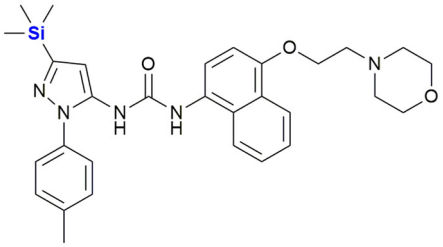

304

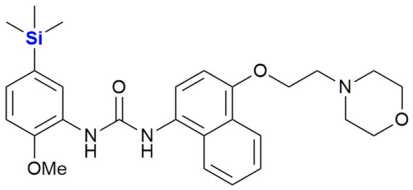

305

Fig. 91 p38 MAP kinase inhibitors BIRP-796 **303** and sila-analogues **304** and **305**.

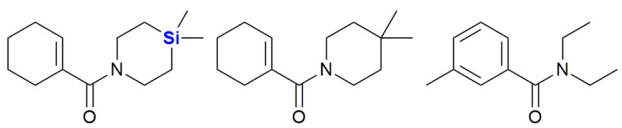

306 307 308

Fig. 92 Sila-piperidine amide mosquito repellent.

In 2021, Sen, Reddy and co-workers identified the sila-piperidine amide **306** (Fig. 92) as a potent mosquito repellent.[469] The investigators demonstrated that **306** provided protection from *Anopheles aegypti* for 756 ± 5 min at a dose of 0.5 mg cm^{-2} and was more effective than its carba-analogue **307** (520 ± 4 min) and the common insect repellent, *N*,*N*-diethyl-3-methyl benzamide (DEET) **308** (616 ± 5 min).

Shete *et al.* reported the synthesis of a series of cannabigerol (**309**, CBG) and cannabidiol (**310**, CBD) analogues, among these the silylated chinones **311** and **312** (Fig. 93). They found that **311** and especially **312** possessed potent anti-inflammatory activity against heme-induced NLRP3 inflammasome by inhibiting several cytokines (IL-1β, TNF-α, IL-6) at concentrations of 10 μM. The compounds showed no cytotoxicity *in vitro* against J774A.1 cells.

The anti-inflammatory activity of CDB-analogue **312** was further investigated *in vivo* and significantly decreased heme-induced IL-1β levels in mice. This suggests that **312** could be

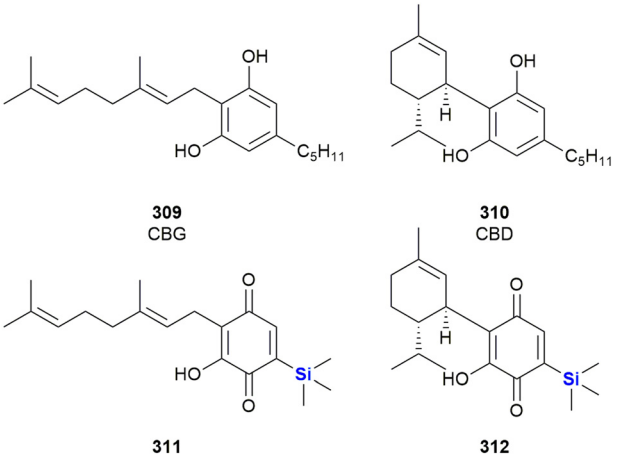

309 CBG 310 CBD

311 312

Fig. 93 Anti-inflammatory silicon-containing CBD-analogues.

a potential drug candidate against diseases such as sickle cell anemia and thalassemia which involve activation of the NLRP3 inflammatory response by hemolysis.[470]

Cardiovascular diseases

Sieburth and co-workers have reported the synthesis and biological evaluation of a range of silanediol peptidomimetics as transition state analogue inhibitors of several hydrolases. That the silanediol group is indeed essential for the activity of such compounds was proven by Sieburth and co-workers by the synthesis of the pair of silanol **313** and silanediol **314** (Fig. 94). While the mixture of diastereomers of **314** inhibited ACE with an IC_{50} of 14 nM, replacing one of the OH groups by a methyl group caused a significant drop of activity of the diastereomeric mixture of **313** (IC_{50} = 3040 nM).[471]

In a subsequent study, Sieburth and co-workers reported the synthesis and biological evaluation of a silanediol peptidomimetic **316** as an angiotensin-converting enzyme

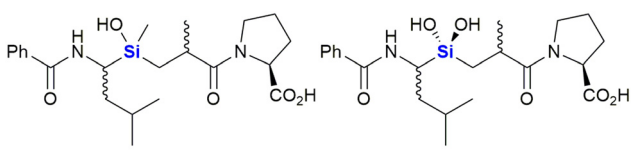

313 314

Fig. 94 Silanol and silanediol peptidomimetic **313** and **314** targeting ACE.

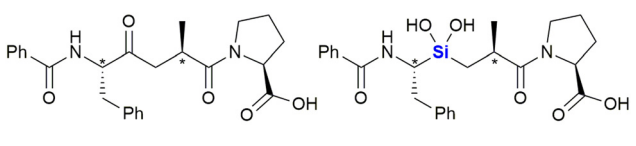

315 316

Fig. 95 Ketone **318** and silanediol **319** targeting ACE. The asterisks indicate variable stereocentres.

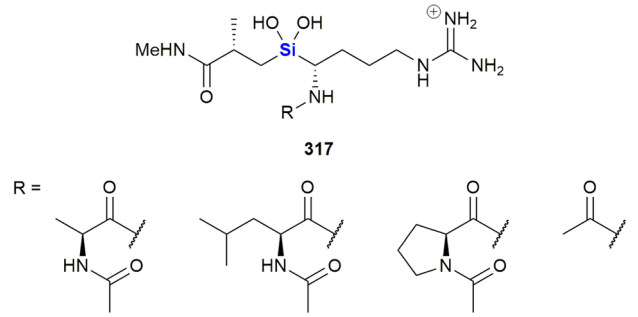

Fig. 96 Silanediol peptidomimetics targeting FXIa.

(ACE) inhibitor,[472] which was based on the ketone inhibitor **315** reported by Almquist and co-workers.(Fig. 95).[473–475]

Inhibition was shown to be highly stereo-dependent. The *R*,*S*,*S* configuration was most active in both the parent ketone **315** (IC_{50} = 1 nM) and the silanediol **316** (IC_{50} = 3.8 nM). In comparison, the other ketone (IC_{50} = 8.2, 46 and 3200 nM) and silanediol diastereomers (IC_{50} = 19, 207 and 72 nM) were significantly less active. Interestingly, in the case of the least active ketone diastereomer (IC_{50} = 3200 nM), the corresponding sila-analogue displayed an unusually low IC_{50} value of 72 nM suggesting that the silanediol may be better able to adapt its conformation for the required biochemical interactions. The Sieburth group also published research based on further efforts towards the development of improved stereoselective syntheses of a variety of silanol peptidomimetics, this time as protease inhibitors.[476] The reader is further referred to a micro review on the subject of silandiols as protease inhibitors by the same authors.[477]

More recently, in 2018, Sieburth and Duong reported on the asymmetric synthesis of silanediol peptidomimetics **317** targeting the serine protease coagulation cascade enzyme FXIa (Fig. 96). These efforts were aimed at the development of a novel thrombosis treatment.[478] The prepared Arg-[Si]-Ala analogues represented the first silanediol dipeptide to carry a guanidine group, and it should be noted that inhibition of Factor Xia catalysis is still to be reported.

The authors further reported on the preparation and structural analysis of silanediols as transition-state-analogue inhibitors of the metalloprotease thermolysin (Fig. 97).[479–481] Notably, the replacement of the phosphinic acid (**318**) with a silanediol afforded an organosilane which was determined to bind to a natural receptor with the silicon atom interacting with the binding site.

The activities reported (K_i = 40 nM) were comparable to previously reported phosphorus analogues like **319** (K_i = 10 nM), this despite the fact that the silanediols are electronically neutral whilst the phosphorus groups are anionic in nature.

Captopril **320** (Fig. 98) is also a competitive inhibitor of the angiotensin converting enzyme (ACE) and used to treat hypertension. Dalkas *et al.* reported the design and synthesis of its silicon-analogue **321**, which was synthesised as a diastereomeric mixture and used as such in *in vitro studies*.[482] So called silacaptopril **321** (IC_{50} = 43 nM) showed lower inhibitory activity against ACE than its carbon analogue **320** (IC_{50} = 6.3 nM). In addition, docking studies revealed that captopril *S*,*S*-**320** and silacaptopril, although modelled *in silico* as pure *S*,*R*-**321**, adopted similar orientations into the ACE ligand binding site. In addition, the modelling software predicted a higher docking score for *R*,*S*-**321**.

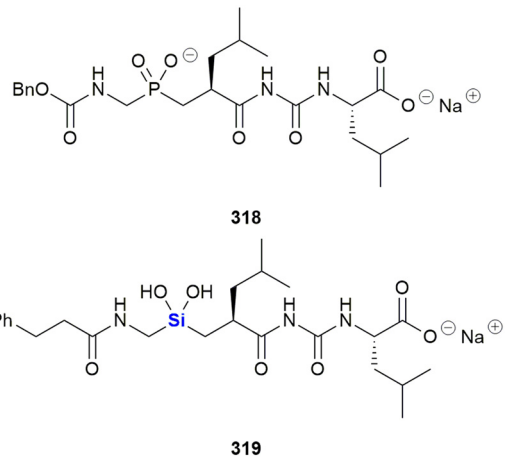

Fig. 97 Silanediol peptidomimetic targeting thermolysin.

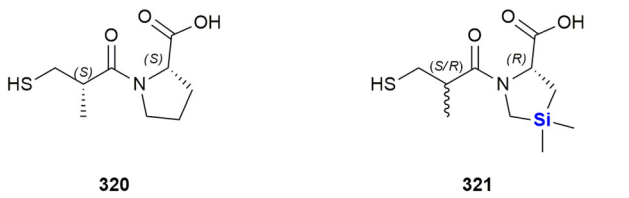

Fig. 98 Captopril **320** and silacaptopril **321**.

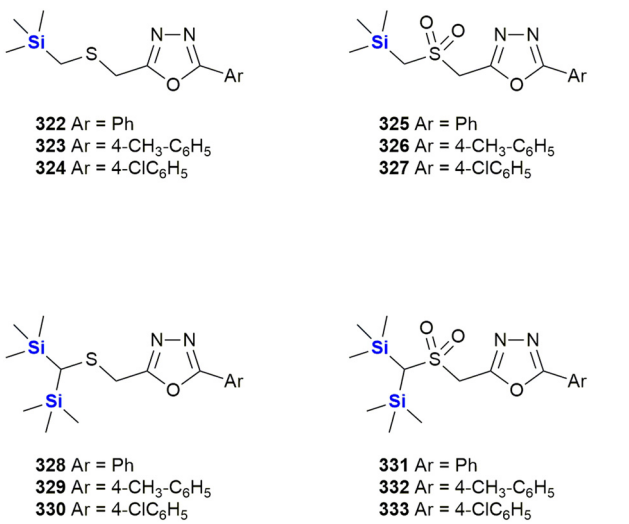

Fig. 99 Anti-allergic silicon-containing oxadiazoles.

Anti-histamine agents

The Reddy group has demonstrated how the incorporation of silicon into oxadiazoles afforded histaminic suppressors **322–327** that were more effective than the typically prescribed anti-histamine, diphenylhydramine (DPH) (Fig. 99).[483] The efficacy of **327** was evaluated using RBL-2H3 as an *in vitro* model and an *in vivo* anaphylactic mouse model. It was observed that the silyl compound suppressed DNP-HAS-induced mast cell degranulation, as well as the expression of THF-α mRNA and Akt phosphorylation in antigen-stimulated RBL-2H3 cells.

The same group later introduced the derivatives **328–333** with two instead of one TMS groups (Fig. 99).[484] Among this set of compounds, the sulphones **331–333** showed higher anti-allergic activity than the thioethers **328–330** and seemed to surpass slightly the activity of their mono-silylated counterparts. While **331** was most active, its cytotoxicity made the other sulphones more promising as potential therapeutic leads.

Diabetes

Tacke and co-workers reported the synthesis and biological evaluation of silicon-containing GPR81 and GPR109A agonists which are potential targets for certain metabolic diseases and type 2 diabetes (Fig. 100).[485] During the study, several 6-sila-4,5,6,7-tetrahydrobenzo[*d*]thiazoles were synthesised, and the role of the quaternary silicon atom was studied by contrasting the activity of the new compounds against their respective non-sila variants **334** and **336**. Sila-analogues **335** and **337** showed high GPR81 and GPR109A potency. The EC_{50}'s of **335** were in the range of 1.0–4.4 μM (GPR81) and 1.2–4.8 μM (GPR109A), while the pyrazole analogues **337** were generally more active with EC_{50}'s in the range of 0.21–2.2 μM (GPR81) and 0.47–1.8 μM (GPR109A). In contrast, the non-silylated parent compounds **334** (EC_{50} = 0.24 μM against GPPR81 and 2.1 μM against GPR109A) and **336** (EC_{50} = 0.018 μM against GPPR81 and 0.25 μM against GPR109A) generally showed higher activity. In terms of metabolic stability, the sila-analogues displayed comparable or slightly improved stabilities relative to **334** and **336**.[485]

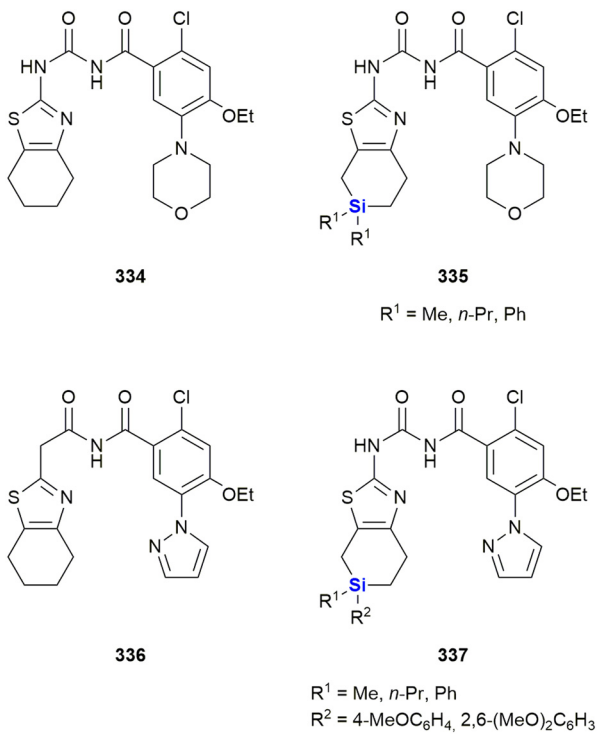

Fig. 100 Silicon-containing GPR81 and GPR109A agonists.

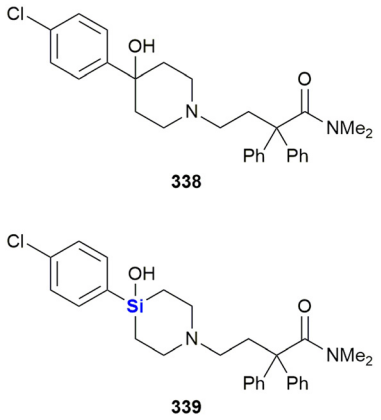

Fig. 101 Loperamide **341** and sila-loperamide **342**.

Anti-diarrheal agents

In 2015, Tacke and co-workers also developed a silicon analogue of loperamide **338**, an opioid receptor agonist which is used clinically as an anti-diarrheal agent. Of note was that the sila-analogue **339** featured a structural carbon–silicon exchange at position 4 of the piperidine ring (Fig. 101). The physiochemical properties of **338** and **339** were found to be very similar and in both instances sub-nanomolar receptor binding affinities and agonist affinity was noted for the μ1 opioid receptor, the main target of loperamide **338**. The compounds differed in their ability to cross Caco-2 cell membranes with the sila-analogue **339** having lower permeability and increased efflux abilities; however, both compounds were strong P-gp substrates and readily oxidised by human liver microsomes.[486]

Neurotropic agents

Some of the of the earliest research involving carbon–silicon switches was reported by Fessenden and Coon in 1965 (some of the initial research by this group also involved potentially

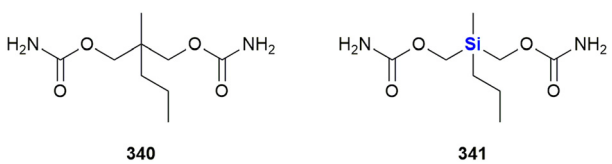

Fig. 102 Meprobamate **340** and sila-meprobamate **341**.

interesting Si-containing pharmacological scaffolds, but without significant biological data being supplied – see for example the following ref. 487 and 488). In an example of interest to this review, these researchers systematically investigated mono- and dicarbamates, such as anxiolytic meprobamate **340** and its sila-analogue **341** (Fig. 102).[489] During this bioactivity investigation it was determined that the sila-analogue **341** (LD_{50} > 1000 mg kg^{-1}) was slightly less toxic than **340** (LD_{50} = 700 mg kg^{-1}), but that the duration of its effects were significantly reduced from 56 min to 13 min.

The use of silicon atom "swaps" as a strategy in the search for and development of neurologically active compounds has attracted attention in light of the ability of silicon to dramatically alter a compounds lipophilicity. As previously mentioned in this review, in their development of anti-bacterials for the treatment of meningitis, Reddy and co-workers showed that increasing the lipophilicity of drugs can lead to improved brain exposure.[434] The use of silicon bioisosteres therefore offers an attractive means of improving efficacy through improved membrane penetration of the blood brain barrier.

One of the earlier examples of utilising this approach was performed by preparing a sila-analogue of budipine **342**, a monoamine uptake inhibitor used as part of a therapy for Parkinson's disease. In the late 1980s, Stasch and colleagues disseminated research focussed on the replacement of the C-atom within the 4,4-diphenyl core of budipine by a Si-atom, thereby providing compound **343** (Fig. 103).[490] This sila-analogue had an increased lipophilicity (relative to the non-Si parent compound), an established advantage for therapeutics acting on the CNS (as in Parkinson's disease therapy) because this compound characteristic has been identified as being very important in improving BBB penetration.[490] In terms of the neuropsychiatric disorder schizophrenia, it is widely accepted that changes in complex neurotransmitter systems (such as the excessive stimulation of dopamine D2 receptors) are impacted, even though the exact pathogenesis mechanism are still under investigation. As such, dopamine over-activity is associated with the psychotic symptoms of schizophrenia, such as delusions, hallucinations and thought disorders. In terms of current treatments, the anti-psychotic agent haloperidol **344** acts by blocking the dopamine D2 receptor, as well as other serotonin receptors (Fig. 104).[491] With this in mind, in 2004, Tacke and co-workers reported research involving the synthesis of the silicon-containing derivative, sila-haloperidol **346**.[492] Upon testing the binding affinities of haloperidol **344** and its silicon-analogue **346** against various recombinant dopamine receptors, the researchers were able to show that sila-substitution of haloperidol had quite clearly modulated the receptor

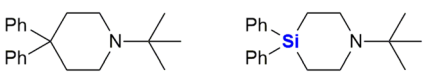

342 **343**

Fig. 103 Budipine **342** and sila-budipine **343**.

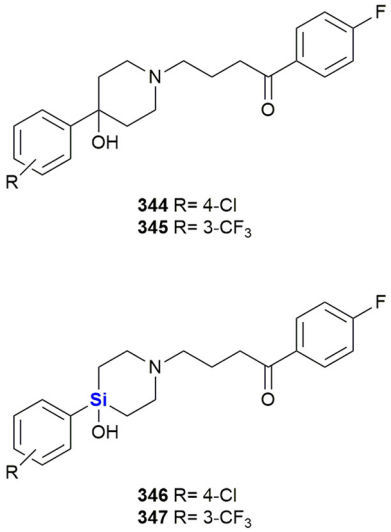

344 R= 4-Cl
345 R= 3-CF_3
346 R= 4-Cl
347 R= 3-CF_3

Fig. 104 Haloperidol **344**, Trifluperidol **345** and sila-analogues.

selectivity profile. These effects suggested that the biochemical impact of haloperidol **344** and sila-haloperidol **346** would differ substantially *in vivo*. Additional research by the group, involving radio-ligand binding studies, revealed that sila-haloperidol **346** had comparable receptor binding affinities to haloperidol **344** for the dopamine hD_1, hD_2, hD_3, hD_4 and hD_5 receptors.[493] The same research group also investigated trifluperidol **345** and its sila analogue **347**.[494] In this case, the sila-analogue was a less effective inhibitor of hD1 and hD2 and showed lower selectivity for the hD2 receptor. In contrast, in the pair of **345** and **347**, the sila-substitution lead to an increase of both inhibitory potency and selectivity for the hD2 receptor.

Tacke *et al.* reported the synthesis of spirocyclic ligands for σ_1 receptors (Fig. 105). The σ_1 receptor is an attractive target for the treatment of several diseases of the CNS such as depression, schizophrenia, anxiety, Alzheimer's and Parkinson's diseases. Compared to their respective carba-analogues **348**, introduction of silicon in the spirocyclic scaffold of **349** increased both the affinity (K_i = 0.3–2.9 mM) and the selectivity for σ_1 ligands.[495]

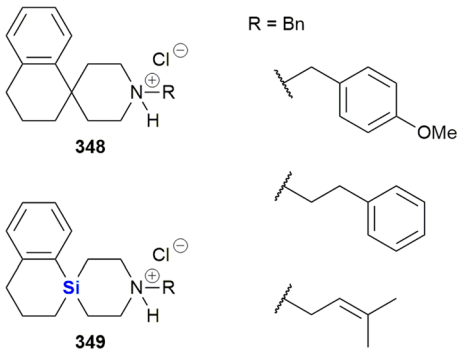

348 **349**

Fig. 105 Spirocyclic σ receptor ligands **348** and sila-analogues **349**.

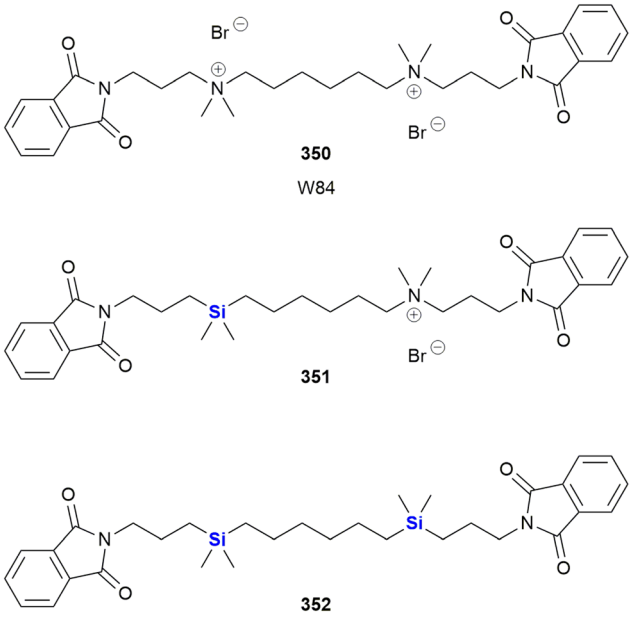

Fig. 106 Silicon-based w84-type allosteric modulators.

Tacke and co-workers also reported on the synthesis of silicon-based W84-type allosteric modulators for ligand binding to muscarinic M_2 receptors (Fig. 106).[496] The non-sila parent compound W84 **350** is known to inhibit the dissociation of the orthosteric ligand [^{3}H] *N*-methylscopolamine, whereas the researchers developed a silicon-containing analogue wherein one ammonium nitrogen atom was exchanged with a silicon atom affording enhanced binding. The silylated compound **351** was further shown to be an M_2-selective allosteric enhancer and therefore did not affect binding at the M_1, M_3, M_4 and M_5 receptors. Interestingly, compound **352** with two silicon atoms instead of nitrogen was completely inactive.[497]

The Tacke research group also reported the synthesis and biological evaluation of sila-venlafaxine **354**, a silicon analogue of the serotonin/noradrenaline reuptake inhibitor venlafaxine **353** (Fig. 107).[498–500] Furthermore, studies suggested that sila-substitution dramatically influenced the pharmacological selectivity profiles of compound **353** with respect to serotonin, noradrenaline and dopamine reuptake inhibition. (*R*)-Sila-venlafaxine **354** showed 10-fold more potent inhibition of noradrenaline transporters than serotonin and dopamine transporters, which might be beneficial for the selective treatment of diseases of the CNS. The venlafaxine analogue **355** with a sila-cyclopentanol instead of a sila-cyclohexanol ring showed lower inhibition of the serotonine transporter than venlafaxine **353** and showed similar activity regarding the reuptake inhibition of serotonin, noradrenaline or dopamine.

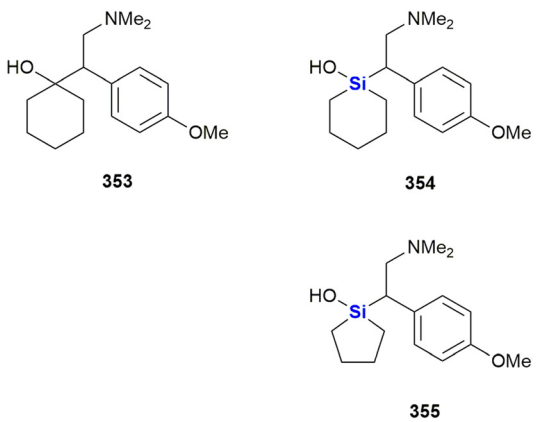

Fig. 107 Venlafaxine **353**, sila-venlafaxine **354** and a related sila-compound **355** as selective noradrenaline reuptake inhibitor.

Zablotskaya and co-workers have extensively studied the effect of incorporating silicon into neurologically active compounds since the early 1990's, during which time several potent psychotropic agents were identified by these researchers (Fig. 108).[289] The group demonstrated that the silylation of aminoalcohols (a strategy previously utilized for pharmacokinetic modulation of this family of compounds)[501] afforded compounds which were agonists or antagonists of choline, and caused an increase in psychotropic activity. It was thereby proposed that the mechanism of action might be linked to the passage of the more hydrophobic silyl derivatives through lipophilic membranes.[289] As part of this research, tetrahydroquinolines **356** and **357** as well as tetrahydroisoquinoline salts **358** and **359** were synthesised and screened for neurotropic activity. Subsequent studies showed that the substituent on the 2-hydroxyethyl side chain influenced the tone of skeletal musculature and movement co-ordination. This activity was found to decrease when moving from the unsubstituted parent compound to bulkier silyl ethers. Furthermore, weak hypothermic activity was noted for derivatives of *N*-(2′-hydroxyethyl) tetrahydroquinolines and almost all the novel compounds showed anti-hypoxic activity (30–55%) and anti-convulsive action on Corazol-induced convulsions, with TMS ether **356** showing the best activity.

Further investigations by Zablotskaya and co-workers, into the hydrolytic stability of trialkylsilyl derivatives of heterocyclic bases **87–90** (Fig. 31) as potentially active compounds, was undertaken to see if the rate of hydrolysis could be controlled by changing the substituents at the silicon atom.[290] The compounds were attractive as the by-products of hydrolysis were determined to be particularly

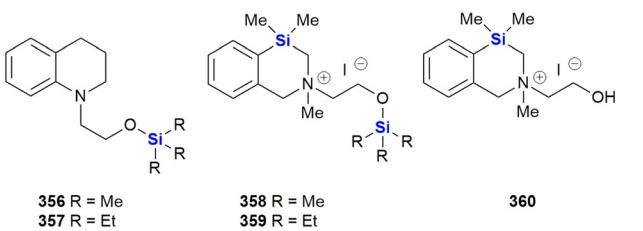

Fig. 108 Silicon-containing compounds displaying psychotropic activity.

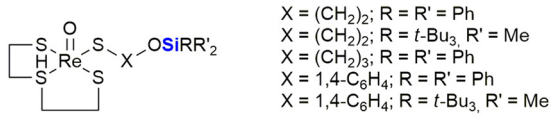

361

Fig. 109 Anti-convulsive silylated rhenium complexes.

non-toxic. Biological assessment of the effect of the compounds on locomotor activity, muscular tone and memory processes showed that the TBDMS protected barbituric acid **88** (R = $SiMe_2t$-Bu) had a higher sedative action and a stronger effect on memory processes, fully suppressing retrograde amnesia and higher anti-stress activity than the unsilylated barbituric acid.

In 1999, rhenium(v)-containing organosilicon complexes **361** were prepared by Lukevics and co-workers, some of which showed anti-convulsive activity and did not affect the skeletal muscle tone and movement co-ordination of mice (Fig. 109). In addition, some of the synthetic derivatives displayed tranquilizing effects increasing the length of barbiturate narcosis by 50%, strengthened the effect of amphetamines, increased motor activity and lowered murine body temperature.[286]

The Zablotskaya group further showed that TMS ethers of hydroxyl-containing thiazole derivatives **362** and **363**, which acted as amphetamine antagonists, possessed sedative effects on mice, and that both the silylated and unsilylated ethers displayed similar activities (Fig. 110).[284]

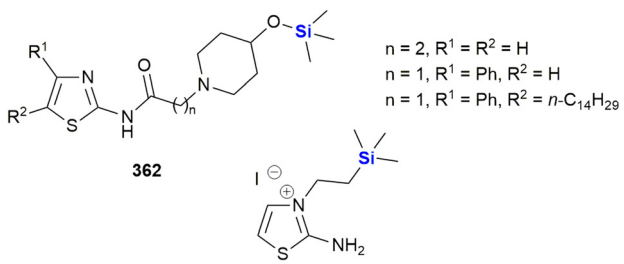

362

363

Fig. 110 Silylated thiazole **365** and thiazolium **366** amphetamine-antagonists.

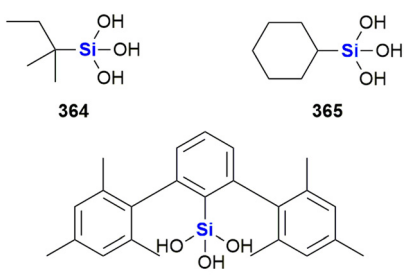

364 365

366

Fig. 111 Stable silanetriols displaying moderate AChE activities.

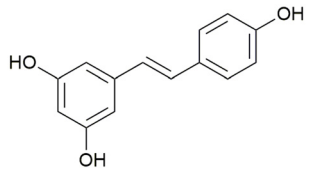

367

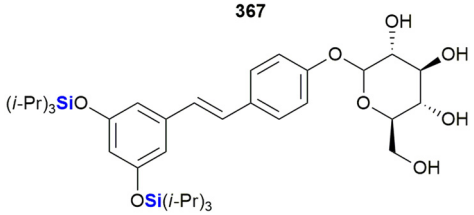

368

Fig. 112 Resveratrol **367** and neuroprotective sila-resveratrol **368**.

In 2011, Pietschnig and co-workers reported the synthesis of three silanetriols **364–366**, designed to act as reversible acetylcholinesterase inhibitors, in their search for potential anti-Alzheimer's agents (Fig. 111).[502] The compounds were found to display moderate activities and negligible cytoxicities in this regard. The most active compound, cyclohexylsilanetriol **365**, exhibited 45% inhibition of acetylcholinesterase relative to galantamine hydrobromide, its activity corresponding to an IC_{50} value of 121 μM.

Furthermore, more recently in 2021, Morales, González-Rey and co-workers designed several silyl resveratrol derivatives and potential neuroprotective agents.[503] Resveratrol **367** has been shown to exhibit neuroprotective properties; however, the low bioavailability of this natural product has limited its utility (Fig. 112). In an attempt to ameliorate this issue, the researchers designed several silyl resveratrol analogues and accessed them synthetically. Notably, compound **368** displayed improved neuroprotective activity relative to resveratrol **367**, when it was screened for toxicity and neuroprotection using a zebra fish embryo model system. In addition, compound **368** also reduced motor-coordination loss in a murine model of Huntington's disease and diminished the progression of autoimmune encephalomyelitis in a multiple sclerosis murine model.

In 2021, Duan, Sun, Wu *et al.* reported synthetic cannabinoids incorporating a carbon-silicon switch in the alkyl chain attached to the benzene ring (Fig. 113).[504] The CBD-derived **369** showed mixed agonistic activity at both the

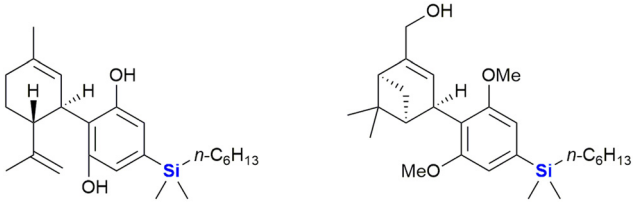

369 370

Fig. 113 Synthetic sila-cannabinoids.

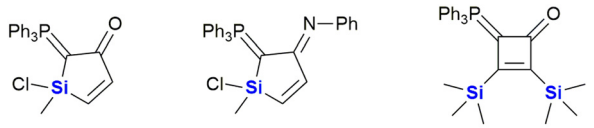

371 372 373

Fig. 114 Silicon-containing AChE inhibitors.

CB1- and CB2-receptor, while **370** was selective for CB2. The novel cannabinoids reduced the proportion of infarcted brain tissue in experimental autoimmune encephalomyelitis (EAE) mice by 50% (**369**) and 90% (**370**) at a dose of 10 mg kg^{-1} or 30 mg kg^{-1}, respectively. The CB2-selective agonist **370** was the more promising therapeutic agent for the treatment of multiple sclerosis, as **369** induced ataxia and tremors due to its CB1 agonist activity.

Last year, El-Hussieny *et al.* reported the synthesis of the two sila-cycles **371** and **372** as well as the disilylated butenone **373** (Fig. 114).[505] These compounds inhibited acetylcholinesterase AChE (IC_{50} = 113–345 nM) but were not investigated further as potential treatments of Alzheimer's disease as in this work a non-silylated compound proved to be more potent.

Hornsperger *et al.* investigated silylated trifluormethylketones as AChE inhibitors for the treatment of Alzheimer's disease with the intention to increase the lipophilicity and duration of action by the incorporation of silicon (Fig. 115). Compound **374** was a very effective inhibitor of AChE, with an even lower dissociation constant K_i = 47 pM than the ammonium ion **375** (K_i = 80 pM). It showed long-lasting, but reversible inhibition of AChE *in vitro* while **375** formed a stable complex with AChE and was found to be an almost irreversible inhibitor. Compound **374** showed dose-dependent inhibition of rat brain AChE with an ED_{50} of 2.5 mg kg^{-1}. Due to its high lipophilicity, **374** could be dermally administered to dogs, thus avoiding a significant first-pass clearance after oral administration. Furthermore, **374** showed a significantly lower toxicity (LD_{50} = 180–250 mg kg^{-1} in mice and rats) than **375**.[506]

In 2021, Song, Jiang and co-workers disclosed the synthesis of the anti-depressant (−)-sila-mesembranol, **376**, a silicon analogue of (−)-mesembranol **377**.[507] Furthermore, the researchers went on to demonstrate that the sila-analogue **376** showed improved activity in two murine depression models, thereby suggesting clinical potential of this compound (Fig. 116).

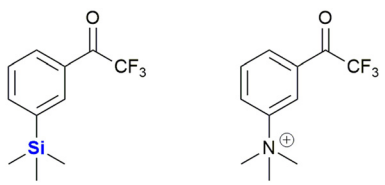

374 375

Fig. 115 Silylated trifluormethylketones as potential Alzheimer drug candidates.

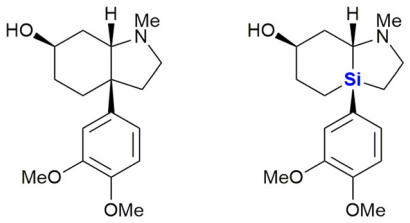

376 377

Fig. 116 Anti-depressant (−)-mesembranol **376** and (−)-sila-mesembranol **377**.

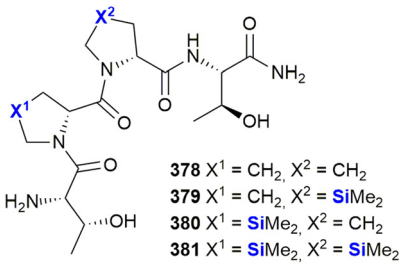

Fig. 117 Silaproline derivatives of the anti-depressant rapastinel.

Madica *et al.* investigated analogues of the anti-depressant tetrapeptide rapastinel **378**, in which one (**379**, **380**) or both (**381**) proline residues were exchanged for a silaproline (Fig. 117).[508] According to predictions, the proline-silaproline switch does not influence the conformational properties of the compounds, but was supposed to increase lipophilicity and stability towards enzymatic degradation. So far, the biological activity of these compounds has not been reported.

Aminoalkylsilanes have been investigated as irreversible inhibitors of monoamine oxidase, an enzyme with several isoforms some which are linked to the metabolism of monoamine neurotransmitters. Inhibitors of these monoamine oxidases, such as **382** (Fig. 118), might therefore exhibit anti-depressant activity.[509] The physiological function of another isoform, benzylamine oxidase, is however not fully understood, but its preponderance in vascular tissues might indicate a cardiovascular function. Of interest was that the aminoalkylsilane **383** caused irreversible inactivation of this isoform.[510]

Miscellaneous

Cavelier, Sarret and co-workers reported the synthesis of the silaproline analogue **384** of the neurotensin[8-13]

382 n=1-3 383

Fig. 118 Silicon-containing amines as irreversible inhibitors of monoamine oxidase.

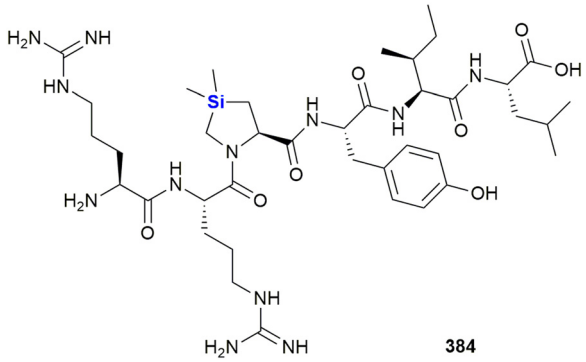

384

Fig. 119 Analgesic silaproline analogue of the neurotensin[8-13] fragment.

pentapeptide fragment (Fig. 119).[511] The presence of the bulky dimethylsilyl-group significantly increased the compound's resistance to proteolytic degradation, a notorious problem in the development and use of peptide therapeutics, and thus increased its bioavailability. Of interest is that **384** showed promising analgesic properties in a range of experimental pain models and did not show the common side-effects associated with opioid therapies.

Silperisone **386** is a centrally acting muscle relaxant and suppresses monosynaptic and polysynaptic spinal reflexes

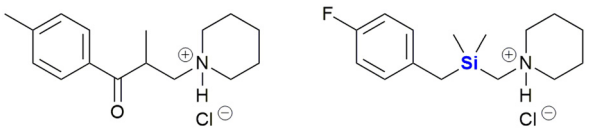

385 386

Fig. 120 Muscle relaxants tolperisone **385** and silperisone **386**.

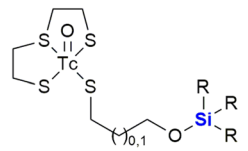

387

R = Et, Ph

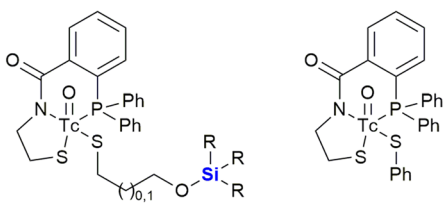

388 389

R = Et, Ph

Fig. 121 ^{99m}Tc complexes with a silylated thiopropanol ligand.

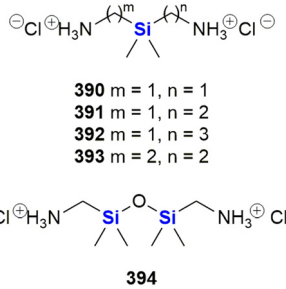

390 m = 1, n = 1
391 m = 1, n = 2
392 m = 1, n = 3
393 m = 2, n = 2

394

Fig. 122 Silicon-containing diamines **390**–**394** as irreversible inhibitors of diamine oxidase.

and is used for the treatment of muscle spasms (Fig. 120). It was developed by Farkas and colleagues as a tolperisone **385** analogue in order to increase duration, oral bioavailability and reduced side effects.[512]

Santos and co-workers introduced silicon into ^{99m}Tc complexes with the aim of increasing the lipophilicity and bioavailability of these radiopharmaceuticals (Fig. 121). Attempts to prepare trimethylsilyl-containing complexes failed, as hydrolysis occurred during the formation of the ^{99m}Tc complex in aqueous phosphate buffer.[513] Ligands with more bulky silyl ether groups were more stable and the resulting radiolabelled complexes **387** (ref. 513) and **388** (ref. 514) were obtained in high yields. Furthermore, the biodistribution of the complexes **388** were investigated in mice. Unexpectedly, they showed lower brain uptake than the non-silylated and less lipophilic reference complex **389**, presumably due to their larger size.

Van Dorsselaer investigated bis(aminoalkyl)silanes **390**–**394** as irreversible inhibitors of diamine oxidase (Fig. 122).[515] This copper-containing enzyme which plays a key role in histamine metabolism and is linked to a range of diseases while its precise role is not clear in any case.[516] Among all tested compounds, only **390** and **392** irreversibly inhibited diamine oxidase while the other compounds were completely inactive and showed neither reversible nor irreversible inhibition. It should also be recognized that the value of *N*-(silylmethyl)amines, -amides, and -amino acids as bioactive molecules has already been reviewed.[256]

In 2022, Singh, Sushma and Priyanka reported the synthesis of organotriethoxysilanes **395** containing a thiosemicarbazone and a triazole group (Fig. 123).[517] The

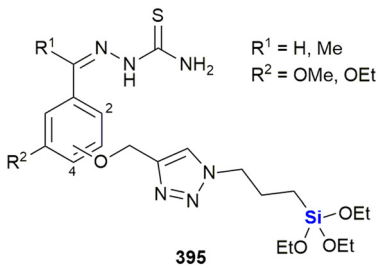

395

Fig. 123 Thiosemicarbazone-triazole linked organotriethoxysilanes as Hg(II) chemosensors.

compounds were used for the selective complexation and detection of Hg(II) ions by fluorescence spectroscopy with a detection limit of ~40 nM. The compounds were only weakly cytotoxic and could therefore be used as chemosensors for Hg(II) ions in living cells. The same group also reported a series of silatranes as fluorescence sensors for a variety of heavy metal ions and investigated their potential biological activity *in silico*.[518–527]

Retinoic acid-related orphan receptors (RORs) regulate DNA transcription, yet their natural ligands are unknown. They exist in the form of three subtypes which are related to a variety of biological functions. RORα is related to neural functions, RORβ is thought to be involved in the processing of sensory information while RORγ is linked to insulin resistance and the immune system. RORs are therefore interesting targets for new therapeutic applications. Toyama *et al.* investigated a library of structurally similar dibenzosiloles which include general structures **397** and **399** as novel inverse agonists (Table 5).[528] In these structures, a dialkylsilane group replaced the amide groups in the parent structures **396** and **398**, which were investigated earlier as RORγ selective inverse agonists.[529]

Very recently, Fujii *et al.* investigated silicon-containing analogues of the multi-target nuclear receptor modulator T0901317 (**400**), in which the sulfonamide functional group was exchanged by a silyl group (Fig. 124).[530] The resulting silicon analogues were investigated as human liver X receptor (hLXR) agonists. While both **401** (EC_{50} = 0.43 μM against hLXRα and EC_{50} = 0.59 μM against hLXRβ) and **402** (EC_{50} = 2.15 μM against hLXRα and EC_{50} = 0.74 μM against hLXRβ) generally showed lower activity than T090131 (EC_{50} = 0.26 μM against hLXRα and hLXRβ) in a luciferase reporter gene assay using HEK293 cells. However, while T0901317 showed no selectivity, by proper choice of the silyl group it was possible to increase the selectivity of the silanes for either of the liver X receptors LXRα or LXRβ.

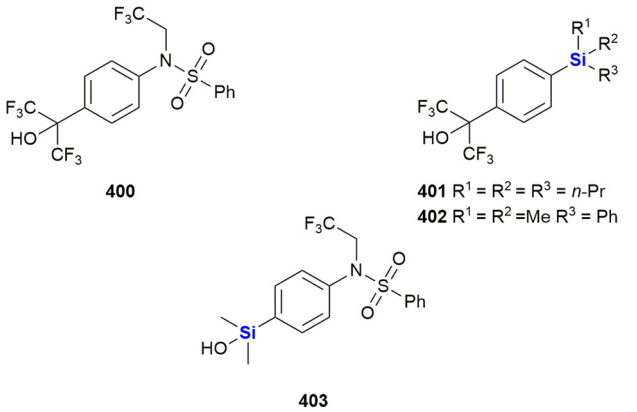

Fig. 124 Liver X receptor agonist T0901317 **400** and silicon containing analogues **401**, **402** and **403**.

The same group also reported the synthesis of the silanol derivative **403** as a multi-target nuclear receptor modulator (Fig. 124). The non-silyl parent compound **400** displays potent, but unselective, activities toward liver X receptor α (hLXRα) and β (hLXRβ), farnesoid X receptor (FXR), pregnane X receptor (PXR) and retinoic acid receptor-related orphan receptor (ROR)γ (EC_{50} = 0.23–3.4 μM). In contrast, the silanol derivative **403** displayed selectivity with significant activity shown only against PXR (EC_{50} = 0.88 μM).[531,532]

Agrichemicals

Silicon has not only found its way into drug discovery related to human diseases but has also found its way into the agrichemical sector. Though not the focus of this review, a few very recent examples will be presented in this section. Of importance here is to appreciate that many of the silicon-switch or Si-derivation strategies applied in medicinal chemistry are also of value in the agrichemical sector, and of course *vice versa*.

Table 5 Dibenzosilole scaffolds acting as novel ROR inverse agonists

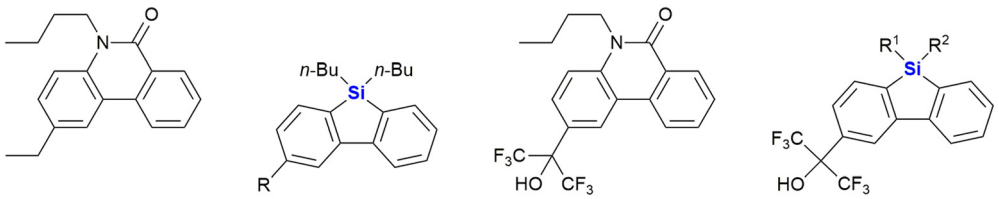

		Inhibition at 10 μM/%						IC_{50}/μM		
Compound	R	RORα	RORβ	RORγ	Compd	R_1	R_2	RORα	RORβ	RORγ
396										
397a	—	37	29	37	**399a**	—	—	7.2	5.7	4.7
397b	$CH(OH)CH_3$	17	<5.0	<5.0	**399b**	*n*-Bu	*n*-Bu	6.2	6.7	5.5
397c	H	22	<5.0	13	**399c**	Me	Me	9.4	(40%)[a]	5.4
397d	Et	7.0	<5.0	18	**399d**	Et	Et	(34%)[a]	(28%)[a]	4.2
397e	$COCH_3$	13	<5.0	<5.0	**399e**	*n*-Bu	Me	7.7	7.0	4.4

[a] Inhibition at 10 μM.

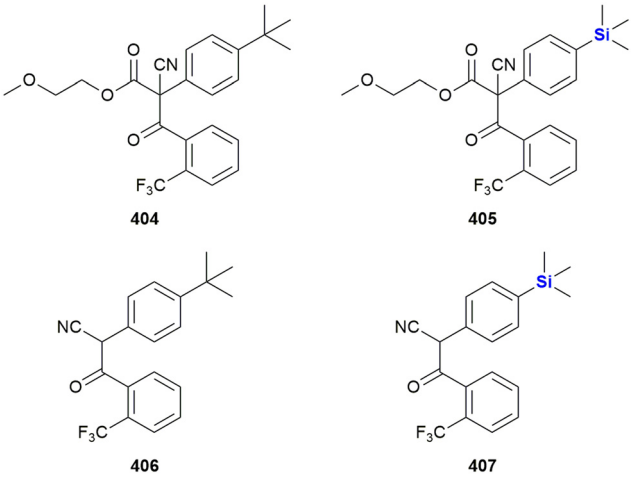

Fig. 125 Acaricidal cyflumetofen **404** and sila-derivatives.

In 2020, Maienfisch and co-workers employed a carbon–silicon switch during their development of the anti-fungal sila-cyflumetofen **405**, based on the beta-ketonitrile acaricide cyflumetofen **404** (Fig. 125).[533] In the development of the sila-analogue the critical for activity *tert*-butyl group was replaced by a TMS group. The researchers found that the silicon analogue retained good activity and had favourable pharmokinetic properties when compared to the parent compound. Sila-cyflumetofen **405** and cyflumetofen **404** both displayed complete inhibition of acaricidal activities at 200 and 50 ppm, respectively. At 12.5 ppm **404** displayed good activity (70–100% inhibition) while the sila-analogue **405** was completely inactive. That being noted, **404** and derivative **405** are prodrug forms which require conversion into the active forms **406** and **407** with carboxylesterase enzymes. In the case of the "active" forms, the sila-analogue **407** was marginally more active than **406** (IC_{50} for oxidoreductase activity was 0.0016 *vs.* 0.0025 μg mL^{-1}).

In 2022, Maienfisch and co-workers investigated the effects of bioisosteric replacement by a carbon–silicon switch on cyflumetofen **404**,[533,534] a compound which is used as an acaricidal succinate dehydrogenase inhibitor (Fig. 126). The researchers found that simply converting the *tert*-butyl group into a trimethylsilyl group led to a complete loss of activity at low concentrations (12.5 mg L^{-1}). However, if at the same time the 2-methoxyethyl ester was replaced with an isopropyl ester (**408**), it was found that the activity had been restored (90% activity at 12.5 mg L^{-1}), even slightly exceeding the activity of **404** (80% activity at 12.5 mg L^{-1}).

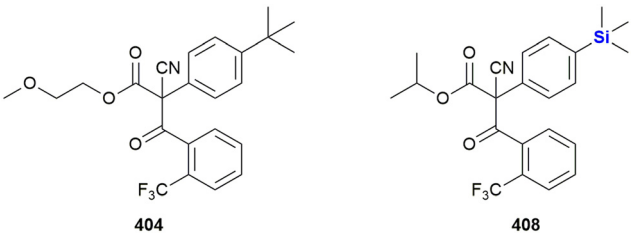

Fig. 126 Acaricidal cyflumetofen **404** and silylated derivative **408**.

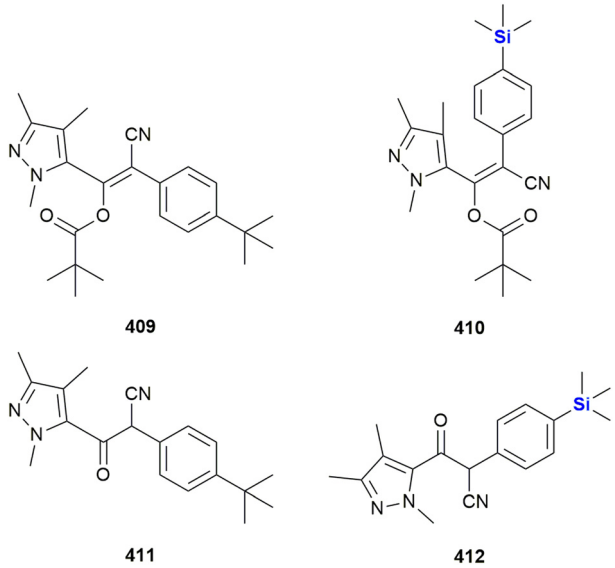

Fig. 127 Acaricidal cyenopyrafen **409** and sila-cyenopyrafen **410** and their respective active forms **411** and **412**.

Zhou *et al.* synthesised a series of silicon containing analogues of cyenopyrafen **409**, a prodrug of the succinate dehydrogenase inhibitor **410** (Fig. 127).[535] Among the synthesised compounds, **410** emerged as the most potent inhibitor with an LC_{50} of 0.062 mg L^{-1} against *Tetranychus cinnabarinus* (carmine spider mite) and slightly surpassed the activity of cyenopyrafen (LC_{50} of 0.141 mg L^{-1}). As the incorporation of silicon in **410** decreased acute toxicity against fish, it might represent a promising lead for the development of more environmentally benign acaricides.

The same group also investigated silicon containing insecticides (Fig. 128).[536] The diamide insecticide **414** was tested against the moth *Mythimna separata* and exhibited a low LC_{50} = 2.00 mg L^{-1}, but unfortunately was less active than its carba-analogue **413** (0.27 mg L^{-1}). In the pair of **415** and **416**, the addition of a trimethylsilyl unit slightly decreased the activity against the moths *Mythimna separata* (LC_{50} = 4.68 mg L^{-1} **415**, LC_{50} = 4.80 mg L^{-1} **416**) and *Plutella xylostella* (LC_{50} = 0.21 mg L^{-1} **415**, LC_{50} = 0.30 mg L^{-1} **416**).[537]

The Maienfisch group also developed a series of succinate dehydrogenase inhibitors by bioisosteric replacement of the amide moiety of difluoromethyl-pyrazol amides by a β-ketonitrile moiety (Fig. 129).[538] It was found that increasing hydrophobic interactions with the target protein increased the potency of the tested compounds. Indeed, the silicon-containing compounds **417–418** were among the most potent fungicides. In particular, **419** showed 91.2% inhibition against *Rhizoctonia solani* at low concentrations of 1 μg mL^{-1} and could be considered a promising agent to prevent Rice Sheath Blight.

Wei *et al.* also reported on the use of a carbon–silicon switch approach in the development of succinate dehydrogenase inhibitors based upon the chemical space surrounding flubeneteram **420**, a recently reported anti-fungal that targets

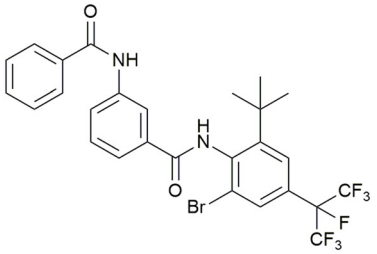

413

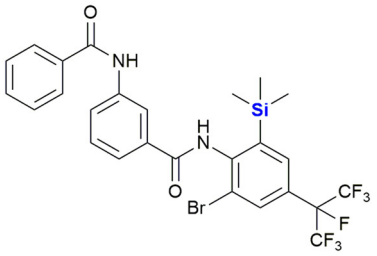

414

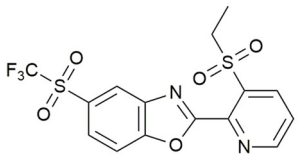

415

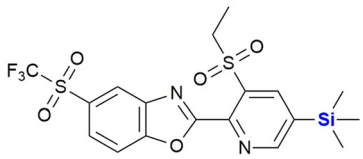

416

Fig. 128 Insecticides **413** and **415** and their sila-analogues **414** and **416**.

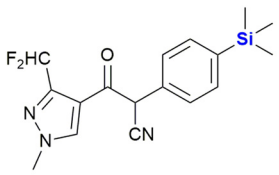

417

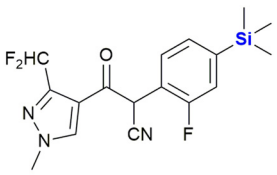

418

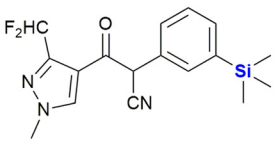

419

Fig. 129 Silicon-containing succinate dehydrogenase inhibitors **417**–**419**.

this enzyme (Fig. 130).[539] Compound **421** was synthesized and found to display improved anti-fungal activities at low concentrations (0.19 mg L^{-1}) against soybean rust control. The

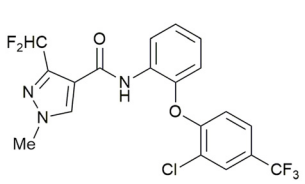

420

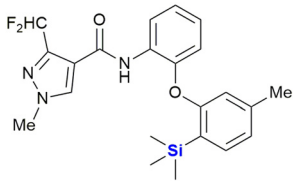

421

Fig. 130 Flubeneteram **420** and sila-analogue **421**.

chlorine–silicon swap was specifically performed to improve van der Waals interactions with succinate dehydrogenase.

Conclusions

As research on silicon containing drug molecules now spans more than six decades and currently sees many research groups actively contributing to the field, it is somewhat perplexing that even though several compounds have entered advanced clinical trials, no silicon-containing drug molecule for the treatment of human diseases and conditions has, to the best of our knowledge, ever proceeded beyond the clinical trial stage. This issue has been repeatedly raised and has generally been answered by the troubles involving the synthesis of silicon containing scaffolds on the one hand and the limited benefits of incorporating silicon on the other. However, we are of the opinion that the rich field of silicon-containing drug molecules deserves a more distinguishing and occasionally a more optimistic perspective, especially given the recent progress in synthetic methods focused on the incorporation of silicon into important drug-like scaffolds.

Most examples covered in this review represent derivatives of natural products and known synthetic small molecule drugs. In these cases, the silyl moiety is introduced to optimise the pharmacological and pharmacokinetic profile but is generally not crucial for the biological activity of the molecule itself. Most derivatisations rely on the formation of silyl ethers, as many alkylchlorosilanes are commercially available at reasonable costs and cover a broad range from small, easily hydrolysable groups which cause a small increase of lipophilicity, to large, bulky groups which are both more stable and more lipophilic. Current advances in late-stage small molecule functionalisations now also include the introduction of silicon-containing groups, which should allow new derivatisations beyond the classical use of silyl ethers.[540] Incorporation of silicon into biologically active scaffolds which are already identified and accessed by simple derivatisation is arguably most likely to yield commercialised silicon-containing drugs in the nearer future.

On the other hand, the use of silicon containing analogues of pharmacologically active compounds, in which silicon atoms replace carbons, or other elements, as a bioisostere has been less explored, mainly due to this being a more challenging synthetic issue. This area is however open to much opportunity, as it has been repeatedly shown that the incorporation of silicon in the actual scaffold of the drug not only can markedly improve the ADME profile, but also

biological activity and selectivity. Given the significant advances in recent Si–C connective chemistry and increased possibilities of asymmetric bond formation to silicon, we will surely see this area advance swiftly, even though chances for commercialized drugs of this kind are currently admittedly low.

Last, we would like to point out an underrepresented opportunity in the field. While the different chemical behaviour and availability of silicon- or carbon-based building blocks is often an obstacle in accessing silicon-containing analogues, it might as well be seen as a chance to access new and unique biologically active scaffolds with no direct carba-analogue by creatively exploiting the unique chemistry of silicon and the broad range of readily available silicon-containing building blocks. This approach is still in its infancy, and so far, the focus has been almost exclusively on silanediols, silanetriols and silatranes. Beyond that, a huge and possibly rewarding chemical space remains to be explored.

References added in proof

During the review of this manuscript a number of papers related to the topic of this review were published. For completeness, they are listed as follows: a) an organocatalytic asymmetric synthetic approach to silicon-centered stereogenic siloxanols[541] or a synthetic approach to silacyclohexanones,[542] both approaches of potential importance to the synthesis of bioactive Si-containing molecules; b) the disclosure of novel silicon ethers as components of ionizable lipids as part of mRNA lipid nanoparticle complexes;[543] the development of silicon-containing subtype-selective estrogen receptor modulators based on the bis(4-hydroxyphenyl)silanol structure;[544] the evaluation of Si-containing β-hydroxyphenyl phosphine borane derivatives as nuclear estrogen receptor ligands;[545] as well as an overview of the innovative studies involving the physical properties of organosilanes generated by way of hydrosilane–organoiodine couplings.[546] Finally, the application of directed evolution to develop enzymes able to cleave the silicon–carbon bonds found in siloxane substances is also of topical interest with respect to this review.[547]

Conflicts of interest

There are no conflicts to declare.

Acknowledgements

This work was supported through the CSIR Parliamentary Grant. DR further acknowledges the National Research Foundation (NRF, South Africa) for funding, Thuthuka grant number 106959 and Competitive Support for Unrated Researchers grant number 116303. FH and WvO gratefully acknowledge Stellenbosch University for postdoctoral funding for FH. WvO also acknowledges Stellenbosch University (research support) and National Research Foundation, South Africa, for funding. Opinions expressed in this publication and the conclusions arrived at are those of the authors and are not necessarily attributed to the CSIR or NRF.

Notes and references

1 J. Michl, *Chem. Rev.*, 1995, **95**, 1135.
2 **https://www.rsc.org/periodic-table/element/14/silicon** (Accessed 3 May 2024).
3 Z. Souri, K. Khanna, N. Karimi and P. Ahmad, *J. Plant Growth Regul.*, 2021, **40**, 906–925.
4 R. Tacke, *Angew. Chem., Int. Ed.*, 1999, **38**, 3015–3018.
5 G. A. Showell and J. S. Mills, *Drug Discovery Today*, 2003, **8**, 551–556.
6 S. J. Barraza and S. E. Denmark, *J. Am. Chem. Soc.*, 2018, **140**, 6668–6684.
7 G. W. Bemis and M. A. Murcko, *J. Med. Chem.*, 1996, **39**, 2887–2893.
8 G. W. Bemis and M. A. Murcko, *J. Med. Chem.*, 1999, **42**, 5095–5099.
9 N. A. Meanwell, *J. Agric. Food Chem.*, 2023, **71**, 18087–18122.
10 P. Steele, *Expert Opin. Ther. Pat.*, 2002, **12**, 3–10.
11 A. K. Franz and S. O. Wilson, *J. Med. Chem.*, 2013, **56**, 388–405.
12 S. E. Thomas, *Oxford Chemistry Primers, Organic Synthesis – The Roles of Boron and Silicon*, Oxford University Press, USA, 1995.
13 A. G. Brook, F. Abdesaken, B. Gutekunst, G. Gutekunst and R. K. Kallury, *J. Chem. Soc., Chem. Commun.*, 1981, 191–192.
14 S. S. Sen, *Angew. Chem., Int. Ed.*, 2014, **53**, 8820–8822.
15 J. S. Mills and G. A. Showell, *Expert Opin. Invest. Drugs*, 2004, **13**, 1149–1157.
16 J. Ackermann, R. Tacke and U. Wannagat, *Liebigs Ann. Chem.*, 1979, 1915–1924.
17 W. Kitching, H. A. Olszowy, G. M. Drew and W. Adcock, *J. Org. Chem.*, 1982, **47**, 5153–5156.
18 M. M. Reichstat, U. B. Mioc, L. J. Bogunovic and S. V. Ribnikar, *J. Mol. Struct.*, 1991, **244**, 283–290.
19 P. W. Kenny, *J. Med. Chem.*, 2022, **65**, 14261–14275.
20 J. Graton, F. Besseau, A. Goupille and J. Y. Le Questel, *J. Mol. Struct.*, 2022, **1266**, 133505.
21 D. V. Woo, J. E. Christian and R. C. Schnell, *Can. J. Pharm. Sci.*, 1979, **14**, 12–14.
22 D. V. Woo, J. E. Christian and R. C. Schnell, *Can. J. Pharm. Sci.*, 1979, **14**, 65–67.
23 D. E. Clark, *Drug Discovery Today*, 2003, **8**, 927–933.
24 X. Dong, X. Yuan, Z. Song and Q. Wang, *Phys. Chem. Chem. Phys.*, 2021, **23**, 12582–12591.
25 P. Luger, B. Dittrich and R. Tacke, *Org. Biomol. Chem.*, 2015, **13**, 9093–9106.
26 P. Luger, M. Weber, C. Hubschle and R. Tacke, *Org. Biomol. Chem.*, 2013, **11**, 2348–2354.
27 N. S. Sarai, B. J. Levin, J. M. Roberts, D. E. Katsoulis and F. H. Arnold, *ACS Cent. Sci.*, 2021, **7**, 944–953.
28 E. Grabitz, M. Reich, O. Olsson and K. Kümmerer, *Sustainable Chem. Pharm.*, 2020, **18**, 100331.
29 C. Rücker, M. Winkelmann and K. Kümmerer, *Environ. Sci. Pollut. Res.*, 2023, **30**, 91492–91500.
30 C. Rücker, E. Grabitz and K. Kümmerer, *Chemosphere*, 2023, **321**, 137858.

31 P. D. Lickiss and K. M. Stubbs, *J. Organomet. Chem.*, 1991, **421**, 171–174.
32 R. D. Crouch, *Tetrahedron*, 2013, **69**, 2383–2417.
33 W. Zhang, W. Guan, J. I. Martinez Alvarado, L. F. T. Novaes and S. Lin, *ACS Catal.*, 2023, **13**, 8038–8048.
34 L. Zheng, X.-X. Nie, Y. Wu and P. Wang, *Eur. J. Org. Chem.*, 2021, **2021**, 6006–6014.
35 Y. Kong and D. Mu, *Chem. – Asian J.*, 2022, **17**, e202200104.
36 W. Yuan and C. He, *Synthesis*, 2022, **54**, 1939–1950.
37 M. Zhang, S. Gao, J. Tang, L. Chen, A. Liu, S. Sheng and A. Q. Zhang, *Chem. Commun.*, 2021, **57**, 8250–8263.
38 X. Pang and X.-Z. Shu, *Chem. – Eur. J.*, 2023, **29**, e202203362.
39 N. Kranidiotis-Hisatomi and M. Oestreich, *Synthesis*, 2023, **55**, 1497–1506.
40 W. C. Xue and M. Oestreich, *ACS Cent. Sci.*, 2020, **6**, 1070–1081.
41 K. M. Korch and D. A. Watson, *Chem. Rev.*, 2019, **119**, 8192–8228.
42 J.-W. Park, *Chem. Commun.*, 2022, **58**, 491–504.
43 F. Ye and L.-W. Xu, *Synlett*, 2021, **32**, 1281–1288.
44 X. Zhang, J. Fang, C. Cai and G. Lu, *Chin. Chem. Lett.*, 2021, **32**, 1280–1292.
45 G. L. Larson and R. J. Liberatore, *Org. Process Res. Dev.*, 2021, **25**, 1719–1787.
46 S. Shamna, J. Fairoosa, C. M. A. Afsina and G. Anilkumar, *J. Organomet. Chem.*, 2022, **960**, 122236.
47 P. P. Pal, S. Ghosh and A. Hajra, *Org. Biomol. Chem.*, 2023, **21**, 2272–2294.
48 J. Gao and C. He, *Chem. – Eur. J.*, 2023, **29**, e202203475.
49 Y. Wu and P. Wang, *Angew. Chem., Int. Ed.*, 2022, **61**, e202205382.
50 Y. M. Cui, Y. Lin and L. W. Xu, *Coord. Chem. Rev.*, 2017, **330**, 37–52.
51 G. C. Nandi, *Eur. J. Org. Chem.*, 2021, **2021**, 587–606.
52 W.-S. Huang, Q. Wang, H. Yang and L.-W. Xu, *Synthesis*, 2022, **54**, 5400–5408.
53 V. Chandrasekhar, R. Boomishankar and S. Nagendran, *Chem. Rev.*, 2004, **104**, 5847–5910.
54 S. Curpanen, G. Poli, J. Oble and A. Perez-Luna, *Eur. J. Org. Chem.*, 2021, **2021**, 1055–1071.
55 M. C. D'Amaral, K. G. Andrews, R. Denton and M. J. Adler, *Synthesis*, 2023, **55**, 3209–3238.
56 S. K. Ghosh, *Asian J. Org. Chem.*, 2022, **11**, e202200227.
57 C. Moberg, *Synthesis*, 2020, **52**, 3129–3139.
58 D. L. Priebbenow, *Adv. Synth. Catal.*, 2020, **362**, 1927–1946.
59 X. Wang, F. Liu, Y. Li, Z. Yan, Q. Qiang and Z.-Q. Rong, *ChemCatChem*, 2020, **12**, 5022–5033.
60 A. Sivaramakrishna, S. Pete, C. Mandar Mhaskar, H. Ramann, D. Venkata Ramanaiah, M. Arbaaz, M. Niyaz, S. Janardan and P. Suman, *Coord. Chem. Rev.*, 2023, **485**, 215140.
61 B. Cheng, P. Lu, H. Zhang, X. Cheng and Z. Lu, *J. Am. Chem. Soc.*, 2017, **139**, 9439–9442.
62 W. Zheng, Y. Xu, H. Luo, Y. Feng, J. Zhang and L. Lin, *Org. Lett.*, 2022, **24**, 7145–7150.
63 L. X. Lu, J. C. Siu, Y. H. Lai and S. Lin, *J. Am. Chem. Soc.*, 2020, **142**, 21272–21278.
64 X.-Y. Lu, H.-Y. Pan, R. Huang, K. Yang, X. Zhang, Z.-Z. Wang, Q.-Q. Tao, G.-X. Yang, X.-J. Wang and H.-P. Zhou, *Org. Lett.*, 2023, **25**, 2476–2481.
65 C. Karmel, Z. Chen and J. F. Hartwig, *J. Am. Chem. Soc.*, 2019, **141**, 7063–7072.
66 W. Sarkar, A. Mishra, A. Bhowmik and I. Deb, *Org. Lett.*, 2021, **23**, 4521–4526.
67 Y.-J. Liu, Y.-H. Liu, Z.-Z. Zhang, S.-Y. Yan, K. Chen and B.-F. Shi, *Angew. Chem., Int. Ed.*, 2016, **55**, 13859–13862.
68 J. Scharfbier, B. M. Gross and M. Oestreich, *Angew. Chem., Int. Ed.*, 2020, **59**, 1577–1580.
69 A. P. Cinderella, B. Vulovic and D. A. Watson, *J. Am. Chem. Soc.*, 2017, **139**, 7741–7744.
70 S. B. J. Kan, R. D. Lewis, K. Chen and F. H. Arnold, *Science*, 2016, **354**, 1048–1051.
71 Q.-C. Gan, Z.-Q. Song, C.-H. Tung and L.-Z. Wu, *Org. Lett.*, 2022, **24**, 5192–5196.
72 H. Li, C. Yang, D. Wang and L. Deng, *Organometallics*, 2023, **42**, 1693–1698.
73 X. Tang, Y. Zhang, Y. Tang, Y. Li, J. Zhou, D. Wang, L. Gao, Z. Su and Z. Song, *ACS Catal.*, 2022, **12**, 5185–5196.
74 C. Qin, Z. Huang, S.-B. Wu, Z. Li, Y. Yang, S. Xu, X. Zhang, G. Liu, Y.-D. Wu, L. W. Chung and Z. Huang, *J. Am. Chem. Soc.*, 2022, **144**, 20903–20914.
75 X.-X. Zhang, Y. Gao, Y.-X. Zhang, J. Zhou and J.-S. Yu, *Angew. Chem., Int. Ed.*, 2023, **62**, e202217724.
76 T. Tani, Y. Sohma and T. Tsuchimoto, *Adv. Synth. Catal.*, 2020, **362**, 4098–4108.
77 S. Chen, X. He, C. Jin, W. Zhang, Y. Yang, S. Liu, Y. Lan, K. N. Houk and X. Shen, *Angew. Chem., Int. Ed.*, 2022, **61**, e202213431.
78 J. B. Gluyas, C. Burschka, S. Dorrich, J. Vallet, H. Gronemeyer and R. Tacke, *Org. Biomol. Chem.*, 2012, **10**, 6914–6929.
79 J. Y. L. Chung, M. Shevlin, A. Klapars and M. Journet, *Org. Lett.*, 2016, **18**, 1812–1815.
80 Q. Li, M. Driess and J. F. Hartwig, *Angew. Chem., Int. Ed.*, 2014, **53**, 8471–8474.
81 H. Fang, K. Xie, S. Kemper and M. Oestreich, *Angew. Chem., Int. Ed.*, 2021, **60**, 8542–8546.
82 W. S. Wang, S. Zhou, L. J. Li, Y. H. He, X. Dong, L. Gao, Q. T. Wang and Z. L. Song, *J. Am. Chem. Soc.*, 2021, **143**, 11141–11151.
83 C. Sedano, R. Velasco, C. Feberero, S. Suárez-Pantiga and R. Sanz, *Org. Lett.*, 2020, **22**, 6365–6369.
84 B.-S. Mu, Y. Gao, F.-M. Yang, W.-B. Wu, Y. Zhang, X. Wang, J.-S. Yu and J. Zhou, *Angew. Chem., Int. Ed.*, 2022, **61**, e202208861.
85 Y. H. Huang, Y. C. Wu, Z. L. Zhu, S. J. Zheng, Z. H. Ye, Q. Peng and P. Wang, *Angew. Chem., Int. Ed.*, 2022, **61**, e202113052.
86 J. Wang, H. Wang, Z. Wang, L. Li, C. Qin and X. Luan, *Chin. J. Chem.*, 2021, **39**, 2659–2667.
87 S. Y. Park, J.-W. Lee and C. E. Song, *Nat. Commun.*, 2015, **6**, 7512.

88 J. Seliger and M. Oestreich, *Angew. Chem., Int. Ed.*, 2021, **60**, 247–251.
89 J. Gao, P.-L. Mai, Y. Ge, W. Yuan, Y. Li and C. He, *ACS Catal.*, 2022, **12**, 8476–8483.
90 X. Xu, J. M. A. van Hengst, Y. Mao, M. Martinez, S. Roda, M. Floor, V. Guallar, C. E. Paul, M. Alcalde and F. Hollmann, *Angew. Chem., Int. Ed.*, 2023, **62**, e202302844.
91 H. Chen, Y. Chen, X. X. Tang, S. F. Liu, R. P. Wang, T. B. Hu, L. Gao and Z. L. Song, *Angew. Chem., Int. Ed.*, 2019, **58**, 4695–4699.
92 J. O. Bauer and C. Strohmann, *Angew. Chem., Int. Ed.*, 2014, **53**, 720–724.
93 H. Zhou, R. Properzi, M. Leutzsch, P. Belanzoni, G. Bistoni, N. Tsuji, J. T. Han, C. Zhu and B. List, *J. Am. Chem. Soc.*, 2023, **145**, 4994–5000.
94 M.-M. Liu, Y. Xu and C. He, *J. Am. Chem. Soc.*, 2023, **145**, 11727–11734.
95 J. H. Chen, B. Cheng, M. Y. Cao and Z. Lu, *Angew. Chem., Int. Ed.*, 2015, **54**, 4661–4664.
96 M. W. Gribble, M. T. Pirnot, J. S. Bandar, R. Y. Liu and S. L. Buchwald, *J. Am. Chem. Soc.*, 2017, **139**, 2192–2195.
97 M. A. Rivero-Crespo, A. Leyva-Perez and A. Corma, *Chem. – Eur. J.*, 2017, **23**, 1702–1708.
98 C. Wang, W. J. Teo and S. Z. Ge, *ACS Catal.*, 2017, **7**, 855–863.
99 J. Guo, X. Z. Shen and Z. Lu, *Angew. Chem., Int. Ed.*, 2017, **56**, 615–618.
100 H. Fang, W. Hou, G. Liu and Z. Huang, *J. Am. Chem. Soc.*, 2017, **139**, 11601–11609.
101 J. Guo, H. L. Wang, S. P. Xing, X. Hong and Z. Lu, *Chem*, 2019, **5**, 881–895.
102 Z. Y. Cheng, S. P. Xing, J. Guo, B. Cheng, L. F. Hu, X. H. Zhang and Z. Lu, *Chin. J. Chem.*, 2019, **37**, 457–461.
103 Z. Y. Zhao, Y. X. Nie, R. H. Tang, G. W. Yin, J. Cao, Z. Xu, Y. M. Cui, Z. J. Zheng and L. W. Xu, *ACS Catal.*, 2019, **9**, 9110–9116.
104 X. W. Gu, Y. L. Sun, J. L. Xie, X. B. Wang, Z. Xu, G. W. Yin, L. Li, K. F. Yang and L. W. Xu, *Nat. Commun.*, 2020, **11**, 2904.
105 S. Park, *Chin. J. Chem.*, 2019, **37**, 1057–1071.
106 S. Nishino, K. Hirano and M. Miura, *Chem. – Eur. J.*, 2020, **26**, 8725–8728.
107 Y. Wan, J. J. Zhu, Q. Y. Yuan, W. Wang and Y. Q. Zhang, *Org. Lett.*, 2021, **23**, 1406–1410.
108 Y. E. You and S. Z. Ge, *Angew. Chem., Int. Ed.*, 2021, **60**, 12046–12052.
109 S. Neogi, A. K. Ghosh, S. Mandal, D. Ghosh, S. Ghosh and A. Hajra, *Org. Lett.*, 2021, **23**, 6510–6514.
110 M. B. Zhong, X. Pannecoucke, P. Jubault and T. Poisson, *Chem. – Eur. J.*, 2021, **27**, 11818–11822.
111 A. Vivien, L. Veyre, R. Mirgalet, C. Camp and C. Thieuleux, *Chem. Commun.*, 2022, **58**, 4091–4094.
112 C.-R. Jiang, C.-L. Zhao, H.-F. Guo and W. He, *Chem. Commun.*, 2016, **52**, 7862–7865.
113 A. Bokka, Y. D. Hua, A. S. Berlin and J. Jeon, *ACS Catal.*, 2015, **5**, 3189–3195.
114 Y. Takeda, K. Shibuta, S. Aoki, N. Tohnai and S. Minakata, *Chem. Sci.*, 2019, **10**, 8642–8647.
115 H. Kondo, K. Itami and J. Yamaguchi, *Chem. Sci.*, 2017, **8**, 3799–3803.
116 N. Gandhamsetty, J. Park, J. Jeong, S. W. Park, S. Park and S. Chang, *Angew. Chem., Int. Ed.*, 2015, **54**, 6832–6836.
117 X. D. Qiu, L. Zhou, H. R. Wang, L. Y. Lu, Y. Ling and Y. A. Zhang, *RSC Adv.*, 2021, **11**, 37083–37088.
118 T. Ahmad, Q. Li, S. Q. Qiu, J. L. Xu, Y. H. Xu and T. P. Loh, *Org. Biomol. Chem.*, 2019, **17**, 6122–6126.
119 J. J. Shen, Q. Gao, G. Z. Wang, M. Tong, L. L. Chen and S. M. Xu, *ChemistrySelect*, 2019, **4**, 11358–11361.
120 J. Zhou, B. Y. Jiang, Y. Fujihira, Z. Y. Zhao, T. Imai and N. Shibata, *Nat. Commun.*, 2021, **12**, 3749.
121 M. Zheng, J. Hou, L. L. Hua, W. Y. Tang, L. W. Zhan and B. D. Li, *Org. Lett.*, 2021, **23**, 5128–5132.
122 Y. Y. Xue, Z. Z. Guo, X. Y. Chen, J. Y. Li, D. P. Zou, Y. J. Wu and Y. S. Wu, *Org. Biomol. Chem.*, 2022, **20**, 989–994.
123 T. Inagaki, S. Sakurai, M. Yamanaka and M. Tobisu, *Angew. Chem., Int. Ed.*, 2022, **61**, e202202387.
124 Z. K. Zhang and X. L. Hu, *ACS Catal.*, 2020, **10**, 777–782.
125 B. Z. Zhao, Y. Q. Li, H. Y. Li, M. Belal, L. Zhu and G. Y. Yin, *Sci. Bull.*, 2021, **66**, 570–577.
126 Z. T. He, X. Q. Tang, L. B. Xie, M. Cheng, P. Tian and G. Q. Lin, *Angew. Chem., Int. Ed.*, 2015, **54**, 14815–14818.
127 C. Chen, W. Sun, L. Y. Liu, J. H. Zhao, Y. J. Huang, X. N. Shi, J. Ding, D. Q. Jiao and B. L. Zhu, *Org. Chem. Front.*, 2021, **8**, 2250–2255.
128 H. Li, W. S. Huang, K. F. Yang, F. Ye, G. W. Yin, Z. Xu and L. W. Xu, *Asian J. Org. Chem.*, 2021, **10**, 2883–2887.
129 S. B. Krause, J. R. McAtee, G. P. A. Yap and D. A. Watson, *Org. Lett.*, 2017, **19**, 5641–5644.
130 K. Matsumoto, J. Huang, Y. Naganawa, H. Guo, T. Beppu, K. Sato, S. Shimada and Y. Nakajima, *Org. Lett.*, 2018, **20**, 2481–2484.
131 J. Ke, W. T. Liu, X. J. Zhu, X. F. Tan and C. He, *Angew. Chem., Int. Ed.*, 2021, **60**, 8744–8749.
132 D. S. Ni and M. K. Brown, *ACS Catal.*, 2021, **11**, 1858–1862.
133 H. Zhang, E. Wang, S. Geng, Z. Liu, Y. He, Q. Peng and Z. Feng, *Angew. Chem., Int. Ed.*, 2021, **60**, 10211–10218.
134 J. Dong, X.-A. Yuan, Z. Yan, L. Mu, J. Ma, C. Zhu and J. Xie, *Nat. Chem.*, 2021, **13**, 182–190.
135 K. Kikushima, Y. Etou, R. Kamura, I. Takeda, H. Ito, M. Ohashi and S. Ogoshi, *Org. Lett.*, 2020, **22**, 8167–8172.
136 L. Zhang and M. Oestreich, *Org. Lett.*, 2018, **20**, 8061–8063.
137 W. Yuan, P. Orecchia and M. Oestreich, *Chem. – Eur. J.*, 2018, **24**, 19175–19178.
138 Z.-Z. Zhao, X. Pang, X.-X. Wei, X.-Y. Liu and X.-Z. Shu, *Angew. Chem., Int. Ed.*, 2022, **61**, e202200215.
139 H. Yamagishi, H. Saito, J. Shimokawa and H. Yorimitsu, *ACS Catal.*, 2021, **11**, 10095–10103.
140 J. Duan, K. Wang, G.-L. Xu, S. Kang, L. Qi, X.-Y. Liu and X.-Z. Shu, *Angew. Chem., Int. Ed.*, 2020, **59**, 23083–23088.
141 J. Zhang, Y. Zhang, S. Geng, S. Chen, Z. Liu, X. Zeng, Y. He and Z. Feng, *Org. Lett.*, 2020, **22**, 2669–2674.

142 V. Murugesan, V. Balakrishnan and R. Rasappan, *J. Catal.*, 2019, **377**, 293–298.
143 T. Yoshida, L. Ilies and E. Nakamura, *Org. Lett.*, 2018, **20**, 2844–2847.
144 K. Hitoshio, H. Yamagishi, J. Shimokawa and H. Yorimitsu, *Chem. Commun.*, 2021, **57**, 6867–6870.
145 H. J. Lee, C. Kwak, D. P. Kim and H. Kim, *Green Chem.*, 2021, **23**, 1193–1199.
146 T. Nagata, T. Inoue, X. J. Lin, S. Ishimoto, S. Nakamichi, H. Oka, R. Kondo, T. Suzuki and Y. Obora, *RSC Adv.*, 2019, **9**, 17425–17431.
147 D. Y. Wang, X. Wen, C. D. Xiong, J. N. Zhao, C. Y. Ding, Q. Meng, H. Zhou, C. Wang, M. Uchiyama, X. J. Lu and A. Zhang, *iScience*, 2019, **15**, 307–315.
148 S. H. Zheng, T. Y. Zhang and H. Maekawa, *J. Org. Chem.*, 2020, **85**, 13965–13972.
149 L. J. You, W. Yuan and C. A. He, *Eur. J. Org. Chem.*, 2021, **2021**, 3079–3082.
150 J. N. Zhao, M. Kayumov, D. Y. Wang and A. Zhang, *Org. Lett.*, 2019, **21**, 7303–7306.
151 B. Su, T. G. Zhou, X. W. Li, X. R. Shao, P. L. Xu, W. L. Wu, J. F. Hartwig and Z. J. Shi, *Angew. Chem., Int. Ed.*, 2017, **56**, 1092–1096.
152 Y. Ma, B. Wang, L. Zhang and Z. Hou, *J. Am. Chem. Soc.*, 2016, **138**, 3663–3666.
153 Y. D. Hua, P. Asgar, T. Avullala and J. Jeon, *J. Am. Chem. Soc.*, 2016, **138**, 7982–7991.
154 H. Fang, L. Guo, Y. Zhang, W. Yao and Z. Huang, *Org. Lett.*, 2016, **18**, 5624–5627.
155 W. B. Liu, D. P. Schuman, Y. F. Yang, A. A. Toutov, Y. Liang, H. F. T. Klare, N. Nesnas, M. Oestreich, D. G. Blackmond, S. C. Virgil, S. Banerjee, R. N. Zare, R. H. Grubbs, K. N. Houk and B. M. Stoltz, *J. Am. Chem. Soc.*, 2017, **139**, 6867–6879.
156 S. H. Liu, P. Pan, H. Q. Fan, H. Li, W. Wang and Y. Q. Zhang, *Chem. Sci.*, 2019, **10**, 3817–3825.
157 J. Wen, B. Dong, J. J. Zhu, Y. Zhao and Z. Z. Shi, *Angew. Chem., Int. Ed.*, 2020, **59**, 10909–10912.
158 C. H. Dai, Y. L. Zhan, P. Liu and P. P. Sun, *Green Chem.*, 2021, **23**, 314–319.
159 S. Liu, S. L. Zhang, Q. Lin, Y. Q. Huang and B. Li, *Org. Lett.*, 2019, **21**, 1134–1138.
160 W. X. Xu, H. L. Teng, Y. Luo, S. J. Lou, M. Nishiura and Z. M. Hou, *Chem. – Asian J.*, 2020, **15**, 753–756.
161 W. Z. Li and Z. X. Wang, *Org. Biomol. Chem.*, 2021, **19**, 5082–5086.
162 J. H. Li, M. Y. Ding and C. Jiang, *Org. Lett.*, 2021, **23**, 9036–9040.
163 Y. F. Li, K. C. Shu, P. Liu and P. P. Sun, *Org. Lett.*, 2020, **22**, 6304–6307.
164 X. Gong, P. Deng and J. H. Cheng, *ChemCatChem*, 2022, **14**, e202200060.
165 G. Pandey, S. K. Tiwari, P. Singh and P. K. Mondal, *Org. Lett.*, 2021, **23**, 7730–7734.
166 T. Thorwart and L. Greb, *Chem. Sci.*, 2023, **14**, 11237–11242.
167 Y. C. Wu, Y. H. Huang, X. Y. Chen and P. Wang, *Org. Lett.*, 2020, **22**, 6657–6661.
168 S. Som, J. Choi, D. Katsoulis and K. L. Lee, *Chem. Sci.*, 2022, **13**, 10759–10764.
169 Z.-B. Yan, M. Peng, Q.-L. Chen, K. Lu, Y.-Q. Tu, K.-L. Dai, F.-M. Zhang and X.-M. Zhang, *Chem. Sci.*, 2021, **12**, 9748–9753.
170 M. D. Visco, J. M. Wieting and A. E. Mattson, *Org. Lett.*, 2016, **18**, 2883–2885.
171 D. Chen, D. X. Zhu and M. H. Xu, *J. Am. Chem. Soc.*, 2016, **138**, 1498–1501.
172 V. Balakrishnan, V. Murugesan, B. Chindan and R. Rasappan, *Org. Lett.*, 2021, **23**, 1333–1338.
173 W. Y. Qi, J. S. Zhen, X. H. Xu, X. Du, Y. H. Li, H. Yuan, Y. S. Guan, X. Wei, Z. Y. Wang, G. H. Liang and Y. Luo, *Org. Lett.*, 2021, **23**, 5988–5992.
174 X. Zhang, P. Y. Geng, G. X. Liu and Z. Huang, *Organometallics*, 2021, **40**, 2365–2370.
175 B. B. Zhan, J. Fan, L. Jin and B. F. Shi, *ACS Catal.*, 2019, **9**, 3298–3303.
176 J. L. Pan, Q. Z. Li, T. Y. Zhang, S. H. Hou, J. C. Kang and S. Y. Zhang, *Chem. Commun.*, 2016, **52**, 13151–13154.
177 P. Liu, J. H. Tang and X. M. Zeng, *Org. Lett.*, 2016, **18**, 5536–5539.
178 J. H. Li and C. Jiang, *Org. Lett.*, 2021, **23**, 5359–5362.
179 S. Bähr, W. Xue and M. Oestreich, *ACS Catal.*, 2019, **9**, 16–24.
180 X. W. Liu, C. Zarate and R. Martin, *Angew. Chem., Int. Ed.*, 2019, **58**, 2064–2068.
181 C. K. Chu, Y. Liang and G. C. Fu, *J. Am. Chem. Soc.*, 2016, **138**, 6404–6407.
182 S. Mallick, E. U. Wurthwein and A. Studer, *Org. Lett.*, 2020, **22**, 6568–6572.
183 T. Y. Zhang, S. H. Zheng, T. Kobayashi and H. Maekawa, *Org. Lett.*, 2021, **23**, 7129–7133.
184 H. F. Guo, X. Chen, C. L. Zhao and W. He, *Chem. Commun.*, 2015, **51**, 17410–17412.
185 M. M. Xing, H. H. Cui and C. Zhang, *Org. Lett.*, 2021, **23**, 7645–7649.
186 B. Yang and Z. X. Wang, *Org. Lett.*, 2019, **21**, 7965–7969.
187 B. Vulovic, A. P. Cinderella and D. A. Watson, *ACS Catal.*, 2017, **7**, 8113–8117.
188 A. A. Toutov, K. N. Betz, D. P. Schuman, W. B. Liu, A. Fedorov, B. M. Stoltz and R. H. Grubbs, *J. Am. Chem. Soc.*, 2017, **139**, 1668–1674.
189 M. Y. Huang, J. M. Yang, Y. T. Zhao and S. F. Zhu, *ACS Catal.*, 2019, **9**, 5353–5357.
190 C. Y. He, L. B. Xie, R. Ding, P. Tian and G. Q. Lin, *Tetrahedron*, 2019, **75**, 1682–1688.
191 T. He, B. Li, L. C. Liu, W. P. Ma and W. He, *Chem. – Eur. J.*, 2021, **27**, 5648–5652.
192 M. F. Wisthoff, S. B. Pawley, A. P. Cinderella and D. A. Watson, *J. Am. Chem. Soc.*, 2020, **142**, 12051–12055.
193 Y. Nakamura, S. Ozawa, S. Yoshida and T. Hosoya, *Chem. Lett.*, 2019, **48**, 1296–1299.
194 C. Bellini, V. Dorcet, J. F. Carpentier, S. Tobisch and Y. Sarazin, *Chem. – Eur. J.*, 2016, **22**, 4564–4583.
195 A. A. Toutov, K. N. Betz, M. C. Haibach, A. M. Romine and R. H. Grubbs, *Org. Lett.*, 2016, **18**, 5776–5779.

196 D. D. Xu, J. C. Chen, J. Y. Li, Y. B. Zhu, S. Y. Wu, J. Q. Zhang, X. Y. Liu and B. M. Fan, *Asian J. Org. Chem.*, 2021, **10**, 1402–1405.
197 Z. C. Wang, H. Q. Fang, G. X. Liu and Z. Huang, *Org. Lett.*, 2021, **23**, 7603–7607.
198 R. Ortega, J. Sanchez-Quesada, C. Lorenz, G. Dolega, A. Karawajczyk, M. Sanz, G. Showell and F. Giordanetto, *Bioorg. Med. Chem.*, 2015, **23**, 2716–2720.
199 T. Ohmura, I. Sasaki and M. Suginome, *Org. Lett.*, 2019, **21**, 1649–1653.
200 W. Reid, J. R. McAtee and D. A. Watson, *Organometallics*, 2019, **38**, 3796–3803.
201 M. Murai, *Asian J. Org. Chem.*, 2022, **11**, e202100651.
202 Y. K. Xu, W. W. Xu, X. Y. Chen, X. A. Luo, H. Y. Lu, M. H. Zhang, X. M. Yang, G. B. Deng, Y. Liang and Y. Yang, *Chem. Sci.*, 2021, **12**, 11756–11761.
203 J. F. Huo, K. B. Zhong, Y. Z. Xue, M. M. Lyu, Y. F. Ping, W. B. Ouyang, Z. X. Liu, Y. Lan and J. B. Wang, *Chem. – Eur. J.*, 2022, **28**, e202200191.
204 J. R. Vale, A. Valkonen, C. A. M. Afonso and N. R. Candeias, *Org. Chem. Front.*, 2019, **6**, 3793–3798.
205 S. Yoshioka, Y. Fujii, H. Tsujino, T. Uno, H. Fujioka and M. Arisawa, *Chem. Commun.*, 2017, **53**, 5970–5973.
206 M. Fischer, C. Burschka and R. Tacke, *Organometallics*, 2014, **33**, 1020–1029.
207 T. He, G. Q. Wang, V. Bonetti, H. F. T. Klare and M. Oestreich, *Angew. Chem., Int. Ed.*, 2020, **59**, 12186–12191.
208 M. Czyzewski, J. D. Sellars, T. Guliashvili, J. Tibbelin, L. Johnstone, J. Bower, M. Box, R. D. M. Davies, H. Ottosson and P. G. Steel, *Chem. Commun.*, 2014, **50**, 2919–2921.
209 H. Arii, Y. Yano, K. Nakabayashi, S. Yamaguchi, M. Yamamura, K. Mochida and T. Kawashima, *J. Org. Chem.*, 2016, **81**, 6314–6319.
210 Y. Yang, R. J. Song, Y. Li, X. H. Ouyang, J. H. Li and D. L. He, *Chem. Commun.*, 2018, **54**, 1441–1444.
211 Y. Qin, J. L. Han, C. W. Ju and D. B. Zhao, *Angew. Chem., Int. Ed.*, 2020, **59**, 8481–8485.
212 J. W. Guo, S. Liu, Q. J. Pang, H. Y. Zhang, L. Gao, L. Chen and Z. L. Song, *Org. Lett.*, 2022, **24**, 726–730.
213 M. H. Zhu, X. W. Zhang, M. Usman, H. J. Cong and W. B. Liu, *ACS Catal.*, 2021, **11**, 5703–5708.
214 X. C. Wang, H. R. Wang, X. F. Xu and D. B. Zhao, *Eur. J. Org. Chem.*, 2021, **2021**, 3039–3042.
215 D. Y. Wang, M. J. Li, X. Y. Chen, M. Y. Wang, Y. Liang, Y. Zhao, K. N. Houk and Z. Z. Shi, *Angew. Chem., Int. Ed.*, 2021, **60**, 7066–7071.
216 K. P. C. Vollhardt, *Angew. Chem., Int. Ed. Engl.*, 1984, **23**, 539–556.
217 A. Gomtsyan, *Chem. Heterocycl. Compd.*, 2012, **48**, 7–10.
218 E. Kabir and M. Uzzaman, *Results Chem.*, 2022, **4**, 100606.
219 W. Wang, L. Gao and Z. Song, *Synthesis*, 2022, **54**, 2749–2764.
220 C. M. Reid, K. N. Fanning, L. S. Fowler and A. Sutherland, *Tetrahedron*, 2015, **71**, 245–251.
221 A. Rene, N. Vanthuyne, J. Martinez and F. Cavelier, *Amino Acids*, 2013, **45**, 301–307.
222 M. Fischer and R. Tacke, *Organometallics*, 2013, **32**, 7181–7185.
223 L. H. Luhning, J. Strehl, M. Schmidtmann and S. Doye, *Chem. – Eur. J.*, 2017, **23**, 4197–4202.
224 Y. Qin, L. H. Li, J. Y. Liang, K. L. Li and D. B. Zhao, *Chem. Sci.*, 2021, **12**, 14224–14229.
225 H. P. Lv, R. D. Laishram, J. C. Chen, R. Khan, Y. B. Zhu, S. Y. Wu, J. Q. Zhang, X. Y. Liu and B. M. Fan, *Chem. Commun.*, 2021, **57**, 3660–3663.
226 D. Limnios and C. G. Kokotos, *ACS Catal.*, 2013, **3**, 2239–2243.
227 K. K. Wang, J. M. Zhou, Y. T. Jiang, M. M. Zhang, C. Wang, D. Xue, W. J. Tang, H. M. Sun, J. L. Xiao and C. Q. Li, *Angew. Chem., Int. Ed.*, 2019, **58**, 6380–6384.
228 K. F. Zhang, L. Yang, Y. F. Hu, C. H. Fan, Y. R. Zhao, L. Bai, Y. L. Li, F. X. Shi, J. Liu and W. Xie, *Angew. Chem., Int. Ed.*, 2020, **59**, 18003–18009.
229 H. Liang, L. J. Wang, Y. X. Ji, H. Wang and B. Zhang, *Angew. Chem., Int. Ed.*, 2021, **60**, 1839–1844.
230 Z. J. Garlets and H. M. L. Davies, *Org. Lett.*, 2018, **20**, 2168–2171.
231 M. P. Wiesenfeldt, T. Knecht, C. Schlepphorst and F. Glorius, *Angew. Chem., Int. Ed.*, 2018, **57**, 8297–8300.
232 Z. Wu, S. B. J. Kan, R. D. Lewis, B. J. Wittmann and F. H. Arnold, *Proc. Natl. Acad. Sci. U. S. A.*, 2019, **116**, 8852–8858.
233 Z. Wu, S. B. J. Kan, R. D. Lewis, B. J. Wittmann and F. H. Arnold, *Proc. Natl. Acad. Sci. U. S. A.*, 2020, **117**, 788–789.
234 J. J. Feng and M. Oestreich, *Angew. Chem., Int. Ed.*, 2019, **58**, 8211–8215.
235 L. Wei, C. Shen, Y. Z. Hu, H. Y. Tao and C. J. Wang, *Chem. Commun.*, 2019, **55**, 6672–6684.
236 D. L. Mu, W. Yuan, S. Y. Chen, N. Wang, B. Yang, L. J. You, B. Zu, P. Y. Yu and C. He, *J. Am. Chem. Soc.*, 2020, **142**, 13459–13468.
237 B. Yang, W. Yang, Y. H. Guo, L. J. You and C. He, *Angew. Chem., Int. Ed.*, 2020, **59**, 22217–22222.
238 L. L. Yang, J. Ouyang, H. N. Zou, S. F. Zhu and Q. L. Zhou, *J. Am. Chem. Soc.*, 2021, **143**, 6401–6406.
239 V. Carreras, C. Besnard, V. Gandon and T. Ollevier, *Org. Lett.*, 2019, **21**, 9094–9098.
240 H. P. Zhang and D. B. Zhao, *ACS Catal.*, 2021, **11**, 10748–10753.
241 Y. J. Zhang, M. Tong, Q. Gao, P. K. Zhang and S. M. Xu, *Tetrahedron Lett.*, 2019, **60**, 1210–1212.
242 Y. Zhang, J. C. Guo, J. N. Han, X. G. Zhou, W. Cao and Z. Q. Fu, *Org. Biomol. Chem.*, 2021, **19**, 6412–6416.
243 R. Chowdhury, A. K. Dubey and S. K. Ghosh, *Asian J. Org. Chem.*, 2021, **10**, 1173–1183.
244 T. Kobayashi, S. Nishino, M. Miura and K. Hirano, *Org. Lett.*, 2022, **24**, 1418–1422.
245 D. C. Bai, F. Wu, L. N. Chang, M. M. Wang, H. Wu and J. B. Chang, *Angew. Chem., Int. Ed.*, 2022, **61**, e202114918.
246 Y. Liu, M. Zhan and P. F. Li, *Chin. J. Chem.*, 2022, **40**, 1028–1032.
247 J. Fotie, C. M. Matherne and J. E. Wroblewski, *Chem. Biol. Drug Des.*, 2023, **102**, 235–254.

248 S. N. Adamovich, E. N. Oborina, A. M. Nalibayeva and I. B. Rozentsveig, *Molecules*, 2022, **27**, 3549.
249 T. Marzo and D. La Mendola, *Inorganics*, 2021, **9**, 46.
250 C. C. Perez, F. R. Benatti, D. P. Martins Jr and A. A. Silva, *Rev. Virtual Quim.*, 2021, **13**, 981–992.
251 R. Ramesh and D. S. Reddy, *J. Med. Chem.*, 2018, **61**, 3779–3798.
252 S. Fujii and Y. Hashimoto, *Future Med. Chem.*, 2017, **9**, 485–505.
253 E. Remond, C. Martin, J. Martinez and F. Cavelier, *Chem. Rev.*, 2016, **116**, 11654–11684.
254 N. F. Lazareva and I. M. Lazarev, *Russ. Chem. Bull.*, 2015, **64**, 1221–1232.
255 B. S. Sekhon, *Res. Pharm. Sci.*, 2013, **8**, 145–158.
256 N. F. Lazareva, *Russ. Chem. Bull.*, 2011, **60**, 615–632.
257 S. Gately and R. West, *Drug Dev. Res.*, 2007, **68**, 156–163.
258 P. K. Pooni and G. A. Showell, *Mini-Rev. Med. Chem.*, 2006, **6**, 1169–1177.
259 W. Bains and R. Tacke, *Curr. Opin. Drug Discovery Dev.*, 2003, **6**, 526–543.
260 R. J. Fessenden and J. S. Fessenden, in *Advances in Organometallic Chemistry*, ed. F. G. A. Stone and R. West, Academic Press, 1980, vol. 18, pp. 275–299.
261 L. R. Garson and L. K. Kirchner, *J. Pharm. Sci.*, 1971, **60**, 1113–1127.
262 S. Fujii, *Med. Chem. Commun.*, 2016, **7**, 1082–1092.
263 D. Lowe, Silicon In Drug Molecules: Not Quite There, in *In the Pipeline*, 2012, **https://www.science.org/content/blog-post/silicon-drug-molecules-not-quite-there**.
264 D. Lowe, Silicon In Drug Molecules, Revisited, in *In the Pipeline*, 2018, **https://www.science.org/content/blog-post/silicon-drug-molecules-revisited**.
265 D. Lowe, Silicon Stays in the Shadows, in *In the Pipeline*, 2017, **https://www.science.org/content/blog-post/silicon-stays-shadows**.
266 D. Lowe, Odd Elements in Drugs: Silicon, in *In the Pipeline*, 2004, **https://www.science.org/content/blog-post/silicon-drug-molecules-not-quite-there**.
267 F. T. Chiu, Y. H. Chang, G. Ozkan, G. Zon, K. C. Fichter and L. R. Phillips, *J. Pharm. Sci.*, 1982, **71**, 542–551.
268 L. T. Farol and K. B. Hymes, *Expert Rev. Anticancer Ther.*, 2004, **4**, 180–188.
269 R. Gniadecki, C. Assaf, M. Bagot, R. Dummer, M. Duvic, R. Knobler, A. Ranki, P. Schwandt and S. Whittaker, *Br. J. Dermatol.*, 2007, **157**, 433–440.
270 K. H. Dragnev, W. J. Petty, S. J. Shah, L. D. Lewis, C. C. Black, V. Memoli, W. C. Nugent, T. Hermann, A. Negro-Vilar, J. R. Rigas and E. Dmitrovsky, *Clin. Cancer Res.*, 2007, **13**, 1794–1800.
271 R. Ramlau, P. Zatloukal, J. Jassem, P. Schwarzenberger, S. V. Orlov, M. Gottfried, J. R. Pereira, G. Temperley, R. Negro-Vilar, S. Rahal, J. K. Zhang, A. Negro-Vilar and Z. E. Dziewanowska, *J. Clin. Oncol.*, 2008, **26**, 1886–1892.
272 M. I. Dawson and Z. Xia, *Biochim. Biophys. Acta, Mol. Cell Biol. Lipids*, 2012, **1821**, 21–56.
273 J. O. Daiss, C. Burschka, J. S. Mills, J. G. Montana, G. A. Showell, I. Fleming, C. Gaudon, D. Ivanova, H. Gronemeyer and R. Tacke, *Organometallics*, 2005, **24**, 3192–3199.
274 M. W. Buttner, C. Burschka, J. O. Daiss, D. Ivanova, N. Rochel, S. Kammerer, C. Peluso-Iltis, A. Bindler, C. Gaudon, P. Germain, D. Moras, H. Gronemeyer and R. Tacke, *ChemBioChem*, 2007, **8**, 1688–1699.
275 J. B. Bauer, W. P. Lippert, S. Dörrich, D. Tebbe, C. Burschka, V. B. Christie, D. M. Tams, A. P. Henderson, B. A. Murray, T. B. Marder, S. A. Przyborski and R. Tacke, *ChemMedChem*, 2011, **6**, 1509–1517.
276 W. P. Lippert, C. Burschka, K. Götz, M. Kaupp, D. Ivanova, C. Gaudon, Y. Sato, P. Antony, N. Rochel, D. Moras, H. Gronemeyer and R. Tacke, *ChemMedChem*, 2009, **4**, 1143–1152.
277 T. Yamakawa, H. Kagechika, E. Kawachi, Y. Hashimoto and K. Shudo, *J. Med. Chem.*, 1990, **33**, 1430–1437.
278 R. Tacke, V. Muller, M. W. Buttner, W. P. Lippert, R. Bertermann, J. O. Daiss, H. Khanwalkar, A. Furst, C. Gaudon and H. Gronemeyer, *ChemMedChem*, 2009, **4**, 1797–1802.
279 K. B. Higginbotham, R. Lozano, T. Brown, Y. Z. Patt, T. Arima, J. L. Abbruzzese and M. B. Thomas, *J. Cancer Res. Clin. Oncol.*, 2008, **134**, 1325–1335.
280 T. Oikawa, S. Fujii, S. Mori, H. Masuno, E. Kawachi and H. Kagechika, *ChemMedChem*, 2022, **17**, e202200176.
281 A. Zablotskaya, I. Segal, Y. Popelis, E. Lukevics, S. Baluja, I. Shestakova and I. Domracheva, *Appl. Organomet. Chem.*, 2006, **20**, 721–728.
282 A. Zablotskaya, I. Segal, Y. Popelis, S. Grinberga, I. Shestakova, V. Nikolajeva and D. Eze, *Appl. Organomet. Chem.*, 2013, **27**, 114–124.
283 A. Zablotskaya, I. Segal, A. Kemme, S. Germane, J. Popelis, E. Lukevics, R. Berger and H. Spies, *Chem. Heterocycl. Compd.*, 2002, 543–555.
284 A. Zablotskaya, I. Segal, S. Germane, I. Shestakova, I. Domracheva, A. Nesterova, A. Geronikaki and E. Lukevics, *Chem. Heterocycl. Compd.*, 2002, **38**, 859–866.
285 A. Zablotskaya, I. Segal, S. Belyakov and E. Lukevics, *Appl. Organomet. Chem.*, 2006, **20**, 149–154.
286 H. Spies, T. Fietz, A. Zablotskaya, S. Belyakov and E. Lukevics, *Chem. Heterocycl. Compd.*, 1999, 116–125.
287 I. Segal, A. Zablotskaya and E. Lukevits, *J. Heterocyclic Chem.*, 2005, 713–725.
288 E. Lukevics, A. Zablotskaya, I. Segal, S. Germane and J. Popelis, *Chem. Heterocycl. Compd.*, 2003, 941–947.
289 E. Lukevics, I. Segal, A. Zablotskaya and S. Germane, *Chem. Heterocycl. Compd.*, 1996, 793–799.
290 E. Lukevics, I. Segal, I. Birgele and A. Zablotskaya, *Chem. Heterocycl. Compd.*, 1998, 1253–1258.
291 E. Lukevics, S. Germane, I. Segal and A. Zablotskaya, *Chem. Heterocycl. Compd.*, 1997, 270–274.
292 A. Zablotskaya, I. Segal, G. Kazachonokh, Y. Popelis, I. Shestakova and V. Nikolajeva, *Silicon*, 2018, **10**, 1129–1138.

293 A. Zablotskaya, I. Segal and E. Lukevics, *Appl. Organomet. Chem.*, 2010, **24**, 150–157.
294 L. Ignatovich, V. Romanov, J. Spura, J. Popelis, I. Domracheva and I. Shestakova, *Chem. Heterocycl. Compd.*, 2012, **47**, 1502–1508.
295 P. C. Lo, C. M. H. Chan, J. Y. Liu, W. P. Fong and D. K. P. Ng, *J. Med. Chem.*, 2007, **50**, 2100–2107.
296 J. T. F. Lau, P. C. Lo, Y. M. Tsang, W. P. Fong and D. K. P. Ng, *Chem. Commun.*, 2011, **47**, 9657–9659.
297 M. Bispo, P. M. R. Pereira, F. Setaro, M. S. Rodriguez-Morgade, R. Fernandes, T. Torres and J. P. C. Tome, *ChemPlusChem*, 2018, **83**, 855–860.
298 C. M. H. Chan, P. C. Lo, S. L. Yeung, D. K. P. Ng and W. P. Fong, *Cancer Biol. Ther.*, 2010, **10**, 126–134.
299 J. M. Park, C. Y. Jung, W. D. Jang and J. Y. Jaung, *ACS Appl. Bio Mater.*, 2021, **4**, 1988–2000.
300 H. Y. Yenilmez, N. Farajzadeh, N. Güler Kuşçulu, D. Bahar, S. Özdemir, G. Tollu, M. Güllü and Z. Altuntaş Bayır, *Chem. Biodiversity*, 2023, **20**, e202201167.
301 H. Y. Yenilmez, N. Farajzadeh, G. Tollu, N. G. Kuşçulu, D. Bahar, S. Özdemir and Z. A. Bayır, *ChemistrySelect*, 2023, **8**, e202300856.
302 G. Y. Atmaca, M. Aksel, M. D. Bilgin and A. Erdoğmuş, *Photodiagn. Photodyn. Ther.*, 2023, **42**, 103339.
303 H. Yalazan, D. Akkaya, G. Seyhan, B. Barut and H. Kantekin, *Appl. Organomet. Chem.*, 2023, **37**, e7040.
304 E. Georgiopoulou, E. Kavetsou, E. Alexandratou, A. Detsi and K. Politopoulos, Comparative characterization of $SiCl_2Pc$ and its cyclodextrin complexes as photosensitizers in photodynamic therapy, in *Translational Biophotonics: Diagnostics and Therapeutics III*, Proc. SPIE, 2023, vol. 12627, p. 1262718, DOI: **10.1117/12.2670864**.
305 N. Farajzadeh, N. Güler Kuşçulu, H. Y. Yenilmez, D. Bahar and Z. Altuntaş Bayır, *Dalton Trans.*, 2022, **51**, 7539–7550.
306 N. Farajzadeh, N. Güler Kuşçulu, H. Y. Yenilmez, D. Bahar and Z. Altuntaş Bayır, *New J. Chem.*, 2022, **46**, 19863–19873.
307 G. Y. Atmaca, M. Aksel, B. Keskin, M. D. Bilgin and A. Erdoğmuş, *Dyes Pigm.*, 2021, **184**, 108760.
308 D. D. Ma, X. Q. Chen, Y. H. Wang, Q. M. Guo, Q. H. Ye, R. T. Guo, S. H. Xiao, Q. Ye, Y. D. Huang and Y. R. Peng, *J. Lumin.*, 2019, **207**, 597–601.
309 Q. Liu, M. Pang, S. Tan, J. Wang, Q. Chen, K. Wang, W. Wu and Z. Hong, *J. Cancer*, 2018, **9**, 310–320.
310 C. Jing, R. L. Wang, H. L. Ou, A. Li, Y. L. An, S. T. Guo and L. Q. Shi, *Chem. Commun.*, 2018, **54**, 3985–3988.
311 K. Z. Chen, S. J. Pan, X. M. Zhuang, H. F. Lv, S. L. Que, S. S. Xie, H. Q. Yang and Y. R. Peng, *J. Nanopart. Res.*, 2016, **18**, 197.
312 A. R. Simioni, F. L. Primo and A. C. Tedesco, *J. Laser Appl.*, 2012, **24**, 012004.
313 K. Mitra and M. C. T. Hartman, *Org. Biomol. Chem.*, 2021, **19**, 1168–1190.
314 C. Uslan and B. Şebnem Sesalan, *Inorg. Chim. Acta*, 2013, **394**, 353–362.
315 W. K. Anderson, R. Kasliwal, D. M. Houston, Y. S. Wang, V. L. Narayanan, R. D. Haugwitz and J. Plowman, *J. Med. Chem.*, 1995, **38**, 3789–3797.
316 A. Varga, P. Hegyes, J. Molnar, I. Mucsi, A. Hever, D. Szabo, S. Kiesig, H. Lage, D. Gaal and J. Nacsa, Substituted disiloxanes, method for the production thereof and the use thereof for reversal of multidrug resistance (MDR), *EP Pat.*, 1432717B1, 1999.
317 J. Molnar, I. Mucsi, J. Nacsa, A. Hever, N. Gyemant, K. Ugocsai, P. Hegyes, S. Kiessig, D. Gaal, H. Lage and A. Varga, *Anticancer Res.*, 2004, **24**, 865–871.
318 A. Zalatnai and J. Molnár, *In Vivo*, 2006, **20**, 137–140.
319 U. Olszewski, R. Zeillinger, M. Demirel Kars, A. Zalatnai, J. Molnar and G. Hamilton, *Anti-Cancer Agents Med. Chem.*, 2012, **12**, 663–671.
320 T. Harukuni, M. Takashi, S. Nobutaka, H. Judit, V. Andrea, E. Helga, M. Ilona, O. Ulrike, H. Gerhard, A. Leonard and M. Joseph, *Anticancer Res.*, 2013, **33**, 2021–2027.
321 O. Wesołowska, K. Michalak, M. Błaszczyk, J. Molnár and K. Środa-Pomianek, *Molecules*, 2020, **25**, 1654.
322 A. M. Thompson, J. W. Blunt, M. H. G. Munro, N. B. Perry and L. K. Pannell, *J. Chem. Soc., Perkin Trans. 1*, 1992, 1335–1342.
323 G. Ş. Karatoprak, E. Küpeli Akkol, Y. Genç, H. Bardakcı, Ç. Yücel and E. Sobarzo-Sánchez, *Molecules*, 2020, **25**, 2560.
324 M. Nakamura, D. Kajita, Y. Matsumoto and Y. Hashimoto, *Bioorg. Med. Chem.*, 2013, **21**, 7381–7391.
325 D. Kajita, M. Nakamura, Y. Matsumoto, M. Ishikawa, Y. Hashimoto and S. Fujii, *Bioorg. Med. Chem. Lett.*, 2015, **25**, 3350–3354.
326 G. Astarita, B. Di Giacomo, S. Gaetani, F. Oveisi, T. R. Compton, S. Rivara, G. Tarzia, M. Mor and D. Piomelli, *J. Pharmacol. Exp. Ther.*, 2006, **318**, 563–570.
327 A. Belfiore, M. Genua and R. Malaguarnera, *PPAR Res.*, 2009, **2009**, 830501.
328 K. Maruyama, M. Nakamura, S. Tomoshige, K. Sugita, M. Makishima, Y. Hashimoto and M. Ishikawa, *Bioorg. Med. Chem. Lett.*, 2013, **23**, 4031–4036.
329 M. F. Boehm, P. Fitzgerald, A. Zou, M. G. Elgort, E. D. Bischoff, L. Mere, D. E. Mais, R. P. Bissonnette, R. A. Heyman, A. M. Nadzan, M. Reichman and E. A. Allegretto, *Chem. Biol.*, 1999, **6**, 265–275.
330 M. Nakamura, M. Makishima and Y. Hashimoto, *Bioorg. Med. Chem.*, 2013, **21**, 1643–1651.
331 D. Kajita, M. Nakamura, Y. Matsumoto, M. Makishima and Y. Hashimoto, *Bioorg. Med. Chem. Lett.*, 2014, **22**, 2244–2252.
332 J. P. M. Antonio, R. F. M. Frade, F. M. F. Santos, J. A. S. Coelho, C. A. M. Afonso, P. M. P. Gois and A. F. Trindade, *RSC Adv.*, 2014, **4**, 29352–29356.
333 O. J. Donadel, T. Martin, V. S. Martin, J. Villar and J. M. Padrón, *Bioorg. Med. Chem. Lett.*, 2005, **15**, 3536–3539.
334 J. M. Padrón, O. J. Donadel, L. G. Leon, T. Martin and V. S. Martin, *Lett. Drug Des. Discovery*, 2006, **3**, 29–34.
335 L. G. Leon, P. O. Miranda, V. S. Martin, J. I. Padron and J. M. Padron, *Bioorg. Med. Chem. Lett.*, 2007, **17**, 3087–3090.
336 U. Sirion, S. Kasemsook, K. Suksen, P. Piyachaturawat, A. Suksamrarn and R. Saeeng, *Bioorg. Med. Chem. Lett.*, 2012, **22**, 49–52.

337 J. Nateewattana, R. Saeeng, S. Kasemsook, K. Suksen, S. Dutta, S. Jariyawat, A. Chairoungdua, A. Suksamrarn and P. Piyachaturawat, *Invest. New Drugs*, 2013, **31**, 320–332.
338 J. Nateewattana, S. Dutta, S. Reabroi, R. Saeeng, S. Kasemsook, A. Chairoungdua, J. Weerachayaphorn, S. Wongkham and P. Piyachaturawat, *Eur. J. Pharmacol.*, 2014, **723**, 148–155.
339 S. Reabroi, A. Chairoungdua, R. Saeeng, T. Kasemsuk, W. Saengsawang, W. M. Zhu and P. Piyachaturawat, *Biomed. Pharmacother.*, 2018, **101**, 414–421.
340 J. Apisornopas, P. Silalai, T. Kasemsuk, A. Athipornchai, U. Sirion, K. Suksen, P. Piyachaturawat, A. Suksamrarn and R. Saeeng, *Bioorg. Med. Chem. Lett.*, 2018, **28**, 1558–1561.
341 C. R. Pungitore, L. G. León, C. García, V. S. Martín, C. E. Tonn and J. M. Padrón, *Bioorg. Med. Chem. Lett.*, 2007, **17**, 1332–1335.
342 H. A. Garro, C. García, V. S. Martín, C. E. Tonn and C. R. Pungitore, *Bioorg. Med. Chem. Lett.*, 2015, **25**, 914–918.
343 N. Khaiwa, N. R. Maarouf, M. H. Darwish, D. W. M. Alhamad, A. Sebastian, M. Hamad, H. A. Omar, G. Orive and T. H. Al-Tel, *Eur. J. Med. Chem.*, 2021, **223**, 113639.
344 E. Martino, S. Della Volpe, E. Terribile, E. Benetti, M. Sakaj, A. Centamore, A. Sala and S. Collina, *Bioorg. Med. Chem. Lett.*, 2017, **27**, 701–707.
345 V. J. Venditto and E. E. Simanek, *Mol. Pharmaceutics*, 2010, **7**, 307–349.
346 D. Sriram, P. Yogeeswari, R. Thirumurugan and T. Ratan Bal, *Nat. Prod. Res.*, 2005, **19**, 393–412.
347 H. Josien, D. Bom, D. P. Curran, Y. H. Zheng and T. C. Chou, *Bioorg. Med. Chem. Lett.*, 1997, **7**, 3189–3194.
348 R. W. Versace, *Expert Opin. Ther. Pat.*, 2003, **13**, 751–760.
349 D. Bom, D. P. Curran, S. Kruszewski, S. G. Zimmer, J. Thompson Strode, G. Kohlhagen, W. Du, A. J. Chavan, K. A. Fraley, A. L. Bingcang, L. J. Latus, Y. Pommier and T. G. Burke, *J. Med. Chem.*, 2000, **43**, 3970–3980.
350 A. H. Van Hattum, H. M. Pinedo, H. M. M. Schlüper, F. H. Hausheer and E. Boven, *Int. J. Cancer*, 2000, **88**, 260–266.
351 A. H. van Hattum, H. M. M. Schlüper, F. H. Hausheer, H. M. Pinedo and E. Boven, *Int. J. Cancer*, 2002, **100**, 22–29.
352 S. Yao, P. Petluru, A. Parker, D. Ding, X. Chen, Q. Huang, H. Kochat and F. Hausheer, *Cancer Chemother. Pharmacol.*, 2015, **75**, 719–728.
353 A. Daud, N. Valkov, B. Centeno, J. Derderian, P. Sullivan, P. Munster, P. Urbas, R. C. DeConti, E. Berghorn, Z. Liu, F. Hausheer and D. Sullivan, *Clin. Cancer Res.*, 2005, **11**, 3009–3016.
354 P. N. Munster and A. I. Daud, *Expert Opin. Invest. Drugs*, 2011, **20**, 1565–1574.
355 N. F. Lazareva, V. P. Baryshok and I. M. Lazarev, *Arch. Pharm.*, 2018, **351**, 1700297.
356 A. K. Franz, P. D. Dreyfuss and S. L. Schreiber, *J. Am. Chem. Soc.*, 2007, **129**, 1020–1021.
357 K. J. Mccormick and W. R. Panje, *Cancer Immunol., Immunother.*, 1986, **21**, 226–232.
358 R. D. Maca and W. R. Panje, *Cancer*, 1982, **50**, 483–489.
359 W. R. Panje, *Arch. Otolaryngol.*, 1981, **107**, 658–663.
360 C. M. Ulrich, J. Bigler and J. D. Potter, *Nat. Rev. Cancer*, 2006, **6**, 130–140.
361 G. A. Bikzhanova, I. S. Toulokhonova, S. Gately and R. West, *Silicon Chem.*, 2007, **3**, 209–217.
362 E. Lukevits, I. Segal, I. Birgele and A. Zablotskaya, *Chem. Heterocycl. Compd.*, 1998, **34**, 1076–1080.
363 A. Szilagyi, F. Fenyvesi, O. Majercsik, I. F. Pelyvas, I. Bacskay, P. Feher, J. Varadi, M. Vecsernyes and P. Herczegh, *J. Med. Chem.*, 2006, **49**, 5626–5630.
364 C. A. Black, J. W. Ucci, J. S. Vorpagel, M. C. Mauck and E. E. Fenlon, *Bioorg. Med. Chem. Lett.*, 2002, **12**, 3521–3523.
365 P. Guo, Y. W. Wang, X. T. Luo, X. L. Qi, L. P. Hou, Z. X. Xie and F. Q. Ye, *Phosphorus, Sulfur Silicon Relat. Elem.*, 2014, **189**, 511–518.
366 J. L. Panayides, V. Mathieu, L. M. Y. Banuls, H. Apostolellis, N. Dahan-Farkas, H. Davids, L. Harmse, M. E. C. Rey, I. R. Green, S. C. Pelly, R. Kiss, A. Kornienko and W. A. L. van Otterlo, *Bioorg. Med. Chem.*, 2016, **24**, 2716–2724.
367 L. Harmse, N. Dahan-Farkas, J. L. Panayides, W. A. L. van Otterlo and C. Penny, *PLoS One*, 2015, **10**, e0138607.
368 M. A. Peterson, M. Oliveira, M. A. Christiansen and C. E. Cutler, *Bioorg. Med. Chem. Lett.*, 2009, **19**, 6775–6779.
369 J. R. Shelton, S. R. Burt and M. A. Peterson, *Bioorg. Med. Chem. Lett.*, 2011, **21**, 1484–1487.
370 J. R. Shelton, C. E. Cutler, M. S. Browning, J. Balzarini and M. A. Peterson, *Bioorg. Med. Chem. Lett.*, 2012, **22**, 6067–6071.
371 J. R. Shelton, C. E. Cutler, M. Oliveira, J. Balzarini and M. A. Peterson, *Bioorg. Med. Chem.*, 2012, **20**, 1008–1019.
372 J. R. Shelton, J. Balzarini and M. A. Peterson, *Bioorg. Med. Chem. Lett.*, 2014, **24**, 5107–5110.
373 A. Lanver and H. G. Schmalz, *Eur. J. Org. Chem.*, 2005, **2005**, 1444–1458.
374 J. Velcicky, A. Lanver, J. Lex, A. Prokop, T. Wieder and H. G. Schmalz, *Chem. – Eur. J.*, 2004, **10**, 5087–5110.
375 C. Hirschhauser, J. Velcicky, D. Schlawe, E. Hessler, A. Majdalani, J. M. Neudorfl, A. Prokop, T. Wieder and H. G. Schmalz, *Chem. – Eur. J.*, 2013, **19**, 13017–13029.
376 D. Schlawe, A. Majdalani, J. Velcicky, E. Hessler, T. Wieder, A. Prokop and H. G. Schmalz, *Angew. Chem., Int. Ed.*, 2004, **43**, 1731–1734.
377 C. Prinz, E. Vasyutina, G. Lohmann, A. Schrader, S. Romanski, C. Hirschhauser, P. Mayer, C. Frias, C. D. Herling, M. Hallek, H. G. Schmalz, A. Prokop, D. Mougiakakos and M. Herling, *Mol. Cancer*, 2015, **14**, 114.
378 R. Dasari, L. M. Banuls, M. Masi, S. C. Pelly, V. Mathieu, I. R. Green, W. A. L. van Otterlo, A. Evidente, R. Kiss and A. Kornienko, *Bioorg. Med. Chem. Lett.*, 2014, **24**, 923–927.
379 G. L. Nelson, C. T. Ronayne, L. N. Solano, S. K. Jonnalagadda, S. Jonnalagadda, J. Rumbley, J. Holy, T. Rose-Hellekant, L. R. Drewes and V. R. Mereddy, *Sci. Rep.*, 2019, **9**, 18266.
380 R. Kitel, A. Byczek-Wyrostek, K. Hopko, A. Kasprzycka and K. Walczak, *Pharmaceuticals*, 2021, **14**, 1079.
381 A. Byczek-Wyrostek, R. Kitel, K. Rumak, M. Skonieczna, A. Kasprzycka and K. Walczak, *Eur. J. Med. Chem.*, 2018, **150**, 687–697.

382 G. G. Llanos, L. M. Araujo, I. A. Jimenez, L. M. Moujir and I. L. Bazzocchi, *Eur. J. Med. Chem.*, 2012, **54**, 499–511.
383 G. G. Llanos, L. M. Araujo, I. A. Jimenez, L. M. Moujir, J. Rodriguez, C. Jimenez and I. L. Bazzocchi, *Eur. J. Med. Chem.*, 2017, **140**, 52–64.
384 N. R. Perestelo, G. G. Llanos, C. P. Reyes, A. Amesty, K. Sooda, S. Afshinjavid, I. A. Jimenez, F. Jayid and I. L. Bazzocchi, *J. Med. Chem.*, 2019, **62**, 4571–4585.
385 R. Zhao, X. Ma, L. Bai, X. Li, K. Mamouni, Y. Yang, H. Liu, A. Danaher, N. Cook, O. Kucuk, R. S. Hodges, L. Gera and D. Wu, *Neoplasia*, 2021, **23**, 1261–1274.
386 H. A. Garro, G. F. Reta, O. J. Donadel and C. R. Pungitore, *Nat. Prod. Commun.*, 2016, **11**, 1289–1292.
387 S. Fujii, Y. Miyajima, H. Masuno and H. Kagechika, *J. Med. Chem.*, 2013, **56**, 160–166.
388 S. Serin, *J. Indian Chem. Soc.*, 2023, **100**, 100939.
389 H. Mousazadeh, M. Milani, N. Zarghami, E. Alizadeh and K. D. Safa, *Basic Clin. Pharmacol. Toxicol.*, 2017, **121**, 390–399.
390 K. D. Safa and H. Mousazadeh, *Monatsh. Chem.*, 2016, **147**, 1951–1961.
391 K. D. Safa and H. Mousazadeh, *Synth. Commun.*, 2016, **46**, 1595–1604.
392 E. Eryilmaz, *Eur. J. Pharm. Sci.*, 2019, **134**, 266–273.
393 M. Deluigi, A. Klipp, C. Klenk, L. Merklinger, S. A. Eberle, L. Morstein, P. Heine, P. R. E. Mittl, P. Ernst, T. M. Kamenecka, Y. He, S. Vacca, P. Egloff, A. Honegger and A. Plückthun, *Sci. Adv.*, 2021, **7**, eabe5504.
394 R. Fanelli, A. Chastel, S. Previti, E. Hindié, D. Vimont, P. Zanotti-Fregonara, P. Fernandez, P. Garrigue, F. Lamare, R. Schollhammer, L. Balasse, B. Guillet, E. Rémond, C. Morgat and F. Cavelier, *Bioconjugate Chem.*, 2020, **31**, 2339–2349.
395 S. Geurs, D. Clarisse, K. De Bosscher and M. D'hooghe, *J. Med. Chem.*, 2023, **66**, 7698–7729.
396 P. A. Marks and R. Breslow, *Nat. Biotechnol.*, 2007, **25**, 84–90.
397 A. S. Madsen, H. M. E. Kristensen, G. Lanz and C. A. Olsen, *ChemMedChem*, 2014, **9**, 614–626.
398 I. S. Ignatyev, M. Montejo, P. G. Rodríguez Ortega and J. J. L. González, *J. Mol. Model.*, 2013, **19**, 1819–1834.
399 D. Davis, H. M. Kim, J. Y. Ramphal, J. R. Spencer, V. W. F. Tai and E. J. Verner, Silanol derivatives as inhibitors of histone deacetylase, WO-2006069096-A2006069091, 2006.
400 M.-F. Zaltariov, M. Turtoi, D. Peptanariu, A.-M. Macsim, L. Clima, C. Cojocaru, N. Vornicu, B.-I. Ciubotaru, A. Bargan, M. Calin and M. Cazacu, *Pharmaceutics*, 2022, **14**, 2838.
401 G. Ping, W. Yue-Wu, L. Xin-Tong, Q. Xiao-Lu, H. Le-Ping, X. Zi-Xin and Y. Fa-Qing, *Phosphorus, Sulfur Silicon Relat. Elem.*, 2014, **189**, 511–518.
402 D. Q. Shi, Q. Chen, Z. H. Li and X. P. Liu, *Phosphorus, Sulfur Silicon Relat. Elem.*, 2005, **180**, 1621–1627.
403 M. El-Hussieny, S. T. Mansour, A. I. Hashem, M. A. Fouad and M. A. Abd-El-Maksoud, *J. Chin. Chem. Soc.*, 2022, **69**, 1908–1923.
404 A. Winer, S. Adams and P. Mignatti, *Mol. Cancer Ther.*, 2018, **17**, 1147–1155.
405 M. J. Camarasa, M. J. Perezperez, A. Sanfelix, J. Balzarini and E. Declercq, *J. Med. Chem.*, 1992, **35**, 2721–2727.
406 M. J. Camarasa, S. Velazquez, A. San-Felix and M. J. Perez-Perez, *Antiviral Chem. Chemother.*, 2005, **16**, 147–153.
407 C. A. Chen, S. M. Sieburth, A. Glekas, G. W. Hewitt, G. L. Trainor, S. Erickson-Viitanen, S. S. Garber, B. Cordova, S. Jeffry and R. M. Klabe, *Chem. Biol.*, 2001, **8**, 1161–1166.
408 C. E. Flitcroft, K. A. Jolliffe and C. S. P. McErlean, *Chem. – Eur. J.*, 2023, **29**, e202301083.
409 S. McN. Sieburth, in *Bio-Inspired Silicon-Based Materials*, ed. P. M. Zelisko, Springer Dordrecht, 2014, vol. 5, pp. 103–123.
410 B. Delord, M. C. Guillorit, J. Lafay, M. L. Andreola, D. Tharaud, L. TarragoLitvak, H. J. A. Fleury and G. Déléris, *Eur. J. Med. Chem.*, 1996, **31**, 111–122.
411 N. Pribut, M. D'Erasmo, M. Dasari, K. E. Giesler, S. Iskandar, S. K. Sharma, P. W. Bartsch, A. Raghuram, A. Bushnev, S. S. Hwang, S. L. Burton, C. A. Derdeyn, A. E. Basson, D. C. Liotta and E. J. Miller, *J. Med. Chem.*, 2021, **64**, 12917–12937.
412 Q. Hao, X. Ling, C. Pannecouque, E. De Clercq and F. Chen, *Chin. Chem. Lett.*, 2023, **34**, 107663.
413 F. Ye, X. Song, J. Liu, X. Xu, Y. Wang, L. Hu, Y. Wang, G. Liang, P. Guo and Z. Xie, *Chem. Biol. Drug Des.*, 2015, **86**, 905–910.
414 A. Han, L. Li, K. Qing, X. Qi, L. Hou, X. Luo, S. Shi and F. Ye, *Bioorg. Med. Chem. Lett.*, 2013, **23**, 1310–1314.
415 B. D. Lesur, J.-B. Danzin and Charles, *N-derivatives of 1-deoxy nojirimycin*, Merrell Pharmaceuticals Inc., Cincinnati, OH, United States, 1996, p. 5536732.
416 A. G. Nair, Q. B. Zeng, O. Selyutin, S. B. Rosenblum, Y. H. Jiang, D. Y. Yang, K. Keertikar, G. W. Zhou, M. P. Dwyer, S. H. Kim, B. Shankar, W. S. Yu, L. Tong, L. Chen, R. Mazzola, J. Caldwell, H. Q. Tang, M. L. Allard, R. N. Buckle, P. J. F. Gauuan, C. L. Holst, G. S. Martin, K. P. Naicker, S. Vellekoop, S. Agrawal, R. Liu, R. Kong, P. Ingravallo, E. Xia, Y. Zhai, A. Nomeir and J. A. Kozlowski, *Bioorg. Med. Chem. Lett.*, 2016, **26**, 1475–1479.
417 A. G. Nair, Q. B. Zeng, O. Selyutin, S. B. Rosenblum, Y. H. Jiang, D. Y. Yang, K. Keertikar, G. W. Zhou, M. Dwyer, S. H. Kim, B. Shankar, W. S. Yu, L. Tong, L. Chen, R. Mazzola, J. Caldwell, H. Q. Tang, S. Agrawal, R. Liu, R. Kong, P. Ingravallo, E. Xia, Y. Zhai, A. Nomeir, E. Asante-Appiah and J. A. Kozlowski, *Bioorg. Med. Chem. Lett.*, 2018, **28**, 1954–1957.
418 E. Rémond, C. Martin, J. Martinez and F. Cavelier, in *Peptidomimetics I*, ed. W. D. Lubell, Springer International Publishing, Cham, 2017, pp. 27–50.
419 B. M. Liu, K. Gai, H. Qin, X. S. Liu, Y. Cao, Q. Lu, D. D. Lu, D. Y. Chen, H. Q. Shen, W. Song, Y. Zhang, X. J. Wang, H. J. Xu and Y. S. Zhang, *Eur. J. Med. Chem.*, 2018, **148**, 95–105.
420 B. M. Liu, K. Gai, H. Qin, J. Wang, X. S. Liu, Y. Cao, Q. Lu, D. D. Lu, D. Y. Chen, H. Q. Shen, W. Song, J. Mei, X. J. Wang, H. J. Xu and Y. S. Zhang, *J. Med. Chem.*, 2020, **63**, 5312–5323.
421 S. K. V. Vernekar, L. Qiu, J. Zhang, J. Kankanala, H. M. Li, R. J. Geraghty and Z. Q. Wang, *J. Med. Chem.*, 2015, **58**, 4016–4028.

422 Y. M. Hu, Y. X. Wang, F. Li, C. L. Ma and J. Wang, *Eur. J. Med. Chem.*, 2017, **135**, 70–76.
423 J. Wang, C. L. Ma, Y. B. Wu, R. A. Lamb, L. H. Pinto and W. F. DeGrado, *J. Am. Chem. Soc.*, 2011, **133**, 13844–13847.
424 Y. M. Kim, S. Farrah and R. H. Baney, *Electron. J. Biotechnol.*, 2006, **9**, 176–180.
425 Y. M. Kim, S. Farrah and R. H. Baney, *Electron. J. Biotechnol.*, 2007, **10**, 252–259.
426 Y.-m. Kim, S. Farrah and R. H. Baney, *Int. J. Antimicrob. Agents*, 2007, **29**, 217–222.
427 D. S. Reddy and R. Ramesh, *Antitubercular compounds and process for the preparation thereof*, Council of Scientific & Industrial Research India, 2014.
428 D. S. Reddy, N. Vasudevan, S. Wagh and R. Ramesh, Novel pyrrole compounds with silicon incorporation, Council of Scientific & Industrial Research India, 2014.
429 N. Vasudevan, Z. Motiwala, R. Ramesh, S. B. Wagh, R. D. Shingare, R. Katte, A. Anand, S. Choudhary, A. Kumar, R. S. Gokhale, K. A. Kulkarni and D. S. Reddy, *Eur. J. Med. Chem.*, 2023, **259**, 115633.
430 R. Ramesh, R. D. Shingare, V. Kumar, A. Anand, B. Swetha, S. Veeraraghavan, S. Viswanadha, R. Ummanni, R. Gokhale and D. S. Reddy, *Eur. J. Med. Chem.*, 2016, **122**, 723–730.
431 M. Martins, M. Viveiros, J. Ramos, I. Couto, J. Molnar, M. Boeree and L. Amaral, *Int. J. Antimicrob. Agents*, 2009, **33**, 479–482.
432 G. J. de Knegt, I. A. J. M. Bakker-Woudenberg, D. van Soolingen, R. Aarnoutse, M. J. Boeree and J. E. M. de Steenwinkel, *Int. J. Antimicrob. Agents*, 2015, **46**, 66–72.
433 S. O. Simons, J. E. Kristiansen, G. Hajos, T. van der Laan, J. Molnár, M. J. Boeree, J. van Ingen, J. B. Christensen, M. Viveiros, Z. Riedl, L. Amaral and D. van Soolingen, *Int. J. Antimicrob. Agents*, 2013, **41**, 488–489.
434 B. Seetharamsingh, R. Ramesh, S. S. Dange, P. V. Khairnar, S. Singhal, D. Upadhyay, S. Veeraraghavan, S. Viswanadha, S. Vakkalanka and D. S. Reddy, *ACS Med. Chem. Lett.*, 2015, **6**, 1105–1110.
435 Y. Wen, S. Lun, Y. Jiao, W. Zhang, T. Hu, T. Liu, F. Yang, J. Tang, B. Zhang, W. R. Bishai and L.-F. Yu, *Chin. Chem. Lett.*, 2023, 108464.
436 R. Cebrián, Q. Li, P. Peñalver, E. Belmonte-Reche, M. Andrés-Bilbao, R. Lucas, M. V. de Paz, O. P. Kuipers and J. C. Morales, *J. Nat. Prod.*, 2022, **85**, 1459–1473.
437 K. Yamada, A. Deb, V. M. Shoba, D. Lim, B. Maji, A. E. Modell and A. Choudhary, *Angew. Chem., Int. Ed.*, 2022, **61**, e202201698.
438 G. Singh, A. Devi, Diksha, Priyanka, N. George, J. Singh, Vikas, R. Yadav and R. Sehgal, *Inorg. Chem. Commun.*, 2023, **153**, 110742.
439 N. Dhingra, J. B. Singh and H. L. Singh, *Dalton Trans.*, 2022, **51**, 8821–8831.
440 H. L. Singh, N. Dhingra and S. Bhanuka, *J. Mol. Struct.*, 2023, **1287**, 135670.
441 S. N. Adamovich, E. K. Sadykov, I. A. Ushakov, E. N. Oborina and L. A. Belovezhets, *Mendeleev Commun.*, 2021, **31**, 204–206.
442 S. N. Adamovich, E. V. Kondrashov, I. A. Ushakov, N. S. Shatokhina, E. N. Oborina, A. V. Vashchenko, L. A. Belovezhets, I. B. Rozentsveig and F. Verpoort, *Appl. Organomet. Chem.*, 2020, **34**, e5976.
443 R. Singh, J. K. Puri, V. K. Chahal, R. P. Sharma, S. Kohli, R. Kant and B. S. Gill, *Synth. React. Inorg., Met.-Org., Nano-Met. Chem.*, 2012, **42**, 823–832.
444 G. Singh, J. Singh, A. Singh, J. Singh, M. Kumar, K. Gupta and S. Chhibber, *J. Organomet. Chem.*, 2018, **871**, 21–27.
445 G. Singh, A. Saroa, S. Girdhar, S. Rani, S. Sahoo and D. Choquesillo-Lazarte, *Inorg. Chim. Acta*, 2015, **427**, 232–239.
446 M. Napiórkowska, M. Cieślak, J. Kaźmierczak-Barańska, K. Królewska, A. Czapla and B. Kuran, *Heterocycl. Commun.*, 2015, **21**, 19–24.
447 G. Singh, G. Sharma, Sanchita, P. Kalra, P. Satija, Pawan, B. Singh, D. Aulakh and M. Wreidt, *ChemistrySelect*, 2020, **5**, 284–292.
448 S. N. Adamovich, I. A. Ushakov, E. N. Oborina, S. V. Lukyanova and V. Y. Komarov, *Int. J. Mol. Sci.*, 2023, **24**, 9965.
449 M. Baghershiroudi, K. D. Safa, K. Adibkia and F. Lotfipour, *J. Iran. Chem. Soc.*, 2018, **15**, 1279–1286.
450 G. R. Jachak, R. Ramesh, D. G. Sant, S. U. Jorwekar, M. R. Jadhav, S. G. Tupe, M. V. Deshpande and D. S. Reddy, *ACS Med. Chem. Lett.*, 2015, **6**, 1111–1116.
451 C. Fu, B. Fu, X. X. Peng and G. J. Liao, *Molecules*, 2017, **22**, 637.
452 A. Bargan, M. F. Zaltariov, A. Vlad, A.-M.-C. Dumitriu, A. Soroceanu, A.-M. Macsim, M. Dascalu, C. D. Varganici, M. Cazacu and S. Shova, *Arabian J. Chem.*, 2020, **13**, 3100–3111.
453 M. Adams, C. de Kock, P. J. Smith, K. M. Land, N. Liu, M. Hopper, A. Hsiao, A. R. Burgoyne, T. Stringer, M. Meyer, L. Wiesner, K. Chibale and G. S. Smith, *Dalton Trans.*, 2015, **44**, 2456–2468.
454 Y. Li, C. de Kock, P. J. Smith, H. Guzgay, D. T. Hendricks, K. Naran, V. Mizrahi, D. F. Warner, K. Chibale and G. S. Smith, *Organometallics*, 2013, **32**, 141–150.
455 M. Adams, T. Stringer, C. de Kock, P. J. Smith, K. M. Land, N. Liu, C. Tam, L. W. Cheng, M. Njoroge, K. Chibale and G. S. Smith, 2016, 45, 19086–19095.
456 Y. Li, C. de Kock, P. J. Smith, K. Chibale and G. S. Smith, *Organometallics*, 2014, **33**, 4345–4348.
457 M. Adams, L. Barnard, C. de Kock, P. J. Smith, L. Wiesner, K. Chibale and G. S. Smith, *Dalton Trans.*, 2016, **45**, 5514–5520.
458 G. Singh, A. Arora, S. S. Mangat, S. Rani, H. Kaur, K. Goya, R. Sehgal, I. K. Maurya, R. Tewari, D. Choquesillo-Lazarte, S. Sahoo and N. Kaur, *Eur. J. Med. Chem.*, 2016, **108**, 287–300.
459 G. Singh, A. Singh, J. Singh, D. Aulakh, M. Wriedt, C. Espinosa, M. A. Esteban, R. Sehgal, K. Goyal and S. Sinha, *New J. Chem.*, 2017, **41**, 15165–15172.
460 G. Singh, A. Singh, K. Chowdhary, P. Satija, Sanchita, P. Kalra, G. Sharma, S. Sinha and R. Sehgal, *Polycyclic Aromat. Compd.*, 2021, **41**, 173–183.

461 G. Singh, A. Arora, P. Kalra, I. K. Maurya, C. E. Ruizc, M. A. Estebanc, S. Sinha, K. Goyal and R. Sehgal, *Bioorg. Med. Chem.*, 2019, **27**, 188–195.
462 D. San Nicolás-Hernández, C. J. Bethencourt-Estrella, A. López-Arencibia, E. Hernández-Álvarez, I. Sifaoui, I. L. Bazzocchi, J. Lorenzo-Morales, I. A. Jiménez and J. E. Piñero, *Biomed. Pharmacother.*, 2023, **157**, 114012.
463 A. Geronikaki, D. Hadjipavlou-Litina, A. Zablotskaya and I. Segal, *Bioinorg. Chem. Appl.*, 2007, **2007**, 92145.
464 F. Kleemiss, P. Puylaert, D. Duvinage, M. Fugel, K. Sugimoto, J. Beckmann and S. Grabowsky, *Acta Crystallogr., Sect. B: Struct. Sci., Cryst. Eng. Mater.*, 2021, **77**, 892–905.
465 F. Kleemiss, A. Justies, D. Duvinage, P. Watermann, E. Ehrke, K. Sugimoto, M. Fugel, L. A. Malaspina, A. Dittmer, T. Kleemiss, P. Puylaert, N. R. King, A. Staubitz, T. M. Tzschentke, R. Dringen, S. Grabowsky and J. Beckmann, *J. Med. Chem.*, 2020, **63**, 12614–12622.
466 D. J. Pérez, U. I. Zakai, S. Guo, I. A. Guzei, Z. Gómez-Sandoval, R. S. Razo-Hernández, R. West and Á. Ramos-Organillo, *Aust. J. Chem.*, 2016, **69**, 662–671.
467 D. J. Pérez, M. I. Díaz-Reval, F. Obledo-Benicio, U. I. Zakai, Z. Gómez-Sandoval, R. S. Razo-Hernández, R. West, M. T. Sumaya-Martínez, K. Pineda-Urbina and Á. Ramos-Organillo, *Eur. J. Pharmacol.*, 2017, **814**, 18–27.
468 M. J. Barnes, R. Conroy, D. J. Miller, J. S. Mills, J. G. Montana, P. K. Pooni, G. A. Showell, L. M. Walsh and J. B. H. Warneck, *Bioorg. Med. Chem. Lett.*, 2007, **17**, 354–357.
469 A. S. Kulkarni, R. Ramesh, S. Walia, S. I. Sayyad, G. B. Gathalkar, S. Balamkundu, M. Joshi, A. Sen and D. S. Reddy, *ACS Omega*, 2021, **6**, 31236–31243.
470 S. S. Shete, F. Iqbal, M. Bhardwaj, U. Nandi, A. Kumar and D. S. Reddy, *ACS Med. Chem. Lett.*, 2023, **14**, 1716–1723.
471 M. W. Mutahi, T. Nittoli, L. Guo and S. M. Sieburth, *J. Am. Chem. Soc.*, 2002, **124**, 7363–7375.
472 J. Kim, G. Hewitt, P. Carroll and S. M. Sieburth, *J. Org. Chem.*, 2005, **70**, 5781–5789.
473 R. G. Almquist, W.-R. Chao, M. E. Ellis and H. L. Johnson, *J. Med. Chem.*, 1980, **23**, 1392–1398.
474 R. F. Meyer, E. D. Nicolaides, F. G. Tinney, E. A. Lunney, A. Holmes, M. L. Hoefle, R. D. Smith, A. D. Essenburg, H. R. Kaplan and R. G. Almquist, *J. Med. Chem.*, 1981, **24**, 964–969.
475 R. G. Almquist, J. Crase, C. Jennings-White, R. F. Meyer, M. L. Hoefle, R. D. Smith, A. D. Essenburg and H. R. Kaplan, *J. Med. Chem.*, 1982, **25**, 1292–1299.
476 Y. Bo, S. Singh, H. Q. Duong, C. Cao and S. M. Sieburth, *Org. Lett.*, 2011, **13**, 1787–1789.
477 S. M. Sieburth and C. A. Chen, *Eur. J. Org. Chem.*, 2006, **2006**, 311–322.
478 H. Q. Duong and S. M. Sieburth, *J. Org. Chem.*, 2018, **83**, 5398–5409.
479 J. Kim, A. Glekas and S. M. Sieburth, *Bioorg. Med. Chem. Lett.*, 2002, **12**, 3625–3627.
480 J. Kim and S. M. Sieburth, *J. Org. Chem.*, 2004, **69**, 3008–3014.
481 D. H. Juers, J. Kim, B. W. Matthews and S. M. Sieburth, *Biochemistry*, 2005, **44**, 16524–16528.
482 G. A. Dalkas, D. Marchand, J.-C. Galleyrand, J. Martinez, G. A. Spyroulias, P. Cordopatis and F. Cavelier, *J. Pept. Sci.*, 2010, **16**, 91–97.
483 G. D. Reddy, S. J. Park, H. M. Cho, T. J. Kim and M. E. Lee, *J. Med. Chem.*, 2012, **55**, 6438–6444.
484 D. R. Guda, S.-J. Park, M.-W. Lee, T.-J. Kim and M. E. Lee, *Eur. J. Med. Chem.*, 2013, **62**, 84–88.
485 M. Geyer, J. A. Baus, O. Fjellström, E. Wellner, L. Gustafsson and R. Tacke, *ChemMedChem*, 2015, **10**, 2063–2070.
486 M. Geyer, E. Wellner, U. Jurva, S. Saloman, D. Armstrong and R. Tacke, *ChemMedChem*, 2015, **10**, 911–924.
487 R. J. Fessenden, J. G. Larsen, M. D. Coon and J. S. Fessenden, *J. Med. Chem.*, 1964, **7**, 695–698.
488 R. J. Fessenden and M. D. Coon, *J. Med. Chem.*, 1964, **7**, 561–562.
489 R. J. Fessenden and M. D. Coon, *J. Med. Chem.*, 1965, **8**, 604–608.
490 J. P. Stasch, H. Russ, U. Schacht, M. Witteler, D. Neuser, M. Gerlach, M. Leven, W. Kuhn, P. Jutzi and H. Przuntek, *Arzneim. Forsch.*, 1988, **38-2**, 1075–1078.
491 A. Schotte, P. F. M. Janssen, A. A. H. P. Megens and J. E. Leysen, *Brain Res.*, 1993, **631**, 191–202.
492 R. Tacke, T. Heinrich, R. Bertermann, C. Burschka, A. Hamacher and M. U. Kassack, *Organometallics*, 2004, **23**, 4468–4477.
493 R. Tacke, F. Popp, B. Muller, B. Theis, C. Burschka, A. Hamacher, M. U. Kassack, D. Schepmann, B. Wunsch, U. Jurva and E. Wellner, *ChemMedChem*, 2008, **3**, 152–164.
494 R. Tacke, B. Nguyen, C. Burschka, W. P. Lippert, A. Hamacher, C. Urban and M. U. Kassack, *Organometallics*, 2010, **29**, 1652–1660.
495 R. Tacke, R. Bertermann, C. Burschka, S. Dörrich, M. Fischer, B. Müller, G. Meyerhans, D. Schepmann, B. Wünsch, I. Arnason and R. Bjornsson, *ChemMedChem*, 2012, **7**, 523–532.
496 S. Duda-Johner, J. O. Daiß, K. Mohr and R. Tacke, *J. Organomet. Chem.*, 2003, **686**, 75–83.
497 J. O. Daiss, S. Duda-Johner, C. Burschka, U. Holzgrabe, K. Mohr and R. Tacke, *Organometallics*, 2002, **21**, 803–811.
498 J. O. Daiss, C. Burschka, J. S. Mills, J. G. Montana, G. A. Showell, J. B. H. Warneck and R. Tacke, *J. Organomet. Chem.*, 2006, **691**, 3589–3595.
499 G. A. Showell, M. J. Barnes, J. O. Daiss, J. S. Mills, J. G. Montana, R. Tacke and J. B. H. Warneck, *Bioorg. Med. Chem. Lett.*, 2006, **16**, 2555–2558.
500 J. O. Daiss, C. Burschka, J. S. Mills, J. G. Montana, G. A. Showell, J. B. H. Warneck and R. Tacke, *Organometallics*, 2006, **25**, 1188–1198.
501 A. H. Beckett, D. C. Taylor and J. W. Gorrod, *J. Pharm. Pharmacol.*, 1975, **27**, 588–593.
502 M. Blunder, N. Hurkes, S. Spirk, M. List and R. Pietschnig, *Bioorg. Med. Chem. Lett.*, 2011, **21**, 363–365.

503 E. Belmonte-Reche, P. Penalver, M. Caro-Moreno, M. L. Mateos-Martin, N. Adan, M. Delgado, E. González-Rey and J. C. Morales, *Eur. J. Med. Chem.*, 2021, **223**, 113655.
504 W. Duan, Y. Sun, M. Wu, Z. Zhang, T. Zhang, H. Wang, F. Li, L. Yang, Y. Xu, Z.-J. Liu, T. Hua, H. Nie and J. Cheng, *Eur. J. Med. Chem.*, 2021, **226**, 113878.
505 M. El-Hussieny, M. A. Abd-El-Maksoud, F. M. Soliman, M. A. Fouad and M. K. El-Ashrey, *J. Enzyme Inhib. Med. Chem.*, 2023, **38**, 2166040.
506 J.-M. Hornsperger, J.-N. Collard, J.-G. Heydt, E. Giacobini, S. Funes, J. Dow and D. Schirlin, *Biochem. Soc. Trans.*, 1994, **22**, 758–763.
507 G. Luo, L. M. Chen, Y. Li, Y. Fan, D. Y. Wang, Y. F. Yang, L. Gao, R. T. Jiang and Z. L. Song, *Org. Chem. Front.*, 2021, **8**, 5941–5947.
508 K. Madica, K. C. Nadimpally and G. J. Sanjayan, *Tetrahedron Lett.*, 2017, **58**, 1568–1571.
509 R. B. Silverman and G. M. Banik, *J. Am. Chem. Soc.*, 1987, **109**, 2219–2220.
510 C. Danzin, J.-N. Collard, P. Marchal and D. Schirlin, *Bioorg. Med. Chem. Lett.*, 1995, **5**, 2363–2366.
511 P. Tétreault, É. Besserer-Offroy, R. L. Brouillette, A. René, A. Murza, R. Fanelli, K. Kirby, A. J. Parent, I. Dubuc, N. Beaudet, J. Côté, J.-M. Longpré, J. Martinez, F. Cavelier and P. Sarret, *Eur. J. Pharmacol.*, 2020, **882**, 173174.
512 S. Farkas, *CNS Drug Rev.*, 2006, **12**, 218–235.
513 T. Kniess, H. Spies, I. Santos and A. Zablotska, *J. Labelled Compd. Radiopharm.*, 2002, **45**, 629–636.
514 C. Fernandes, T. Kniess, L. Gano, S. Seifert, H. Spies and I. Santos, *Nucl. Med. Biol.*, 2004, **31**, 785–793.
515 V. V. Dorsselaer, D. Schirlin, P. Marchal, F. Weber and C. Danzin, *Bioorg. Chem.*, 1996, **24**, 178–193.
516 M. C. J. Wolvekamp and R. W. F. de Bruin, *Dig. Dis.*, 1994, **12**, 2–14.
517 G. Singh, Sushma, Priyanka, Diksha, Mohit, S. Gupta, M. Angeles Esteban, C. Espinosa-Ruíz and D. González-Silvera, *J. Mol. Struct.*, 2022, **1255**, 132446.
518 G. Singh, Tamana, A. Devi, A. Saini, Y. Thakur, S. Khurana, S. Sharma, T. Diskit and K. N. Singh, *Dyes Pigm.*, 2023, **219**, 111537.
519 G. Singh, A. Devi, Tamana, P. Malik, S. Khurana, J. Stanzin, D. Sharma, Mithun and Heena, *Spectrochim. Acta, Part A*, 2023, **299**, 122854.
520 G. Singh, Mohit, Diksha, Pawan, P. Satija, Sushma, S. Sharma, S. Gupta and K. N. Singh, *Inorg. Chim. Acta*, 2023, **545**, 121263.
521 G. Singh, S. Gupta, S. Sharma, A. Devi, S. Khurana, P. Malik, S. Devi, Heena and Vikas, *Environ. Nanotechnol., Monit. Manage.*, 2023, **20**, 100831.
522 G. Singh, Diksha, Mohit, Priyanka, A. Devi, S. Devi, H. Kaur, J. Singh and G. Singh, *New J. Chem.*, 2023, **47**, 12608–12619.
523 G. Singh, Diksha, Mohit, Suman, Sushma, A. Devi, S. Gupta, C. Espinosa-Ruíz and M. Angeles Esteban, *Inorg. Chim. Acta*, 2022, **537**, 120926.
524 G. Singh, A. Devi, Mohit, P. Satija, Sushma, Vikas, D. Gonzalez-Silvera, C. Espinosa-Ruiz and M. Angeles Esteban, *Inorg. Chim. Acta*, 2022, **542**, 121126.
525 G. Singh, A. Devi, Mohit, Diksha, Suman, A. Saini, J. D. Kaur, S. Gupta and Vikas, *New J. Chem.*, 2022, **46**, 21717–21729.
526 G. Singh, A. Saini, Mohit, Pawan, Diksha, Sushma, Suman, Priyanka and P. Satija, *Inorg. Chem. Commun.*, 2022, **146**, 110090.
527 G. Singh, G. Sharma, P. Satija, A. Singh, Pawan, C. E. Ruiz, D. G. Silvera, M. A. Esteban and S. Soni, *ChemistrySelect*, 2020, **5**, 15055–15060.
528 H. Toyama, M. Nakamura, Y. Hashimoto and S. Fujii, *Bioorg. Med. Chem.*, 2015, **23**, 2982–2988.
529 Y. Nishiyama, M. Nakamura, T. Misawa, M. Nakagomi, M. Makishima, M. Ishikawa and Y. Hashimoto, *Bioorg. Med. Chem.*, 2014, **22**, 2799–2808.
530 N. Namba, T. Noguchi-Yachide, Y. Matsumoto, Y. Hashimoto and S. Fujii, *Bioorg. Med. Chem.*, 2022, **66**, 116792.
531 H. Toyama, H. Shirakawa, M. Komai, Y. Hashimoto and S. Fujii, *Bioorg. Med. Chem.*, 2018, **26**, 4493–4501.
532 H. Toyama, S. Sato, H. Shirakawa, M. Komai, Y. Hashimoto and S. Fujii, *Bioorg. Med. Chem. Lett.*, 2016, **26**, 1817–1820.
533 C. Zhou, J. G. Cheng, R. Beadle, F. G. Earley, Z. Li and P. Maienfisch, *Bioorg. Med. Chem.*, 2020, **28**, 115509.
534 C. Zhou, X. Wang, X. Quan, J. Cheng, Z. Li and P. Maienfisch, *Nongye Yu Shipin Kexue*, 2022, **70**, 11063–11074.
535 C. Zhou, Z. Li, X. Qian, J. Cheng and P. Maienfisch, *Nongye Yu Shipin Kexue*, 2023, **71**, 18239–18249.
536 X. Quan, L. Xu, Z. Li and P. Maienfisch, *Nongye Yu Shipin Kexue*, 2023, **71**, 18188–18196.
537 L. Xu, X. Quan, Z. Li and P. Maienfisch, *Nongye Yu Shipin Kexue*, 2023, **71**, 18250–18259.
538 C. Zhou, X. Sun, W. Fu, Z. Li, J. Cheng and P. Maienfisch, *Nongye Yu Shipin Kexue*, 2023, **71**, 5483–5495.
539 G. Wei, M.-W. Huang, W.-J. Wang, Y. Wu, S.-F. Mei, L.-M. Zhou, L.-C. Mei, X.-L. Zhu and G.-F. Yang, *J. Agric. Food Chem.*, 2021, **69**(13), 3965–3971.
540 I. F. Yu, J. W. Wilson and J. F. Hartwig, *Chem. Rev.*, 2023, **123**, 11619–11663.
541 J. J. Dalton, A. Bernal Sánchez, A. T. Kelly, J. C. Fettinger and A. K. Franz, *ACS Catal.*, 2024, **14**, 1005–1012.
542 E. Ramesh, L. D. Nandawadekar, R. S. Rao and D. S. Reddy, *Org. Lett.*, 2023, **25**, 6881–6885.
543 R. Holland, K. Lam, S. Jeng, K. McClintock, L. Palmer, P. Schreiner, M. Wood, W. Zhao and J. Heyes, *ACS Nano*, 2024, **18**, 10374–10387.
544 Y. Matsumoto, Y. Hashimoto and S. Fujii, *RSC Adv.*, 2023, **13**, 27359–27362.
545 Y. Miyajima, T. Noguchi-Yachide, K. Ochiai and S. Fujii, *RSC Med. Chem.*, 2024, **15**, 119–126.
546 Y. Yamanoi, *Acc. Chem. Res.*, 2023, **56**, 3325–3341.
547 N. S. Sarai, T. J. Fulton, R. L. O'Meara, K. E. Johnston, S. Brinkmann-Chen, R. R. Maar, R. E. Tecklenburg, J. M. Roberts, J. C. T. Reddel, D. E. Katsoulis and F. H. Arnold, *Science*, 2024, **383**, 438–443.